

AD _____

Award Number: DAMD17-02-1-0375

TITLE: CBP and Extracellular Matrix-Induced Apoptosis in p53(-)
HMECs: A Model of Early Mammary Carcinogenesis

PRINCIPAL INVESTIGATOR: Victoria L. Seewaldt, M.D.

CONTRACTING ORGANIZATION: Duke University Medical Center
Durham, North Carolina 27710

REPORT DATE: September 2004

TYPE OF REPORT: Annual

PREPARED FOR: U.S. Army Medical Research and Materiel Command
Fort Detrick, Maryland 21702-5012

DISTRIBUTION STATEMENT: Approved for Public Release;
Distribution Unlimited

The views, opinions and/or findings contained in this report are those of the author(s) and should not be construed as an official Department of the Army position, policy or decision unless so designated by other documentation.

20050415 032

REPORT DOCUMENTATION PAGEForm Approved
OMB No. 074-0188

Public reporting burden for this collection of information is estimated to average 1 hour per response, including the time for reviewing instructions, searching existing data sources, gathering and maintaining the data needed, and completing and reviewing this collection of information. Send comments regarding this burden estimate or any other aspect of this collection of information, including suggestions for reducing this burden to Washington Headquarters Services, Directorate for Information Operations and Reports, 1215 Jefferson Davis Highway, Suite 1204, Arlington, VA 22202-4302, and to the Office of Management and Budget, Paperwork Reduction Project (0704-0188), Washington, DC 20503

1. AGENCY USE ONLY (Leave blank)		2. REPORT DATE September 2004	3. REPORT TYPE AND DATES COVERED Annual (1 Sep 03 - 31 Aug 04)	
4. TITLE AND SUBTITLE CBP and Extracellular Matrix-Induced Apoptosis in p53(-) HMECs: A Model of Early Mammary Carcinogenesis			5. FUNDING NUMBERS DAMD17-02-1-0375	
6. AUTHOR(S) Victoria L. Seewaldt, M.D.				
7. PERFORMING ORGANIZATION NAME(S) AND ADDRESS(ES) Duke University Medical Center Durham, North Carolina 27710 E-Mail: Seewa001@mc.duke.edu			8. PERFORMING ORGANIZATION REPORT NUMBER	
9. SPONSORING / MONITORING AGENCY NAME(S) AND ADDRESS(ES) U.S. Army Medical Research and Materiel Command Fort Detrick, Maryland 21702-5012			10. SPONSORING / MONITORING AGENCY REPORT NUMBER	
11. SUPPLEMENTARY NOTES				
12a. DISTRIBUTION / AVAILABILITY STATEMENT Approved for Public Release; Distribution Unlimited				12b. DISTRIBUTION CODE
13. ABSTRACT (Maximum 200 Words) Interactions between normal mammary epithelial cells (HMECs) and extracellular matrix (ECM) are important for mammary gland homeostasis and loss of ECM-sensitivity is an early event in mammary carcinogenesis. The purpose of this grant is to investigate how the CREBP-binding protein (CBP) might target the elimination of damaged HMECs. We have observed that 1) suppression of CBP results in apoptosis-resistance through impaired laminin expression and 2) CBP promotes induction of interferon-regulated genes during apoptosis. These findings will provide novel targets for chemoprevention and are being used to develop markers for response to current prevention strategies.				
14. SUBJECT TERMS Prevention, CREBP-binding protein, extracellular matrix, apoptosis				15. NUMBER OF PAGES 168
				16. PRICE CODE
17. SECURITY CLASSIFICATION OF REPORT Unclassified	18. SECURITY CLASSIFICATION OF THIS PAGE Unclassified	19. SECURITY CLASSIFICATION OF ABSTRACT Unclassified	20. LIMITATION OF ABSTRACT Unlimited	

NSN 7540-01-280-5500

Standard Form 298 (Rev. 2-89)
Prescribed by ANSI Std. Z39-18
298-102

Table of Contents

Cover.....1

SF 298.....2

Introduction.....3

Body.....3

Key Research Accomplishments.....8

Reportable Outcomes.....8

Conclusions.....9

References.....9

Appendices.....9

INTRODUCTION:

Interactions between normal mammary epithelial cells (HMECs) and extracellular matrix (ECM) are important for mammary gland homeostasis; loss of ECM-sensitivity is thought to be an early event in mammary carcinogenesis. The CREBP binding protein (CBP) is known to regulate both proliferation and apoptosis but the role of CBP in ECM-signaling is poorly characterized. **The purpose of this grant is to investigate how CBP might regulate apoptosis in HMECs. Major findings to date and progress in fulfillment of Specific Aim I:** We investigated the relationship between CBP expression and sensitivity to prepared ECM (rECM)-induced growth arrest and apoptosis in an *in vitro* model of early mammary carcinogenesis. Suppression of CBP expression in HMECs by antisense oligonucleotides (ODNs) resulted in loss of rECM-mediated growth regulation, polarity, and apoptosis. Chromatin immunoprecipitation studies (ChIP) and reporter studies demonstrated that inhibition of CBP protein expression resulted in 1) loss of CBP-occupancy of the *LAMA3A* promoter and 2) a decrease in *LAMA3A* promoter activity. rECM-resistance correlated with 1) loss of CBP occupancy of the *LAMA3A* promoter, 2) decreased *LAMA3A* promoter activity, and 3) loss of laminin-5 α 3-chain mRNA and protein expression. These observations suggest a critical role for CBP in rECM-mediated growth regulation, polarity, and apoptosis through modulation of *LAMA3A* activity and laminin-5 α 3-chain expression. Expression of CBP in rECM-resistant cells resulted in induction of laminin-5 α 3-chain expression and restoration of apoptosis-sensitivity. Suppression of CBP expression in apoptosis-resistant cells resulted in 1) loss of CBP occupancy of the *LAMA3A* promoter, 2) loss of laminin-5 α 3-chain expression, and 3) apoptosis-resistance. **Major findings to date and progress in fulfillment of Specific Aim II:** CBP is a known regulator of interferon (IFN)-signaling and dysregulated expression of IFN-signal transduction genes has been observed during mammary carcinogenesis. We hypothesize that the level of CBP expression is critical for the induction of IFN-activated transcription during rECM-mediated apoptosis in HMEC-E6 cells. We observed that CBP regulates induces expression of interferon regulated genes in the absence of interferon release. rECM promotes CBP occupancy of the IRF-1 promoter and upregulation of IRF-1 mRNA and protein. Inhibition of IRF-1 signaling by siRNA directed against IRF-1 blocks IRF-1 expression, induction of interferon regulated genes, and apoptosis resistance.

BODY:

SPECIFIC AIM I: Does the level of the CREBP binding protein (CBP) protein expression in normal human mammary epithelial cells (HMECs) determine sensitivity to prepared extracellular matrix (rECM)-mediated apoptosis? [See appended manuscript Dietze et al.]

1a) Suppression of CBP in early passage HMECs by antisense oligonucleotides (ODNs). Antisense ODNs were utilized to suppress CBP protein expression in HMECs to test whether the level of CBP protein expression might be important for rECM-sensitivity. Relative levels of CBP protein expression were tested by Western analysis. Early passage HMEC vector controls (HMEC-LXSN) and early passage apoptosis-sensitive HMECs transduced with human papillomavirus-16 E6 protein (HMEC-E6) treated with the active, CBP-specific ODN, A3342V, exhibited a 65% and 72% respective decrease in CBP protein expression relative to untreated controls. Cells treated with the inactive CBP ODN, scrA3342V, did not exhibit a significant decrease in CBP protein expression.

1b) Suppression of CBP enhances proliferation in rECM. Treatment of early passage HMEC-LXSN controls and HMEC-E6 cells with CBP-specific ODNs resulted in enhanced proliferation in rECM-culture as measured by 1) physical growth parameters and 2) Ki-67 staining. Both early passage HMEC-LXSN controls and HMEC-E6 cells treated with active CBP-specific ODNs (A33243V) demonstrated a continued increase in sphere diameter from Day 7-9 in rECM culture. In contrast, early passage HMEC-LXSN controls and HMEC-E6 cells treated with inactive ODNs (scrA33243V) did not exhibit an increase in sphere diameter after Day 7. Treatment of early passage HMEC-LXSN and HMEC-E6 cells with CBP-specific ODNs (A33243V) resulted in continued Ki-67 staining at 9 and 11 days in rECM culture. In contrast, Ki-67 staining at 9 and 11 days were markedly reduced in HMEC-LXSN and HMEC-E6 cells treated with inactive ODNs (scrA33243V). These observations show that suppression of CBP protein expression in early passage HMEC-E6 cells and HMEC-LXSN controls resulted in enhanced proliferation in rECM culture.

1c) Suppression of CBP protein results in altered localization and expression of biochemical markers of polarity. Early passage HMEC-E6 cells and HMEC-LXSN controls treated with active CBP ODNs (A33423V) exhibited a loss of epithelial polarity as evidenced by dispersed and intracellular staining of 1) E-cadherin and 2) the tight junction-associated protein, ZO-1. In contrast, early passage HMEC-LXSN controls and HMEC-E6 cells treated with inactive CBP ODNs (scrA33423V) demonstrated expression of E-cadherin and ZO-1 at the cell-cell junction, consistent with a correctly polarized epithelium. These observations indicate that suppression of CBP protein expression in HMECs by antisense ODNs promotes a loss of epithelial polarity in rECM culture.

1d) Suppression of CBP inhibits apoptosis in rECM culture. Early passage HMEC-E6 cells were treated with CBP-specific antisense ODNs to test whether suppression of CBP protein expression blocked apoptosis in rECM culture. Early passage HMEC-E6 treated with CBP-specific antisense ODNs (A33423V) formed large irregular clusters in rECM and did not undergo apoptosis as assessed by either electron microscopy or TUNEL-staining. In contrast, early passage HMEC-E6 cells treated with inactive CBP ODNs underwent apoptosis on Day 7 as assessed by either morphologic criteria or TUNEL-staining. Similar to early passage HMEC-E6 cells, early passage HMEC-LXSN cells treated CBP-specific, antisense ODNs (A33423V) formed large irregular clusters in rECM. Early passage HMEC-LXSN controls treated with inactive ODN (scrA33423V) formed a morphologically organized, ascus-like structure and did not undergo apoptosis consistent with what has been previously observed for early passage HMEC-LXSN untreated controls. These observations demonstrate that suppression of CBP protein expression in early passage HMEC-E6 cells by antisense ODNs blocks apoptosis in rECM culture.

A second HMEC strain, AG11134, was tested to ensure that these observations were not HMEC strain-specific. Similar to observations made in HMEC strain AG11132 above, 1) early passage AG11134-E6 cells treated with inactive CBP ODN (scrA33423V) were sensitive to rECM-growth regulation and underwent apoptosis at Day 7, 2) early passage AG11134-LXSN controls treated with antisense-CBP ODN (A99424V) were resistant to rECM growth arrest and did not undergo apoptosis at Day 7-9, and 3) early passage AG11134-LXSN controls

treated with CBP-specific antisense ODNs were resistant to rECM-mediated growth regulation and did not undergo apoptosis (data not shown).

1e) Laminin-5 expression is decreased in rECM resistant, late passage HMEC-E6 cells. We previously observed that sensitivity to rECM-apoptosis in early passage HMEC-E6 cells required polarized expression of $\alpha 3/\beta 1$ -integrin. Differential gene expression studies, semi-quantitative RT-PCR, and Western analysis were performed to test whether the loss of sensitivity to rECM-mediated growth regulation, polarity, and apoptosis observed in late passage HMEC-E6 cells correlated with altered expression of laminin-5 and/or $\alpha 3/\beta 1$ -integrin mRNA. Differential gene expression studies demonstrated decreased expression of all three laminin-5 chains ($\alpha 3$, $\beta 3$, and $\gamma 2$) in apoptosis-resistant, late passage HMEC-E6 cells relative to early passage HMEC-LXSN controls and early passage HMEC-E6 cells grown in rECM. Semi-quantitative RT-PCR confirmed a 98% decrease in laminin-5 $\alpha 3$ -chain ($p \leq 0.01$), an 88% decrease in laminin-5 $\beta 3$ -chain ($p \leq 0.01$), and a 75% decrease in laminin-5 $\gamma 2$ -chain ($p \leq 0.01$) mRNA expression relative to early passage HMEC-LXSN controls. There was no significant change in the level of $\alpha 3/\beta 1$ -integrin mRNA expression. Western analysis similarly demonstrated an 85% ($p < 0.001$) decrease in laminin-5 $\alpha 3$ -chain protein expression in apoptosis-resistant, late passage HMEC-E6 cells relative to early passage HMEC-LXSN controls. Expression of laminin-5 $\alpha 3$ -chain protein did not significantly vary between early passage HMEC-LXSN cells and early passage HMEC-E6 cells (Figure 6 d). There was a 130% ($p < 0.002$) increase in laminin-5 $\alpha 3$ -chain protein in late passage HMEC-LXSN controls relative to early passage HMEC-LXSN cells. These observations demonstrate that the presence of rECM-resistance in late passage HMEC-E6 cells correlates with a loss of laminin-5 mRNA and protein expression.

1f) Lack of polarized expression of laminin- $\alpha 3$ and integrin- $\alpha 3$ proteins in late passage HMEC-E6 cells grown in rECM. Early and late passage HMEC-LXSN controls and HMEC-E6 cells were grown in rECM and tested for 1) laminin-5 $\alpha 3$ -chain and 2) $\alpha 3$ - and $\beta 1$ -integrin expression by immunohistochemistry (clones P5H10, P1F2, and P4C10, respectively). Early and late passage HMEC-LXSN controls and early passage HMEC-E6 cells exhibited polarized basal expression of laminin-5 $\alpha 3$ -chain and $\alpha 3$ - and $\beta 1$ -integrins. In contrast, late passage, CBP-“poor” HMEC-E6 cells grown in rECM demonstrated disorganized plasma membrane and cytosolic expression of both laminin-5 $\alpha 3$ -chain and $\alpha 3$ -integrin. As predicted by differential gene expression studies and Western analysis, there was also a qualitative decrease in laminin-5 $\alpha 3$ -chain expression in late passage HMEC-E6 cells relative to controls. Late passage HMEC-E6 cells grown in rECM exhibited polarized basal $\beta 1$ -integrin expression but had an increase in the amount of cytosolic expression relative to early passage cells. These observations demonstrate a loss of polarized expression of laminin-5 $\alpha 3$ -chain and $\alpha 3$ -integrin in rECM-resistant late passage HMEC-E6 cells.

1g) Suppression of CBP expression in HMECs alters both laminin- $\alpha 3$ and integrin- $\alpha 3$ protein expression in rECM culture. We observed that late passage HMEC-E6 cells grown in rECM culture exhibit 1) reduced levels of CBP protein expression and 2) disorganized expression of both laminin-5 $\alpha 3$ -chain and $\alpha 3$ -integrin. This observation led us to hypothesize that suppression of CBP in HMECs would alter laminin-5 $\alpha 3$ -chain and $\alpha 3$ -integrin expression and/or distribution. CBP protein expression was suppressed in early passage HMEC-E6 cells

and HMEC-LXSN controls by treatment with CBP-specific, antisense ODN (A99424V). HMECs with suppressed CBP expression exhibited disorganized plasma membrane and cytosolic distribution of laminin-5 α 3-chain and α 3-integrin. β 1-integrin expression was observed at the basal surface. In contrast, early passage HMEC-LXSN controls and HMEC-E6 cells treated with inactive CBP ODN (scrA99424V) exhibited polarized basal expression of laminin-5 α 3-chain and α 3- and β 1-integrins. These observations demonstrate that suppression of CBP protein expression in HMECs alters the distribution of both laminin-5 α 3-chain and α 3-integrin.

1h) Decreased CBP expression in rECM-resistant late passage HMEC-E6 cells correlates with decreased LAMA3A promoter activity. We tested whether the observed decrease in CBP and laminin-5 α 3-chain expression in late passage HMEC-E6 cells correlated with decreased LAMA3A promoter activity. Early and late passage HMEC-E6 and passage-matched HMEC-LXSN controls were transiently transfected with a CAT reporter coupled to the LAMA3A promoter sequence (1403 bp, GenBank Accession Number AF279435) and grown in rECM culture. rECM-sensitive early passage HMEC-E6 cells and early and late passage HMEC-LXSN controls exhibited a similar level of LAMA3A activity. In contrast, rECM-resistant, late passage HMEC-E6 cells with decreased CBP and laminin-5 α 3-chain expression exhibited a 91% decrease in LAMA3A promoter activity relative to early passage HMEC-E6 cells ($p \leq 0.01$). These experiments demonstrate in HMECs a positive correlation between 1) the level of CBP and laminin-5 α 3-chain protein expression and 2) LAMA3A promoter activity.

1i) LAMA3A promoter activity in HMECs with suppressed CBP protein expression. We next tested whether suppression of CBP protein expression resulted in decreased LAMA3A promoter activity. LAMA3A-CAT reporter activity was compared in early passage HMEC-LXSN and HMEC-E6 cells treated with either CBP-specific antisense ODNs (A33423V) or inactive ODNs (scrA33423V). A 92% and 89% decrease ($p < 0.01$) in LAMA3A promoter activity was observed, respectively, in early passage HMEC-LXSN and HMEC-E6 cells grown in rECM and treated with CBP-specific ODNs (A33423V) relative to cells treated with inactive ODNs (scrA33423V). No significant difference in LAMA3A promoter activity was observed in HMECs treated with or without inactive ODNs. These observations demonstrate that suppression of CBP expression in HMECs results in a reduction in LAMA3A promoter activity.

1j) Lack of CBP occupancy of the human laminin 5 (LAMA3A) promoter correlates with rECM-resistance. The human LAMA3A promoter contains three AP-1 sites at positions -387, -185, and -127 (Miller et al., 2001). The AP-1 site, at position -185, has been previously shown to be critical for basal activity in mammary epithelial cells. Chromatin immunoprecipitation (ChIP) was performed in rECM-resistant, CBP-"poor" late passage HMEC-E6 cells and controls to test whether the observed 1) decrease in laminin-5 α 3-chain expression and 2) loss of LAMA3A activity correlated with a lack of CBP binding to the 277 bp AP-1-"rich" site of the LAMA3A promoter (position -402 to -125). Early and late passage HMEC-LXSN control cells and rECM-sensitive, early passage HMEC-E6 cells grown in rECM demonstrated CBP binding to the AP-1-"rich" site of the LAMA3A promoter. In contrast, rECM-resistant, late passage HMEC-E6 cells, with decreased CBP and laminin-5 α 3-chain expression, failed to demonstrate CBP binding. These observations suggest that a decrease in CBP expression might promote loss of CBP occupancy of the AP-1-"rich" site of the LAMA3A promoter.

1k) Suppression of CBP expression in HMECs results in loss of CBP occupancy of the *LAMA3A* promoter. Early passage HMEC-E6 cells were treated with active CBP ODNs and tested by ChIP to determine whether suppression of CBP protein expression resulted a loss of CBP occupancy of the AP-1-“rich” region of the *LAMA3A* promoter. Early passage HMEC-E6 cells treated with CBP-specific ODNs, and grown in rECM, did not demonstrate CBP occupancy of the *LAMA3A* promoter. In contrast, early passage HMEC-E6 controls, treated with inactive ODNs, and grown in rECM demonstrated CBP-occupancy (Figure 10 b). These observations demonstrate that suppression of CBP expression in HMEC-E6 cells by antisense ODNs results in a loss of CBP occupancy of the AP-1-“rich” site of the *LAMA3A* promoter. Since the AP-1 site, at position -185, is critical for basal activity in mammary epithelial cells, these observations provide a mechanism by which loss of CBP expression might promote loss of *LAMA3A* promoter activity and laminin-5 α 3-chain expression in HMECs.

1e) Expression of CBP in apoptosis-resistant cells results in increased expression of laminin-5 and restoration of apoptosis-sensitivity in rECM culture. We used retroviral-mediated gene transfer to express CBP in late passage rECM-resistant cells with suppressed levels of CBP. Protein levels of CBP in our transduced were comparable to that observed in parental and rECM-sensitive HMEC-E6 cells. Expression of CBP in rECM-resistant cells resulted in restoration of 1) laminin-5 α 3-chain expression and 2) apoptosis sensitivity. These observations highlight a critical role for CBP in regulating rECM-apoptosis and laminin-5 expression.

SPECIFIC AIM II: Does CBP modulate interferon (IFN)-signal transduction during rECM-mediated apoptosis in HMEC-E6 cells?

2a) Microarray analysis of induced gene transcripts. To investigate the molecular mechanism of rECM-induced apoptosis, we analyzed the expression profiles of HMEC-E6 cells and passage matched HMEC-LXSN controls treated with and without rECM for 6 hrs. Analysis was performed using Hu6800 cDNA microarrays (Affymetrics). Twenty-four interferon-response genes (IRGs) were significantly upregulated in treated HMEC-E6 cells but not in treated HMEC-LXSN controls. Differential expression was confirmed by quantitative RT-PCR in triplicate, normalized to actin. The upregulated genes included IFI 9-27, interferon regulatory factor-1 (IRF-1), ISG15, ISG-54, MX-A, interferon gamma inducible protein 16, STAT-1 alpha, STAT-1 beta, IFI-6-16, and ISG12. Based on these observations, we hypothesized that IRGs 1) may participate in or 2) may be a marker for rECM- induced apoptosis of HMEC-E6 cells.

2b) Interferon-alpha, -beta, and -gamma are not induced by rECM. Assays for interferon-alpha, -beta, and -gamma were performed in HMEC-E6 cells and HMEC-LX controls treated with rECM to determine whether rECM induced interferon production in HMEC-E6 cells correlated with the induction of apoptosis. ELISA assays determined that interferon release was not observed 15 mins-24 hrs following tamoxifen treatment of HMEC-E6 cells (data not shown). These data show that rECM-induced apoptosis in HMEC-E6 cells results in induction of IRGs in the absence of interferon release.

2c) Interferon regulatory factor-1 (IRF-1) is induced by rECM. IRF-1 is a transcriptional regulator that has been shown to promote apoptosis following DNA-damage and is critical for mammary gland involution. Differential gene expression studies demonstrated that IRF-1 mRNA was induced by rECM in HMEC-E6 cells at 6 hrs. Semi-quantitative reverse transcriptase-polymerase chain reaction (RT-PCR) and western analysis was performed to determine the kinetics of IRF-1 mRNA and protein induction. We observed that IRF-1 mRNA and protein was induced by rECM in HMEC-E6 cells but not in HMEC-LXSN controls. IRF-1 mRNA induction in HMEC-E6 cells was first observed at 30 min (5-fold) and was maximally induced at 3 hrs (7-fold). IRF-1 protein induction was first observed at 30 min (1.5-fold) and was maximally induced at 3 hrs (2.3-fold). These observations demonstrate that IRF-1 mRNA and protein are induced by rECM starting at 30 min.

2d) Suppression of IRF-1 expression results in loss of IRG induction: We developed two siRNA constructs directed against IRF-1. Expression of these constructs resulted in a >80% suppression of IRF-1 expression. Treatment of apoptosis-sensitive cells with rECM resulted in a loss of rECM-growth regulation and polarity and well as loss of IRG induction.

2e) AKT activity is critical for induction of rECM-mediated apoptosis: AKT is an important regulator of cell survival and loss of AKT activity is known to promote apoptosis. We observe that rECM-induced apoptosis is associated with loss of AKT-activity and phosphorylation at Ser-473. This is an important observation since we also observe that AKT phosphorylation at Ser-473 is critical cell surface-regulated, tamoxifen-induced apoptosis in HMEC-E6 cells. Expression of a constitutively active AKT blocked the induction of apoptosis and resulted in loss of rECM-regulated growth arrest. Inhibition of $\alpha3/\beta1$ -integrin signaling also resulted in loss of AKT phosphorylation at Ser-473. These results highlight a potential role for AKT in regulating rECM-mediated apoptosis. Work is on-going to investigate whether AKT plays a role in activating CBP.

KEY RESEARCH ACCOMPLISHMENTS:

- 1) Demonstration that suppression of the CREBP binding protein (CBP) results in loss of cellular polarity and apoptosis resistance.
- 2) Evidence that CBP regulates expression of laminin-5 through binding to the laminin 5 promoter (*LAMA3A*).
- 3) Demonstration that suppression of CBP expression blocks CBP recruitment to *LAMA3A*.
- 4) Demonstration that prepared extracellular matrix (rECM) promotes induction of interferon regulated genes (IRGs), including interferon regulatory factor-1 (IRF-1) in the absence of interferon production.
- 5) Identifying that IRF-1 expression is critical for interferon regulated gene (IRG) expression and induction of apoptosis.
- 6) Demonstration that AKT is important for rECM-mediated apoptosis.

Reportable Outcomes:

- 1) Manuscripts:

- a. Dietze, E.C., Bowie, M.L., Troch, M.M., and Seewaldt, V.L. CBP Modulates Reconstituted Extracellular Matrix-Growth Regulation, -Polarity, and -Apoptosis in Human Mammary Epithelial Cells. Submitted to Journal of Cell Science.
- b. Bowie, M.L., Dietze, E.C., Delrow, E., Bean, G.R., Troch, M., Marjoram, R., Seewaldt, V.L. Interferon regulatory factor-1 is critical for tamoxifen-mediated apoptosis in human mammary epithelial cells. *Oncogene*, in press, 2004.
- c. Bean, G.R., Scott, J.V., Yee, L., Ratliff, B., Fabian, C., Kimler, B., Zalles, C., and Seewaldt, V.L. Methylation of the retinoic acid receptor beta in mammary epithelial cells obtained by RPFNA. Submitted *Cancer Epidemiology, Biomarkers, and Prevention*, submitted, 2004.
- d. Troch, M., Bowie, M.L., and Seewaldt, V.L. rECM regulates AKT activity in acutely damaged mammary epithelial cells. In preparation.
- e. Bowie, M.L., Troch, M., and Seewaldt, V.L. rECM promotes induction of IRF-1 in acutely damaged mammary epithelial cells. In preparation.

- 2) **Funding granted:** AVON/NCI Developing markers of breast cancer risk in breast fine needle aspiration. NIH/NCI CA6843-AV13.

Funding pending:

- a. AVON/NCI Contralateral risk markers in women with primary breast cancer. Priority score 1.7. Award notice pending. NIH/NCI CA6843-AV43.
- b. R01 submitted 6/04, Markers of Breast Cancer Risk and Prevention.
- c. DOD Multidisciplinary Postdoctoral Fellowship, Permila Harrell, PI; Victoria Seewaldt, Mentor.

Conclusions:

In this report we demonstrate that suppression of the CREBP binding protein (CBP) results in apoptosis-resistance and loss of epithelial polarity and that CBP is critical for laminin-5 expression. These observations are important for 1) identifying improved targets for breast cancer prevention and 2) developing novel markers to test for response to chemoprevention agents. Information gained in this report is currently being translated to benefit women at risk for breast cancer prevention in our multi-institutional cohort. We have obtained funding for this cohort and are currently using markers in developed in this proposal to identify risk in high-risk women.

References:

None.

Appendices

- 1) Dietze, E.C., Bowie, M.L., Troch, M.M., and Seewaldt, V.L. CBP regulates apoptosis in human mammary epithelial cells: a three-dimensional model of breast cancer. Submitted to *Journal of Cell Science*.
- 2) Dietze, E.C., Troch, M.M., Heffner, J.B., Bean, G.R., and Seewaldt, V.L. Tamoxifen and tamoxifen ethyl bromide induce apoptosis in acutely damaged mammary

epithelial cells through modulation of AKT activity. *Oncogene*, 23: 3851-3862, 2004.

- 3) Bowie, M.L., Troch, M., Dietze, E.C., and Seewaldt, V.L. Interferon regulatory factor-1 is critical for tamoxifen-mediated apoptosis in human mammary epithelial cells. *Oncogene*, accepted, 2004.
- 4) Bean G., Scott, V., Yee, L., Fabian, C., Kimler, B., Zalles, C., and Seewaldt, V.L. Retinoic acid receptor-beta2 promoter methylation in random periareolar fine needle aspiration. Submitted, *Cancer Epidemiology, Biomarkers, and Prevention*, 2004.

CBP loss and resistance to rECM-induced apoptosis

CBP regulates apoptosis in human mammary epithelial cells: a three-dimensional model of breast cancer progression

Eric C. Dietze¹, Michelle L. Bowie¹, Krzysztof Mrózek², Elizabeth Caldwell³, Cassandra Neal³, Robin J. Marjoram¹, Michelle M. Troch¹, Gregory R. Bean¹, Kazunari K. Yokoyama⁴, Brooke Ratliff¹, and Victoria L. Seewaldt^{1*}

¹Division of Medical Oncology, Duke University, Durham, N.C. 27710

²Division of Hematology and Oncology, Ohio State University, Columbus, OH 43210

³Fred Hutchinson Cancer Research Center, Seattle, WA 98109

⁴RIKEN, Tsukuba Institute, Ibaraki 305-0074, Japan

* Author for correspondence:

Victoria Seewaldt
Box 2628
Duke University Medical Center
Durham, NC 27710
Telephone: (919) 668-2455
Fax: (919) 668-2458
email: seewa001@mc.duke.edu

Key words: CBP, Breast cancer, Extracellular matrix, Apoptosis, Human mammary epithelial cells

Summary

Interactions between normal mammary epithelial cells (HMECs) and extracellular matrix (ECM) are important for mammary gland homeostasis; loss of ECM-sensitivity is thought to be an early event in mammary carcinogenesis. The CREBP binding protein (CBP) regulates both proliferation and apoptosis but the role of CBP in ECM-signaling is poorly characterized. We investigated the relationship between CBP expression and sensitivity to prepared ECM (rECM) induced-growth arrest and -apoptosis in a model of mammary carcinogenesis. Prior genetic studies suggested that chromosome 16p harbored a gene that was critical for rECM-sensitivity. In this study, detailed cytogenetic analysis demonstrated that rECM-resistant HMECs exhibited loss at chromosome 16p13 (CBP locus) and loss of CBP protein expression. Suppression of CBP expression in HMECs by antisense oligonucleotides resulted in rECM-resistance. Chromatin immunoprecipitation and reporter studies demonstrated that rECM-resistance correlated with 1) loss of CBP occupancy of the *LAMA3A* promoter, 2) decreased *LAMA3A* promoter activity, and 3) loss of laminin-5 α 3-chain expression. Inhibition of CBP protein expression resulted in 1) loss of CBP-occupancy of the *LAMA3A* promoter and 2) a decrease in *LAMA3A* promoter activity. These observations suggest a critical role for CBP in rECM-mediated growth regulation and apoptosis through modulation of *LAMA3A* activity and laminin-5 α 3-chain expression.

Introduction

Breast tissue is composed of mammary epithelial cells that rest on extracellular matrix (ECM). Interactions between epithelial cells and ECM regulate normal growth, polarity, and apoptosis (Folkman and Moscona, 1978; Petersen et al., 1992; Strange et al., 1992; Zutter et al., 1995; Ilic et al., 1998; Farrelly et al., 1999; Stupack and Cheresch, 2002). Loss of ECM-signaling is thought to be an early event in mammary carcinogenesis and is postulated to promote some of the phenotypic changes observed during malignant progression (Petersen et al., 1992; Howlett et al., 1995; Mercurio et al., 2001; Farrelly et al., 1999; Hood and Cheresch, 2002; Stromblad et al., 2002). Carcinogenesis is hypothesized to be a multistep process resulting from the progressive accumulation of genetic damage. While loss or mutation of specific tumor suppressor genes such as *TP53* promotes mammary carcinogenesis, not all damaged epithelial cells progress to malignancy and many are thought to be eliminated by apoptosis (Fabian et al., 1996; Ashkenazi and Dixit, 1998; Rohan et al., 1998). Mammary gland homeostasis requires a coordinated balance between proliferation and programmed cell death. ECM-signaling is thought to play an important role in regulating this balance (Petersen et al., 1992; Howlett et al., 1995; Farrelly et al., 1999; Mercurio et al., 2001; Hood and Cheresch, 2002; Stupack and Cheresch, 2002). Loss of ECM-signaling is thought to result in apoptosis-resistance and may promote mammary carcinogenesis by preventing the apoptotic elimination of damaged mammary epithelial cells.

Laminins are ECM glycoproteins that promote mammary gland homeostasis by regulating cell adhesion, migration, proliferation, differentiation, and angiogenesis (Aberdam et al., 2000). Laminins have three distinct protein subunits, designated α , β , and γ . Laminin-5 ($\alpha 3A$, $\beta 3$, and $\gamma 1$) is the most abundant ECM glycoprotein produced by mammary epithelial cells (D'Ardenne et al., 1991). Laminin-5 functions as a ligand for $\alpha 3\beta 1$ - and $\alpha 6\beta 4$ -integrins and has been implicated in adhesion, migration, and invasion. Recent reports indicate that binding of the laminin-5 $\alpha 3$ -chain globular LG3 domain to $\alpha 3\beta 1$ -integrin

CBP Loss and Resistance to ECM-induced apoptosis

mediates cell adhesion and migration (Shang et al., 2001). Deregulation of laminin-5 expression is observed during carcinogenesis. While benign ductal and lobular epithelial cells demonstrate continuous laminin-5 staining at the epithelial-stromal interface, primary breast cancers and breast cancer cells exhibit loss of laminin-5 α 3- and γ 2-chain expression (Martin et al., 1998; Henning et al., 1999). Loss of laminin-5 α 3-chain expression has also been observed in prostate cancer, while epigenetic inactivation of all three laminin-5-encoding genes have been observed in lung cancer cells (Hao et al., 2001; Sathyanarayana et al., 2003). There is also evidence that increased laminin-5 γ 2-chain expression and cleavage may be associated with tissue remodeling and tumor invasion. Matrix metalloproteinase (MMP)-dependent mammary gland involution coincides with binding of the laminin-5 γ 2-chain MMP-cleavage fragment, DIII, to the epidermal growth factor receptor (Schenk et al., 2003). Mammary glands from β 1,4-galactosyltransferase 1-null mice exhibit excess mammary gland branching associated with 1) decreased laminin-5 α 3-chain expression, 2) increased expression and cleavage of laminin-5 γ 2-chain, and 3) increased matrix metalloproteinase expression (Steffgen et al., 2002). Increased expression of laminin-5 γ 2-chain is at the invasive front of tumors associated with poor prognosis (Pyke et al., 1994; Yamamoto et al., 2001; Niki et al., 2002) and cooperative interactions between laminin-5 γ 2-chain and MMPs are associated with an aggressive phenotype in melanoma (Seftor et al., 2001). These observations suggest that deregulation of laminin-5-signaling may be important for cancer progression.

We previously developed an *in vitro* model of early mammary carcinogenesis to investigate the potential role of ECM-signaling in eliminating acutely “damaged” HMECs (Seewaldt et al., 2001a). Acute cellular damage was modeled by either 1) retroviral-mediated expression of the Human Papillomavirus Type-16 (HPV-16) E6 protein (HMEC-E6) or 2) treatment with p53-specific antisense oligonucleotides (ODNs). We observed that while HMEC controls grown in rECM underwent growth arrest on Day 7, HMEC-E6 and p53(-) HMEC-AS cells underwent apoptosis (Seewaldt et al., 2001a). While the acute expression of either HPV-16 E6 or suppression of p53 in HMECs promoted sensitivity to rECM-

CBP Loss and Resistance to ECM-induced apoptosis

mediated apoptosis, HMEC-E6 cells passaged in non-rECM culture rapidly acquired resistance to both rECM-mediated growth arrest and apoptosis associated with 1) loss of genetic material from chromosome 16 and 2) loss of polarized expression of the laminin-5 receptor, $\alpha 3 \beta 1$ -integrin (Seewaldt et al., 2001a). These observations lead us to hypothesize that 1) 16p might harbor a gene(s) whose loss and/or rearrangement may promote rECM-resistance and 2) laminin-5/ $\alpha 3 \beta 1$ -integrin-growth regulation and -polarity signals may be critical for targeting the elimination of acutely "damaged" HMECs.

In these studies, HPV-16 E6 was expressed in HMECs as a model of acute cellular damage. E6 interacts with a large number of cellular proteins critical for normal growth regulation and apoptosis (O'Connor, 2000). HPV-16 E6 binds to p53 and targets it for ubiquitin-mediated degradation and also abrogates transcription of p53 (Zimmermann et al., 1999; O'Connor, 2000; zur Hausen, 2000). E6 has been shown to interact with the CREBP-binding protein, CBP, in the C/H1 and C/H3 domains as well as with sequences near the carboxy-terminus (O'Connor, 2000; Patel et al., 1999). HPV-16 E6 protein also activates telomerase (Klingelhutz et al., 1996), binds to Bak (Thomas and Banks, 1999), physically interacts with the focal adhesion proteins, paxillin and fibulin-1, and interacts with the transcriptional regulator, interferon regulatory factor-3 (Ronco et al, 1998). Taken together, these observations provide evidence that expression of HPV-16 E6 leads to marked cellular disruption. However, the response of HMECs expressing HPV-16 E6 to growth in rECM was identical to HMECs treated with p53 antisense oligonucleotides and grown in rECM (Seewaldt et al., 2001a). Thus, the altered response to growth in rECM appears to be primarily a function of p53 expression.

Detailed cytogenetic analysis performed for this report indicated that chromosome 16p13 is the critical area whose loss and/or rearrangement promoted rECM-resistance (Seewaldt et al., 2001a). CBP is a nuclear protein located at chromosome band 16p13.3 that regulates proliferation, differentiation, and apoptosis (Giles et al., 1997; Yao et al., 1998). CBP is a key integrator of diverse signaling pathways

CBP Loss and Resistance to ECM-induced apoptosis

including those regulated by retinoids, p53, estrogen, and BRCA1 (Kawasaki et al., 1998; Robyr et al., 2000). Chromosomal loss at 16p13 has been reported to occur in a majority of benign and malignant papillary neoplasms of the breast and loss or amplification of 16p is frequently observed in premalignant breast lesions (Lininger et al., 1998; Tsude et al., 1998; Aubele et al., 2000). Taken together, these observations suggest that loss of CBP expression might promote mammary carcinogenesis.

Prior studies indicated that $\alpha 3\beta 1$ -integrin-growth mediated regulation signals and the presence of laminin in rECM might be critical for targeting the elimination of acutely damaged HMECs (Seewaldt et al., 2001a). Little is known about the regulation of laminin-5 gene transcription in normal mammary epithelial tissue or about the molecular mechanism underlying the loss of laminin-5 expression observed in early breast carcinogenesis (Miller et al., 2000). The human *LAMA3A* promoter is known to contain three binding sites of the dimeric transcription factor activating protein-1 (AP-1) (Virolle et al., 1998; Miller et al., 2001). It has been recently observed that the second AP-1 binding site present in the human *LAMA3A* promoter at position -185 base pairs is critical for baseline transcription of laminin-5 $\alpha 3$ -chain (Miller et al., 2001). CBP is known to interact with AP-1 response elements (Benkoussa et al., 2002). However, the relationship between CBP and laminin-5 expression in mammary epithelial cells has not been studied.

This report describes a novel role for CBP in mediating sensitivity to rECM-growth regulation and -apoptosis through induction of laminin-5 $\alpha 3$ -chain expression. Observations in our model system have important implications as they predict a critical role for CBP in regulating mammary homeostasis and targeting the elimination of acutely "damaged" HMECs through a laminin-5 $\alpha 3$ -signaling pathway.

Materials and Methods

Cell Culture and Media

Normal human mammary epithelial cell (HMEC) strains AG11132 and AG11134 (M. Stampfer #172R/AA7 and #48R, respectively) were purchased from the National Institute of Aging, Cell Culture Repository (Coriell Institute, National Institute of Aging). HMEC strains AG11132 and AG11134 were established from normal tissue obtained at reduction mammoplasty, have a limited life span in culture, and fail to divide after approximately 20 to 25 passages. HMECs exhibit a low level of estrogen receptor staining characteristic of normal mammary epithelial cells. HMECs were grown in Mammary Epithelial Cell Basal Medium (Clonetics, San Diego, CA) supplemented with 4 μ l/ml bovine pituitary extract (Clonetics #CC4009), 5 μ g/ml insulin (Sigma, St. Louis, MO), 10 ng/ml epidermal growth factor (UBI Lake Placid, NY), 0.5 μ g/ml hydrocortisone (Sigma), 10^{-5} M isoproterenol (Sigma), and 10 mM HEPES buffer (Sigma) [Standard Media]. Cells were cultured at 37°C in a humidified incubator with 5% CO₂/95% air. Mycoplasma testing was performed as previously reported (Seewaldt et al., 1997).

Retroviral Transduction

Expression of HPV-16 E6: The LXS_N16E6 retroviral vector containing the HPV-16 E6 coding sequence was provided by D. Galloway (Fred Hutchinson Cancer Research Center, Seattle, WA) (Demers et al., 1996). HMECs (passage 8) were plated in four T-75 tissue culture flasks (Corning, Corning, NY) in Standard Medium and grown to 50% confluency. Transducing virions from either the PA317-LXS_N16E6 or the control PA317-LXS_N (without insert) retroviral producer line were added at a multiplicity of infection at 1:1 in the presence of 4 μ g/ml Polybrene (Sigma) to log-phase cells grown in T-75 flasks (Seewaldt et al., 1995). The two remaining T-75 flasks were not infected with virus. After 48 hours, two flasks containing transduced cells and one flask with untransduced cells were passaged 1:3

CBP Loss and Resistance to ECM-induced apoptosis

(passage 9) and selected with Standard Media containing 300 μ g/ml G418 (GIBCO, Grand Island, NY) for four to seven days, until 100% of control, untransduced cells were dead. Cells were passaged 1:3 at the completion of selection (passage 10), and were maintained in the absence of selection before immediately proceeding to apoptosis experiments. The fourth flask of unselected, untransduced parental control cells was passaged in parallel with the selected, transduced experimental and vector control cells. Parental AG11132 cells were designated HMEC-P. Transduced AG11132 cells expressing the HPV-16 E6 construct were designated HMEC-E6 and vector control cells were designated HMEC-LXSN. All cells were maintained in Standard Media after transfection in the absence of selection to ensure that any observed chromosomal abnormalities or apoptosis-resistance was not due to continued exposure to selections. All experiments were performed on mass cultures.

Expression of CBP: Construction of the retroviral vector harboring the coding sequences for CBP were generated from the pcDNA3 recombinant plasmid by methods previously described (Seewaldt et al., 1995). The pcDNA3 plasmid was digested with BamHI and the released plasmid inserted in the BamHI cloning site of the dephosphorylated pLXSN plasmid. Correct orientation and sequence was verified by direct sequencing. Ten micrograms of purified pLCBPSN retroviral construct plasmid was transfected via CellfectinTM (Invitrogen) into the PE 501 murine ecotropic retrovirus packaging cell line (Seewaldt et al., 1995). The supernatant was harvested and used to infect the PA317 amphotropic packaging cell line. These cells were selected, and individual foci of resistant cells were isolated and expanded. Producer clones expressing the appropriate-sized MuLV LTR-initiated CBP were identified by RT-PCR and supernates from these producers titered on NIH3T3 thymidine kinase negative target cells. Retroviral transduction and selection was performed as described above to express CBP in late passage (passage 16) HMEC-E6 cells. Expression of the exogenous construct was confirmed by PCR and protein expression was confirmed by Western analysis as described below.

CBP Loss and Resistance to ECM-induced apoptosis
Cytogenetic Analysis of Early and Late Passage HMECs

Spectral karyotypic analyses (SKY) of HMEC-LXSN controls (passages 10 and 16) and HMEC-E6 cells (passages 10 and 18) were performed as previously described (Mrozek et al., 1993; Schrock et al., 1996; Seewaldt et al., 1997; Seewaldt et al., 2001a; Seewaldt et al., 2001b).

Western Blotting

Preparation of cellular lysates and immunoblotting were performed as previously described (Seewaldt et al., 1997; Seewaldt et al., 1999). For p53 expression, the membrane was incubated with a 1:100 dilution of mouse anti-human p53 (Oncogene Science Ab-2). For CBP expression, the blocked membrane was incubated with 1:200 dilution of the CBP C20 antibody (Santa Cruz Biotechnology). For laminin-5 expression, the membrane was incubated with a 1:100 dilution of the C-19 antibody to the laminin-5 α 3-chain (Santa Cruz). Loading control was provided by 1:200 dilution of the I-19 antibody to beta-actin (Santa Cruz). All p53, CBP, and laminin bands were normalized to actin. The resulting film images were digitized and quantitated using Kodak 1D Image Analysis Software (Eastman Kodak).

HMEC Culture in rECM

HMECs were grown in rECM as previously described (Seewaldt et al., 2001a). One hundred microliters of rECM (Growth Factor Depleted MatrigelTM, Collaborative Research, Bedford, MA) were added per well to a 48 well plate and allowed to gel at 37°C for 20 min. Transduced HMECs were trypsinized, counted, and pelleted. Approximately 1×10^4 cells were resuspended in 100 μ l rECM on ice, gently overlaid on the initial undercoating of extracellular matrix, and allowed to gel at 37°C for 20 min. Standard Media was then added and wells were inspected to ensure there was an equal distribution of cells in each well. Cells were grown for 5 to 13 days in culture.

Cell Growth and Proliferation in rECM Culture

CBP Loss and Resistance to ECM-induced apoptosis

Cell growth in rECM culture was determined using the following procedure: The size of the 20 largest growing spherical cell colonies was measured with an eye-piece equipped with a micrometer spindle. Proliferation was assessed by Ki67 staining index, whereby five micron sections were immunostained with antibody directed against Ki-67. Cells were scored visually (100-500 cells) for immunopositive nuclei. The proliferation index was calculated by dividing the number of immunopositive cells as a percentage of the total number of cells scored.

Detection of Apoptosis by In Situ TUNEL

HMECs were grown in rECM for 5 to 11 days and prepared for TUNEL staining as previously described (Seewaldt et al., 2001a). Two hundred cells were scored. The apoptotic index was determined by expressing the number of TUNEL positive cells as a percentage of the total number of cells scored.

Transmission Electron Microscopy

HMECs were grown in contact with rECM as described above. Electron microscopy was as previously described (55-57). Fifty colonies were scored for the presence of apoptosis by morphologic criteria that included 1) margination of chromatin, 2) nuclear condensation, 3) cell shrinkage, and 4) formation of apoptotic bodies (Majno and Joris, 1995).

Immunostaining

HMECs were grown in rECM as described above and embedded in O.C.T. (Miles), snap frozen, and 7 μ sections obtained. For integrin and laminin immunostaining, cells were fixed for 20 min at RT with 2% formaldehyde in 0.1 M sodium cacodylate and 0.1 M sucrose at pH 7.2, permeabilized with 0.1% Triton X-100 for 10 min at RT, and blocked with 0.5% HD-BSA in PBS for 1 hr at RT. Cells were incubated with primary antibody diluted in PBS with 0.5% HD-BSA for 1 hr at RT and washed 6 times with PBS at RT. Antibodies against integrin subunits $\alpha 3$ (P1F2, P1B5) and $\beta 1$ (P4C10) were a generous gift of William Carter and have been previously described (Carter and Wayner, 1987; Wayner et al., 1988;

CBP Loss and Resistance to ECM-induced apoptosis

Carter et al., 1990a; Carter et al., 1990b). Monoclonal antibody P5H10 directed against the $\alpha 3$ chain of laminin-5 was also a generous gift of William Carter. For immunofluorescence, cells were incubated with either FITC- or Rhodamine-conjugated goat anti-mouse antibody at a 1:200 antibody dilution (Santa Cruz) in PBS with 0.5% HD-BSA for 30 min at RT and washed as described above. Sections were mounted in 30% glycerol in PBS and visualized for immunofluorescence using a Zeiss LSM 410 fluorescence microscope (Carl Zeiss, Jena, Germany).

Suppression of CBP Expression

Nine antisense oligonucleotides (ODNs) to human CBP were generated by the PAS program (Ugai et al., 1999). The CBP antisense A3342V ODN (24-mer, nucleotide position 3342-3363) was initially chosen on the basis of selective inhibition of CBP protein expression in MCF-7 cells (data not shown); suppression was confirmed in HMECs. Inactive CBP ODN scrA3342V (22 mer, nucleotide position 3342-3363) was chosen to be the scrambled sequence of the antisense ODN 1) to ensure identical nucleotide content and minimize differences potentially attributable to nucleic acid content and 2) selected based on lack of suppression of CBP in MCF-7 and HMECs. See Table 1 for a list of ODNs. The first and last three nucleotides of all ODNs were phosphorothioate modified to increase their stability *in vitro*. Early passage HMEC-LXSN controls and HMEC-E6 cells were plated in T-75 flasks in Standard Media. After allowing 24 hr for attachment, cell cultures were treated for 72 hr with either active or inactive ODNs (0.001 to 0.1 μ M final concentration). Every 24 hr the culture media was replaced by new Standard Media containing fresh ODNs. Western analysis was performed to confirm 1) suppression of CBP expression as described above and 2) lack of suppression of the related co-activator p300. The resulting film images were digitized and quantitated using Kodak 1D Image Analysis Software.

CBP-Suppression in rECM Culture

CBP Loss and Resistance to ECM-induced apoptosis

Early passage HMEC-LXSN controls and HMEC-E6 cells were trypsinized and approximately 1×10^4 cells were resuspended in 100 μ l rECM containing either active or inactive CBP-specific ODNs (0.01 to 0.1 μ M final concentration) on ice. rECM cultures were prepared as above and overlaid with Standard Media containing active or inactive CBP-specific ODNs (0.01 to 0.1 μ M final concentration). Overlay media were changed every 24 hours to ensure a constant supply of ODNs. The diameter of the growing colonies was determined and cells were prepared for electron microscopy and immunostaining as described above.

Large-Scale rECM Culture

Large-scale rECM culture was utilized to prepare total RNA or protein lysate for analysis utilizing techniques previously developed by the laboratory of Minna Bissell (Roskelley et al., 1994). Early and late passage HMEC-E6 cells and HMEC-LXSN controls were plated in T-75 flasks, previously treated with poly(2-hydroxyethyl methacrylate) (Poly-HEME). Cells were grown in Standard Media with 5% (vivo) rECM.

Differential Gene Expression Studies

Cells were grown in rECM utilizing large-scale rECM culture techniques as described above. Isolation of total RNA was as previously described (Seewaldt et al., 1995). RNA integrity was confirmed by electrophoresis, and samples were stored at -80°C until used. All RNA combinations used for array analysis were obtained from cells that were matched for passage number, cultured under the identical growth conditions, and harvested at identical confluency. cDNA synthesis and probe generation for cDNA array hybridization were obtained by following the standardized protocols provided by AffymetrixTM (Affymetrix, Santa Clara, California).

CBP Loss and Resistance to ECM-induced apoptosis

Expression data for approximately 5,600 full-length human genes was collected using Affymetrix GeneChip HuGeneFLTM arrays, following the standardized protocols provided by the manufacturer. Data were collected in triplicate using independent biological replicates (Baldi and Long, 2001). Array images were processed using Affymetrix MAS 5.0 software, filtered for probe saturation, employed a global array scaling target intensity of 1000, and collected the signal intensity value for each gene. For each set of replicate measurements, gene signal intensity values were averaged and array-level normalization was performed relative to the β -actin averaged value. Normalized values were log-transformed and an additional gene-level normalization was performed using the LXS-ECM data set. Data was imported into *Cluster/TreeView* software (<http://rana.lbl.gov/EisenSoftware.htm>), where heat maps were generated.

Semi-Quantitative RT-PCR

To confirm microarray data, relative transcript levels were analyzed by semiquantitative reverse transcriptase-polymerase chain reaction (RT-PCR). Five micrograms of total RNA was used in first-strand cDNA synthesis with Superscript II reverse transcriptase (Invitrogen). PCR reaction conditions were optimized for integrin- α 3 (*ITGA3*), integrin- β 1 (*ITGB1*), laminin- α 3 (*LAMA3*), laminin- β 3 (*LAMB3*), and laminin- γ 2 (*LAMC2*). Primer sequences were obtained from published sources as follows: *ITGA3* (Hashida et al., 2002), *ITGB1* (Hsu et al., 2001), *LAMA3* (forward primer (Virolle et al., 2002), *LAMB3* and *LAMC2* (Manda et al., 2000). A 50 μ l reaction was set up containing 100 nM forward primer, 100 nM reverse primer, 250 μ M of each dNTP, 10 mM Tris-HCl, 1.5 mM MgCl₂, 50 mM KCl, pH 8.3, 2.5 units Taq polymerase, and 2.0 μ l cDNA. Reaction conditions for beta-actin were 300 nM forward primer, 300 nM reverse primer, 250 μ M of each dNTP, 10 mM Tris-HCl, 1.5 mM MgCl₂, 50 mM KCl, pH 8.3, 2.5 units Taq polymerase, and 2.0 μ l cDNA in a total volume of 50 μ l. Products were amplified with Applied Biosciences GeneAmp PCR system 2400 (Applied Biosciences).

CBP Loss and Resistance to ECM-induced apoptosis

Preliminary reactions were performed to determine the PCR cycle number of linear amplification for each primer set. The primer sets, cycling conditions, and cycle numbers used are indicated in Table 2. Ten microliters of PCR product were analyzed by electrophoresis in 1.2-1.5% agarose gels containing ethidium bromide, visualized under UV light, and quantitated. All samples were performed in triplicate and normalized to beta-actin as the control.

LAMA3A Reporter Studies

A 1403 bp region of the laminin-5 $\alpha 3$ (*LAMA3*) promoter corresponding to GenBank Accession Number AF279435 was amplified with PCR primers, sense 5'-AAG CTT AAG TTT TCC CAT CCG CAA C-3' and antisense 5'-TCT AGA GCT GAC CGC CTC ACT GC-3' (45). The PCR product was cloned into pCRII (Invitrogen), digested out with HindIII and BamHI, and cloned into the reporter plasmid pBLCAT5 (American Type Culture Collection, Manassas, VA). Cells were transfected with the resultant pBLLAMA3aCAT5 reporter plasmid using previously published transfection conditions and controls (Seewaldt et al., 1997). Transfection control was provided by the pCMV-GH plasmid (Seewaldt et al., 1997). Transfected cells were plated in Standard Media in T-25 flasks pre-treated with Poly-HEME, treated with 5% (vivo) rECM for 24 hr, and harvested for CAT activity assays as previously described (Seewaldt et al., 1997). CAT reporter activity was normalized to GH concentration (Nichols Institute, San Juan Capistrano, CA) and total protein as previously described (Seewaldt et al., 1997).

LAMA3A Chromatin Immunoprecipitation

Occupancy of the AP-1-“rich” region of *LAMA3A* promoter from positions -387 to -127 was tested by chromatin immunoprecipitation (ChIP). ChIP was performed by published methods with some modifications (Yahata et al., 2001). Early and late passage HMEC-E6 cells and HMEC-LXSN controls were plated in T-25 flasks treated with Poly-HEME and grown in Standard Media with 5% (vivo)

CBP Loss and Resistance to ECM-induced apoptosis

rECM. Preliminary experiments were run to determine optimal sonication and formaldehyde cross-linking time. Once optimized, cells were harvested, pelleted, and treated with 1% formaldehyde for 15-20 minutes to cross-link cellular proteins. The formaldehyde was quenched by adding 1.0 ml of 250 mM glycine followed by a 5 min RT incubation. Cells were then rinsed twice in ice cold PBS containing Protease Inhibitor Cocktail [4 µg/ml epibestatin hydrochloride, 2 µg/ml calpain inhibitor II, 2 µg/ml pepstatin A, 4 µg/ml mastoparan, 4 µg/ml leupeptin hydrochloride, 4 µg/ml aprotinin, 1 mM TPCK, 1 mM phenylmethylsulfonyl fluoride, and 100 µM TLCK], pelleted, and resuspended in Lysis Buffer [1% SDS, 10 mM EDTA, 50 mM Tris-HCl at pH 8.1, and 1x Protease Inhibitor Cocktail. Samples were then sonicated 3 x 15 seconds each with a 1 min incubation on ice in between pulses on a Branson sonifier model 250 at 50% duty and maximum mini probe power. Supernatants were diluted (1:10) in Dilution Buffer [1% Triton X-100, 2 mM EDTA, 150 mM NaCl, 20 mM Tris-HCl at pH 8.1, 1x Protease Inhibitor Cocktail], and precleared with 2 µg of sheared salmon sperm DNA, 20 µl normal human serum, and 45 µl of protein A-sepharose [50% slurry in 10 mM Tris-HCl at pH 8.1, 1 mM EDTA]. Human anti-CBP antibody (A22, Santa Cruz) was added to the precleared lysate, and placed on a shaker at 4°C, followed by the addition of 45 µl of protein A-sepharose and 2.0 µg sheared salmon sperm DNA, and then incubated an additional 1 hour on a shaker at 4°C. Sepharose beads were then collected and washed sequentially for 10 min each in TSE I (0.1% SDS, 1% Triton X-100, 2 mM EDTA, 20 mM Tris-HCl at pH 8.1, 150 mM NaCl), TSE II (0.1% SDS, 1% Triton X-100, 2 mM EDTA, 20 mM Tris-HCl at pH 8.1, 500 mM NaCl), and buffer III (0.25 M LiCl, 1% NP-40, 1% deoxycholate, 1 mM EDTA, 10 mM Tris-HCl at pH 8.1). Beads were washed once with TE buffer and DNA eluted with 100 µl of 1% SDS-0.1 M NaHCO₃. The eluate was heated at 65°C overnight to reverse the formaldehyde cross-linking. DNA fragments were recovered by phenol/chloroform extraction followed by ethanol precipitation and then amplified by using PCR primers, sense 5'-AAG CTT AAG TTT TCC CAT CCG CAA C-3' and antisense 5'-TCT AGA GCT GAC CGC CTC ACT GC-3'. Thirty microliters of PCR product were

CBP Loss and Resistance to ECM-induced apoptosis

analyzed by electrophoresis in 1.5% agarose gels containing ethidium bromide and visualized under UV light. All samples were tested in triplicate.

Results

Late passage HMEC-E6 cells acquire resistance to rECM-induced apoptosis associated with rearrangement of the CBP locus at chromosome 16p13.

Previous cytogenetic analysis suggested that chromosome 16p harbored a gene(s) whose loss and/or rearrangement might play a role in resistance to rECM-mediated growth control and apoptosis (Seewaldt et al., 2001a). In this study, detailed SKY-based cytogenetic analysis was performed on late passage HMEC-E6 cells to identify gene rearrangements that might pinpoint the chromosomal location of potential gene(s) whose loss might promote rECM-resistance. Chromosomal rearrangements and deletions involving 16p were surveyed in 35 unique late passage HMEC-E6 cells (Fig. 1A). A majority of chromosomal changes involving 16p were whole chromosome or whole chromosome arm deletions, however, 1) one rECM-resistant cell with a 16p deletion retained material proximal to 16p12, while 2) a second rECM-resistant cell exhibited an unbalanced translocation $\text{der}(16)\text{t}(13;16)(\text{q1?2};\text{p13})$ that affected band 16p13 (Fig. 1B). These observations indicated that the gene of importance was located in the distal region of 16p, at 16p13. Chromosomal band 16p13 is the locus of the CBP gene (Giles et al., 1997; Yao et al., 1998). Since CBP is known to play a role in growth regulation and apoptotic signaling, we hypothesized that loss of CBP protein expression might promote rECM-resistance in HMEC-E6 cells.

Resistance to rECM-mediated growth regulation and apoptosis correlates with a decrease in CBP protein expression.

CBP Loss and Resistance to ECM-induced apoptosis

Expression of the exogenous HPV-16 E6 construct and suppression of p53 protein expression was tested by Northern and western analysis (Fig. 2A, B). Western analysis tested whether rECM-resistant late passage HMEC-E6 cells exhibited decreased expression of CBP. CBP protein expression was markedly decreased in late passage, rECM-resistant HMEC-E6 cells relative to early passage, rECM-sensitive HMEC-E6 cells and HMEC-LXSN controls. Late passage HMEC-E6 cells exhibited a 95% ($p < 0.0001$) and 92% ($p < 0.0001$) respective decrease in CBP protein expression relative to early passage HMEC-LXSN controls and early passage HMEC-E6 cells (Fig. 2C). In contrast, there was no significant decrease in CBP protein expression in late passage HMEC-LXSN controls relative to early passage cells (Fig. 2C). These observations in late passage HMEC-E6 cells 1) demonstrate that rECM-resistance correlates with decreased CBP protein expression and 2) are consistent with cytogenetic analysis demonstrating loss or rearrangement of the CBP locus at 16p13.

Antisense ODNs suppress CBP in early passage HMECs.

Antisense ODNs were utilized to suppress CBP protein expression in HMECs to test whether the level of CBP protein expression might be important for rECM-sensitivity. Relative levels of CBP protein expression were tested by Western analysis. Early passage HMEC-LXSN control and early passage HMEC-E6 cells treated with the active, CBP-specific ODN, A3342V, exhibited a 65% ($p < 0.0001$) and 81% ($p < 0.0001$) respective decrease in CBP protein expression relative to untreated controls (Fig. 2D). Cells treated with the inactive CBP ODN, scrA3342V, did not exhibit a statistically significant decrease in CBP protein expression (Fig. 2D). A second HMEC strain, AG11134, was tested to ensure that these observations were not strain-dependent (data not shown).

Suppression of CBP enhances proliferation in rECM.

Treatment of early passage HMEC-LXSN controls and HMEC-E6 cells with CBP-specific ODNs resulted in enhanced proliferation in rECM-culture as measured by 1) sphere diameter and 2) Ki-67

CBP Loss and Resistance to ECM-induced apoptosis

staining. Both early passage HMEC-LXSN controls and HMEC-E6 cells treated with active CBP-specific ODNs (A3324V) demonstrated a continued increase in sphere diameter from Day 7-11 in rECM culture (Fig. 3A, B) and data not shown). In contrast, early passage HMEC-LXSN controls and HMEC-E6 cells treated with inactive ODNs (scrA3342V) did not exhibit any increase in sphere diameter after Day 7 (Fig. 3A, B). Treatment of early passage HMEC-LXSN and HMEC-E6 cells with CBP-specific ODNs (A3342V) resulted in continued Ki-67 staining at 9 and 11 days in rECM culture (Fig. 3C, D). In contrast, Ki-67 staining at 9 and 11 days was markedly reduced in HMEC-LXSN and HMEC-E6 cells treated with inactive ODNs (scrA3342V) and untreated cells (Fig. 3C, D) and data not shown). These observations show that suppression of CBP protein expression in early passage HMEC-E6 cells and HMEC-LXSN controls results in enhanced proliferation in rECM culture.

Suppression of CBP inhibits apoptosis in rECM culture.

Early passage HMEC-E6 cells were treated with CBP-specific antisense ODNs to test whether suppression of CBP protein expression blocked apoptosis in rECM culture. Early passage HMEC-E6 cells treated with CBP-specific antisense ODNs (A3342V) formed large irregular clusters in rECM and did not undergo apoptosis on Days 7-11 as assessed by electron microscopy and TUNEL-staining (Fig. 4B, D). In contrast, early passage HMEC-E6 cells treated with inactive CBP ODNs underwent apoptosis on Day 7 as assessed by either morphologic criteria or TUNEL-staining (Fig. 4C, D). Similar to early passage HMEC-E6 cells, early passage HMEC-LXSN cells treated with CBP-specific, antisense ODNs (A3342V) formed large irregular clusters in rECM and did not undergo apoptosis (Fig. 4A). Early passage HMEC-LXSN controls treated with inactive ODN (scrA3342V) formed a morphologically organized, ascinus-like structure and did not undergo apoptosis, consistent with what has been previously observed for early passage HMEC-LXSN untreated controls (Fig. 4E and data not shown) (Seewaldt et al., 2001a). These observations demonstrate that suppression of CBP protein expression in HMEC-E6 cells by antisense ODNs blocks apoptosis in rECM culture.

CBP Loss and Resistance to ECM-induced apoptosis

A second HMEC strain, AG11134, was tested to ensure that these observations were not HMEC strain-specific. Similar to observations made in HMEC strain AG11132 above, 1) early passage AG11134-E6 cells treated with inactive CBP ODN (scrA3342V) were sensitive to rECM-growth regulation and underwent apoptosis at Day 7, 2) early passage AG11134-LXSN controls treated with antisense-CBP ODN (A99424V) were resistant to rECM growth arrest and did not undergo apoptosis on Days 7-11, and 3) early passage AG11134-LXSN controls treated with CBP-specific antisense ODNs were resistant to rECM-mediated growth regulation and did not undergo apoptosis (data not shown).

Expression of CBP in rECM-resistant, late passage HMEC-E6 cells promotes apoptosis.

Retroviral-mediated gene expression was utilized to express CBP in rECM-resistant late passage HMEC-E6 cells. RT-PCR and Western analysis confirmed expression of exogenous expression of CBP (Fig. 5A and data not shown). As previously observed, late passage HMEC-E6 cells exhibited an 89% ($p < 0.0001$) decrease in CBP protein levels relative to early passage HMEC-E6 cells. Retroviral-mediated exogenous expression of CBP in late passage HMEC-E6 cell resulted in CBP protein levels that were similar (114%) to that of early passage HMEC-E6 cells. Since CBP protein levels are thought to be tightly regulated, it is important that the level of CBP protein expression in transduced late passage HMEC-E6 cells was not significantly greater than baseline CBP levels in early passage HMEC-E6 cells, HMEC-LXSN vector controls, and parental HMECs (Fig. 5A and data not shown). Exogenous expression of CBP in late passage HMEC-E6 cells resulted in reduced proliferation on Days 5-11 relative to late passage HMEC-E6 cells transduced with the empty LXSN vector alone. Proliferation in rECM-culture was measured by 1) physical growth parameters and 2) Ki-67 staining. Late passage HMEC-E6 cells expressing exogenous CBP did not exhibit an increase in sphere diameter after Day 7 and exhibited a decrease in Ki-67 staining (Fig. 5B, C). In contrast, late passage HMEC-E6 cells transduced with the empty LXSN retroviral vector alone and in rECM culture demonstrated a continued increase in sphere diameter on Days 7-9 and no decrease in Ki-67 staining on Days 7-11 (Fig. 5B, C). Late passage HMEC-E6 cells 1) expressing exogenous CBP and 2) LXSN controls were tested for the

CBP Loss and Resistance to ECM-induced apoptosis

presence of apoptosis by morphologic criteria and by TUNEL staining. Late passage HMEC-E6 cells transduced with CBP underwent apoptosis on Day 7 as assessed by either morphologic criteria or TUNEL-staining (Fig. 5D, E). In contrast, HMEC-E6 cells expressing the empty LXSXN retroviral vector formed large irregular clusters in rECM and did not undergo apoptosis (Fig. 5D, E). These observations demonstrate that expression of CBP protein expression in rECM-resistant late passage HMEC-E6 cells promotes sensitivity to rECM-mediated growth arrest and apoptosis.

Laminin-5 expression is decreased in rECM resistant, late passage HMEC-E6 cells.

We previously observed that sensitivity to rECM-apoptosis in early passage HMEC-E6 cells required polarized expression of $\alpha 3/\beta 1$ -integrin (Seewaldt et al., 2001a). Differential gene expression studies, semi-quantitative RT-PCR, and Western analysis were performed to test whether the loss of sensitivity to rECM-mediated growth regulation, polarity, and apoptosis observed in late passage HMEC-E6 cells correlated with altered expression of laminin-5 and/or $\alpha 3/\beta 1$ -integrin mRNA. Differential gene expression studies demonstrated decreased expression of all three laminin-5 chains ($\alpha 3$, $\beta 3$, and $\gamma 2$) in apoptosis-resistant, late passage HMEC-E6 cells relative to early passage HMEC-LXSXN controls and early passage HMEC-E6 cells grown in rECM (Fig. 6A). Semi-quantitative RT-PCR confirmed a 98% decrease in laminin-5 $\alpha 3$ -chain ($p \leq 0.001$), a 58% decrease in laminin-5 $\beta 3$ -chain ($p \leq 0.01$), and a 45% decrease in laminin-5 $\gamma 2$ -chain ($p \leq 0.001$) mRNA expression relative to early passage HMEC-LXSXN controls (Fig. 6B, C). Late passage HMEC-E6 cells also exhibited an 87% decrease in laminin-5 $\alpha 3$ -chain ($p \leq 0.001$), a 45% decrease in laminin-5 $\beta 3$ -chain ($p \leq 0.01$), and a 36% decrease in laminin-5 $\gamma 2$ -chain ($p \leq 0.001$) mRNA expression relative to early passage HMEC-E6 controls (Fig. 6B, C). There was no significant change in the level of $\alpha 3/\beta 1$ -integrin mRNA expression (Fig. 6A-C).

Laminin-5 $\alpha 3$ -chain protein has been shown previously to exhibit both a processed and unprocessed form (Aumailley et al., 2003). Western analysis demonstrated that late passage HMEC-E6 cells exhibited a 72% ($p < 0.0001$) and 59% ($p < 0.0001$) respective decrease in unprocessed and processed laminin-5 $\alpha 3$ -chain protein relative to early passage HMEC-LXSXN cells (Fig. 6D, E). Late passage HMEC-E6 cells exhibited a 74% ($p < 0.0001$) decrease in processed laminin-5 $\alpha 3$ -chain protein expression relative to

CBP Loss and Resistance to ECM-induced apoptosis

early passage HMEC-E6 cells but only a small 10% and non-statistically significant ($p=0.064$) decrease in unprocessed laminin-5 $\alpha 3$ -chain protein expression. These observations demonstrate that the presence of rECM-resistance in late passage HMEC-E6 cells correlates with a loss of processed laminin-5 $\alpha 3$ -chain protein expression.

Lack of polarized expression of laminin- $\alpha 3$ and integrin- $\alpha 3$ proteins is observed in late passage HMEC-E6 cells grown in rECM.

Early and late passage HMEC-LXSN controls and HMEC-E6 cells were grown in rECM and tested for 1) laminin-5 $\alpha 3$ -chain and 2) $\alpha 3$ - and $\beta 1$ -integrin expression and distribution by immunohistochemistry (clones P5H10, P1F2, and P4C10, respectively). Early and late passage HMEC-LXSN controls and early passage HMEC-E6 cells exhibited polarized basal expression of laminin-5 $\alpha 3$ -chain and $\alpha 3$ - and $\beta 1$ -integrins (Fig. 7A-F and data not shown). In contrast, late passage, CBP-“poor” HMEC-E6 cells grown in rECM demonstrated disorganized plasma membrane and cytosolic expression of $\alpha 3$ -integrin (Fig. 7G). As predicted by differential gene expression studies and Western analysis, there was also a qualitative decrease in laminin-5 $\alpha 3$ -chain expression in late passage HMEC-E6 cells relative to controls (Fig. 7H). Late passage HMEC-E6 cells grown in rECM exhibited polarized basal $\beta 1$ -integrin expression but had increased cytosolic expression relative to early passage cells (data not shown). A second HMEC strain, AG1134 was tested to ensure that these observations were not strain specific (data not shown). These observations demonstrate a loss of polarized expression of laminin-5 $\alpha 3$ -chain and $\alpha 3$ -integrin in rECM-resistant late passage HMEC-E6 cells.

Suppression of CBP expression in HMECs alters both laminin- $\alpha 3$ and $\alpha 3$ -integrin protein distribution in rECM culture.

We observed that late passage HMEC-E6 cells grown in rECM culture exhibit 1) reduced levels of CBP protein expression and 2) disorganized expression of both laminin-5 $\alpha 3$ -chain and $\alpha 3$ -integrin. This observation led us to hypothesize that suppression of CBP in HMECs would alter laminin-5 $\alpha 3$ -chain and $\alpha 3$ -integrin expression and/or distribution. CBP protein expression was suppressed in early passage HMEC-E6 cells and HMEC-LXSN controls by treatment with CBP-specific, antisense ODN

CBP Loss and Resistance to ECM-induced apoptosis

(A99424V). HMECs with suppressed CBP expression exhibited disorganized plasma membrane and cytosolic distribution of $\alpha 3$ -integrin (Fig. 8A, B) and qualitatively reduced levels of laminin-5 $\alpha 3$ -chain expression (Fig. 8E, F). $\beta 1$ -integrin expression was observed at the basal surface (data not shown). In contrast, early passage HMEC-LXSN controls and HMEC-E6 cells treated with inactive CBP ODN (scrA99424V) exhibited polarized basal expression of laminin-5 $\alpha 3$ -chain and $\alpha 3$ - and $\beta 1$ -integrins (Fig. 8C, D, G, H and data not shown). These observations demonstrate that suppression of CBP protein expression in HMECs alters the distribution of both laminin-5 $\alpha 3$ -chain and $\alpha 3$ -integrin.

Decreased CBP expression in rECM-resistant late passage HMEC-E6 cells correlates with decreased LAMA3A promoter activity.

We tested whether the observed decrease in CBP and laminin-5 $\alpha 3$ -chain expression in late passage HMEC-E6 cells correlated with decreased *LAMA3A* promoter activity. Early and late passage HMEC-E6 and passage-matched HMEC-LXSN controls were transiently transfected with a CAT reporter coupled to the *LAMA3A* promoter sequence (1403 bp, GenBank Accession Number AF279435) and grown in rECM culture. rECM-sensitive, early passage HMEC-E6 cells and early and late passage HMEC-LXSN controls exhibited a similar level of *LAMA3A* activity (Fig. 9A). In contrast, rECM-resistant, late passage HMEC-E6 cells with decreased CBP and laminin-5 $\alpha 3$ -chain expression exhibited a 91% decrease in *LAMA3A* promoter activity relative to early passage HMEC-E6 cells ($p \leq 0.01$) (Fig. 9A). These experiments demonstrate in HMECs a positive correlation between 1) the level of CBP and laminin-5 $\alpha 3$ -chain protein expression and 2) *LAMA3A* promoter activity.

LAMA3A promoter activity is decreased in HMECs with suppressed CBP protein expression.

We next tested whether suppression of CBP protein expression resulted in decreased *LAMA3A* promoter activity. *LAMA3A*-CAT reporter activity was compared in early passage HMEC-LXSN and HMEC-E6 cells treated with either CBP-specific antisense ODNs (A3342V) or inactive ODNs (scrA3342V). A 92% ($p < 0.001$) and 89% decrease ($p < 0.001$) in *LAMA3A* promoter activity was observed, respectively, in early passage HMEC-LXSN and HMEC-E6 cells grown in rECM and treated with CBP-specific ODNs (A3342V) relative to cells treated with scrambled ODNs (scrA3342V) (Fig. 9B). No significant

CBP Loss and Resistance to ECM-induced apoptosis

difference in *LAMA3A* promoter activity was observed in HMECs treated with or without scrambled ODNs. A second HMEC strain, AG1134, was tested to ensure that these observations were not strain-specific (data not shown). These observations demonstrate that suppression of CBP expression in HMECs results in a reduction in *LAMA3A* promoter activity.

Lack of CBP occupancy of the LAMA3A promoter correlates with rECM-resistance.

The human *LAMA3A* promoter contains three AP-1 sites at positions -387, -185, and -127 (Miller et al., 2001). The AP-1 site, at position -185, has been previously shown to be critical for basal activity in mammary epithelial cells (Miller et al., 2001). Chromatin immunoprecipitation (ChIP) was performed in rECM-resistant, CBP-“poor” late passage HMEC-E6 cells and controls to test whether the observed 1) decrease in laminin-5 α 3-chain expression and 2) loss of *LAMA3A* activity correlated with a lack of CBP binding to the 277 bp AP-1-“rich” site of the *LAMA3A* promoter (position -402 to -125) (Miller et al., 2001). Early and late passage HMEC-LXSN control cells and rECM-sensitive, early passage HMEC-E6 cells grown in rECM demonstrated CBP binding to the AP-1-“rich” site of the *LAMA3A* promoter. In contrast, rECM-resistant, late passage HMEC-E6 cells, with decreased CBP and laminin-5 α 3-chain expression, demonstrated markedly decreased CBP binding (Fig. 10A). These observations suggest that a decrease in CBP expression might promote loss of CBP occupancy of the AP-1-“rich” site of the *LAMA3A* promoter.

Suppression of CBP expression in HMECs results in loss of CBP occupancy at the AP-1-“rich” region of the LAMA3A promoter.

Early passage HMEC-E6 cells were treated with active CBP ODNs and tested by ChIP to determine whether suppression of CBP protein expression resulted a loss of CBP occupancy of the AP-1-“rich” region of the *LAMA3A* promoter. Early passage HMEC-E6 cells treated with CBP-specific ODNs, and grown in rECM, demonstrated a loss of CBP occupancy of the *LAMA3A* promoter (Fig. 10B). This decreased *LAMA3A* promoter occupancy corresponded with a marked decrease in laminin-5 α 3-chain mRNA expression (Fig. 10C). In contrast, early passage HMEC-E6 controls, treated with inactive ODNs and grown in rECM, demonstrated CBP-occupancy of *LAMA3A* and normal levels of laminin-5

CBP Loss and Resistance to ECM-induced apoptosis

α 3-chain mRNA expression (Fig. 10B, C). These observations demonstrate that suppression of CBP expression in HMEC-E6 cells by antisense ODNs results in a loss of CBP occupancy of the AP-1-“rich” site of the *LAMA3A* promoter. Since the AP-1 site, at position -185, is critical for basal activity in mammary epithelial cells (Miller et al., 2001), these observations provide a potential mechanism by which loss of CBP expression might promote loss of *LAMA3A* promoter activity and laminin-5 α 3-chain expression in HMECs.

Expression of CBP in rECM-resistant, late passage HMEC-E6 cells restores laminin- α 3 expression.

Retroviral-mediated gene expression was utilized to express CBP in rECM-resistant late passage HMEC-E6 cells as previously shown (Fig. 5). Late passage HMEC-E6 cells exhibited an 89% ($p < 0.0001$) decrease in CBP protein levels relative to early passage HMEC-E6 cells and retroviral-mediated exogenous expression of CBP in late passage HMEC-E6 cell resulted in CBP protein levels that were similar (114%) to that of early passage HMEC-E6 cells (Fig. 5A). Laminin α -3 exhibited a 74% decrease ($p < 0.01$) in protein expression when late passage HMEC-E6 cells were compared to early passage HMEC-E6 cells (Fig. 5A). Retroviral-mediated exogenous expression of CBP in late passage HMEC-E6 cells was associated with a 142% increase ($p < 0.01$) in laminin α -3 expression as compared to early passage HMEC-E6 cells (Fig. 5A). These observations demonstrate that restoration of CBP protein expression in rECM-resistant late passage HMEC-E6 cells was also associated with restoration of laminin α -3 expression.

Discussion

Interactions between mammary epithelial cells and ECM are important for mammary gland homeostasis; loss of ECM-sensitivity is thought to be an early event in mammary carcinogenesis. CBP is a tightly regulated transcription factor that regulates proliferation, differentiation, and apoptosis. In this report,

CBP Loss and Resistance to ECM-induced apoptosis

we show that suppression of CBP expression promotes loss of sensitivity to rECM-growth regulation and -apoptosis through loss of laminin-5 α 3-chain expression.

Current models suggest that CBP is present in limiting amounts and transcriptional regulation may be, in part, achieved through competition for this cofactor, as only partial suppression of CBP is required for a phenotype in the CBP heterozygote “knock out” mouse (Kawasaki et al., 1998; Yao et al., 1998; Shang et al., 2000). In our model system, CBP was suppressed by either gene loss/rearrangement following stable expression of HPV16 E6 protein or employing AS-ODNs directed against CBP. E6 protein can bind to the C/H3 domain of CBP and suppress CBP function (Goodman and Smolik, 2000). In our model system, AS-ODN directed to CBP resulted in both decreased growth and suppression of apoptosis of E6 expressing cells grown in rECM (Figs. 3 and 4). As demonstrated by ChIP in this report, CBP is recruited to the *LAMA3A* promoter in HMEC-E6 cells (Fig. 10). In other work, we have also shown that HMEC-E6 cells retain their sensitivity to retinoic acid (Seewaldt et al., 1999a), which requires CBP, and that CBP is recruited to the *IRF-1* promoter is required in tamoxifen stimulated apoptosis of HMEC-E6 cells (unpublished data). Furthermore, we have demonstrated that sensitivity to rECM induced apoptosis of HMEC-E6 cells is a function of p53 suppression (Dietze et al., 2001; Seewaldt et al., 2001a). Clearly, CBP function is not blocked by E6 in HMEC-E6 cells.

In this report, we show that only partial suppression of CBP protein expression in HMECs is required for rECM- and apoptosis-resistance. Consistent with observations in our *in vitro* system, partial suppression of CBP protein levels in virgin CBP(+/-) heterozygote mice results in a 90% incidence of severe mammary gland hyperplasia and hyperlactation (Yao, personal communication). Taken together, these observations provide evidence that partial suppression of CBP protein expression in mammary epithelial cells promotes resistance to rECM-growth regulation and -apoptosis.

CBP Loss and Resistance to ECM-induced apoptosis

We also demonstrate a novel mechanism by which loss of CBP occupancy of the AP-1-“rich” region of the *LAMA3A* promoter may promote early mammary carcinogenesis by inhibiting expression of laminin-5 α 3-chain expression. AP-1 response elements are *cis*-acting DNA sequences known to regulate a wide range of cellular processes, including proliferation, apoptosis, survival, and differentiation (Shaulian and Karin, 2002). CBP is known to interact with the AP-1 response element (Horvai et al., 1997; Benkoussa et al., 2002) and participate in activation of AP-1 (Arias et al. 1994; Kwok et al., 1994; Kamei et al., 1996). While much is known about CBP/AP-1 interactions, the role of CBP and AP-1 in early mammary carcinogenesis is poorly defined. It has been recently shown that retinoic acid receptors inhibit AP-1 activity through regulating extracellular signal-regulated kinase and CBP recruitment to an AP-1-responsive promoter (Benkoussa et al., 2002). Here we report a novel mechanism by which CBP occupancy of the AP-1-“rich” region of the *LAMA3A* promoter is important for regulating laminin-5 α 3-chain expression. Both the mouse and human *LAMA3A* promoter contain an AP-1-“rich” region (Virolle et al., 1998; Millet et al., 2001). The second AP-1 binding site present in both the mouse and human *LAMA3A* promoter is critical for baseline transcription of laminin-5 α 3-chain (Virolle et al., 1998; Millet et al., 2001). We show that suppression of CBP results in loss of *LAMA3A* promoter activity and laminin-5 α 3-chain expression and 2) blocks the apoptotic elimination of acutely “damaged” HMEC-E6 cells. The decreased production of laminin 5- α 3 correlated with loss of CBP occupancy of the AP-1-“rich” region of the *LAMA3A* promoter. Taken together, these observations suggest that 1) CBP occupancy of the *LAMA3A* promoter promotes laminin-5 α 3-chain expression and 2) loss of CBP occupancy inhibits laminin-5 α 3-chain expression and may promote survival of acutely “damaged” HMECs.

In contrast to our observation that suppression of CBP inhibits laminin-5 α 3-chain expression in HMECs, it has been previously observed that overexpression of the related co-activator p300 inhibits laminin-5 production in MCF-10A cells (Miller et al., 2000). One potential explanation for these

CBP Loss and Resistance to ECM-induced apoptosis

seemingly divergent results may lie in differences in cell type. MCF-10A is an immortalized human breast epithelial cell line that exhibits complex chromosomal rearrangements (Yoon et al., 2002). Our CBP suppression studies were performed in either early passage HMEC-LXSN control cells or in early passage HMEC-E6 cells. These transduced cell strains are not immortalized and previous cytogenetic analysis demonstrates the absence of chromosomal rearrangements in early passage transduced HMECs (Seewaldt et al., 2001). It is also possible that the difference between these previous studies and our results can be accounted for by differences between CBP and p300 activities. While p300 and CBP have many overlapping functions, there is ample evidence that they also have distinct activities. For example, CBP and p300 play distinct roles during retinoic acid-induced differentiation in F9 cells (Kawasaki et al., 1998; Ugai et al., 1999), and p300, but not CBP, has been shown to be transcriptionally regulated by BRCA1 in breast cancer cell lines (Fan et al. 2002).

In this study, we observe that suppression of CBP results in loss of laminin-5 α 3-chain expression. Observations in our model system are consistent with prior studies showing loss of laminin-5 α 3-chain expression during early carcinogenesis (Hao et al., 2001, Sathyanarayana, et al., 2003) but do not explain the seemingly paradoxical observation that increased laminin-5 γ 2-chain expression and cleavage is associated with tumor invasion (Pyke et al., 1994; Seftor et al., 2001; Yamamoto et al., 2001). However, the rECM-resistant cells used in this model system are 1) not transformed and 2) do not exhibit invasion in *in vitro* assays, and therefore represent a model of pre-invasive breast cancer, rather than a model of invasion.

Tumorigenesis is thought to be a multistep process; there is increasing evidence that epigenetic changes, including DNA methylation and coactivator/corepressor shifts, may play an important role modulating gene expression during carcinogenesis. For example, it has been recently found that transcription of the E-cadherin gene is down-regulated during early carcinogenesis by both promoter hypermethylation and

CBP Loss and Resistance to ECM-induced apoptosis

modulation of coactivator/corepressor expression (Thiery, 2003). Similar to what has been observed for E-cadherin regulation, prior studies have demonstrated that laminin-5 α 3-chain expression can be inhibited by hypermethylation (Sathyanarayana, 2003) and here we provide evidence for a second epigenetic mechanism, coactivator modulation, that regulates expression of laminin-5 α 3-chain. Recently there is new evidence that loss of E-cadherin expression may be temporary and that epigenetic control over the expression of E-cadherin would make it possible for E-cadherin to be produced in aggressive primary and metastatic breast tumors (Thiery, 2003). This model of differential regulation of E-cadherin expression may be valuable in reconciling the potentially divergent observations that 1) laminin-5 α 3-chain expression is lost during early mammary carcinogenesis and 2) increased laminin-5 γ 2-chain expression is associated with tumor invasion and an aggressive phenotype (Pyke et al., 1994, Seftor et al., 2001; Yamamoto et al., 2001; Niki et al., 2002). Further studies will be necessary to determine the role of epigenetic silencing of laminin-5 α 3-chain expression in early mammary carcinogenesis.

In summary, observations in our model system predict that a partial reduction of CBP expression results in 1) loss of CBP occupancy of the AP-1-“rich” region of the *LAMA3A* promoter, 2) decreased *LAMA3A* promoter activity, and 3) reduced expression of laminin-5 α 3-chain protein. We also observe that loss of CBP/laminin 5- α 3 expression blocks rECM-growth regulation and -apoptosis *in vitro* and thereby may promote the clonal expansion of “damaged” HMECs *in vivo*. These observations have potential clinical implications and suggest that suppression of CBP may promote a cellular environment that may increase the risk of subsequent invasive breast cancer.

Acknowledgments:

This work is supported by NIH/NCI grants 2P30CA14236-26 [V.L.S., E.C.D.], R01CA88799 [V.L.S.],

CBP Loss and Resistance to ECM-induced apoptosis

R01CA98441 [V.L.S.], 5-P30CA16058 [K.M.], NIH/NIDDK grant 2P30DK 35816-11 [V.L.S.], DAMD-98-1-851 and DAMD-010919 [V.L.S.], American Cancer Society Award CCE-99898 [to V.L.S.], a V-Foundation Award [V.L.S.], a Susan G. Komen Breast Cancer Award [V.L.S., E.C.D.], and a Charlotte Geyer Award [V.L.S.]. The authors are indebted to Judy Goombridge and Franque Remington for the preparation of electron microscopy specimens. We gratefully acknowledge William Carter for the gift of integrin-specific antibodies. The authors wish to thank Mr. and Mrs. Jack and Marcia Slane for the generous gift of the Zeiss LSM 410 fluorescence microscope to the Duke University Comprehensive Cancer Center. The authors also wish to acknowledge T.P. Yao for sharing his unpublished observations.

References

- Aberdam, D., Virolle, T., Simon-Assmann, P., and Yoshida, K.** (2000). Transcriptional regulation of laminin gene expression. *Microscopy Res. & Tech.* **51**, 228-237.
- Arias, J., Alberts, A.S., Brindle, P., Claret, F.X., Smeal, T., Karin, M., Feramisco, J., and Montminy, M.** (1994). Activation of cAMP and mitogen responsive genes relies on a common nuclear factor. [comment]. *Nature* **370**, 226-229.
- Ashkenazi, A., and Dixit, V.M.** (1998). Death receptors: signaling and modulation. *Science* **281**, 1305-1308.
- Aubele, M.M., Cummings, M.C., Mattis, A.E., Zitzelsberger, H.F., Walch, A.K., Kremer, M., Hofler, H., and Werner, M.** (2000). Accumulation of chromosomal imbalances from intraductal proliferative lesions to adjacent in situ and invasive ductal breast cancer. *Diag. Mol. Path.* **9**, 14-19.
- Aumailley, M., El Khal, A., Knoss, N., and Tunggal, L.** (2003). Laminin 5 processing and its integration into the ECM. *Matrix Biol.* **22**, 49-54.
- Baldi, P., and Long, A.D.** (2001). A Bayesian framework for the analysis of microarray expression data: regularized t-test and statistical inferences of gene changes. *Bioinformatics* **17**, 509-519.
- Benkoussa, M., Brand, C., Delmotte, M.H., Formstecher, P., and Lefebvre, P.** (2002). Retinoic acid receptors inhibit AP1 activation by regulating extracellular signal-regulated kinase and CBP recruitment to an AP1-responsive promoter. *Mol. Cell. Biol.* **22**, 4522-4534.
- Carter, W.G., Wayner, E.A., Bouchard, T.S., and Kaur, P.** (1990a). The role of integrins alpha 2 beta 1 and alpha 3 beta 1 in cell-cell and cell-substrate adhesion of human epidermal cells. *J. Cell Biol.* **110**, 1387-1404.
- Carter, W.G., Kaur, P., Gil, S.G., Gahr, P.J., and Wayner, E.A.** (1990b). Distinct functions for integrins alpha 3 beta 1 in focal adhesions and alpha 6 beta 4/bullous pemphigoid antigen in a new stable anchoring contact (SAC) of keratinocytes: relation to hemidesmosomes. *J. Cell Biol.* **111**, 3141-3154.

CBP Loss and Resistance to ECM-induced apoptosis

- D'Ardenne, A.J., Richman, P.I., Horton, M.A., McAulay, A.E., and Jordan, S.** (1991). Co-ordinate expression of the alpha-6 integrin laminin receptor sub-unit and laminin in breast cancer. *J. Pathol.* **165**, 213-220.
- Demers, G.W., Espling, E., Harry, J.B., Etscheid, B.G., and Galloway, D.A.** (1996). Abrogation of growth arrest signals by human papillomavirus type 16 E7 is mediated by sequences required for transformation. *J. Virol.* **70**, 6862-6869.
- Dietze, E.C., Caldwell, L.E., Grupin, S.L., Mancini, M., and Seewaldt, V.L.** (2001). Tamoxifen but not 4-hydroxytamoxifen initiates apoptosis in p53(-) normal human mammary epithelial cells by inducing mitochondrial depolarization. *J. Biol. Chem.* **276**, 5384-5394.
- Dietze, E.C., Troch, M.M., Bowie, M.L., Yee, L., Bean, G., and Seewaldt, V.L.** (2002). Induction of CBP/p300 is required for ATRA sensitivity in mammary epithelial cells. *Biochem. Biophys. Res. Commun.* **302**, 841-848.
- Fabian, C.J., Kamel, S., Zalles, C., and Kimler, B.F.** (1996). Identification of a chemoprevention cohort from a population of women at high risk for breast cancer. *J. Cell Biochem., Suppl.* **25**, 112-122.
- Fan, S., Ma, Y.X., Wang, C., Yuan, R.Q., Meng, Q., Wang, J.A., Erdos, M., Goldberg, I.D., Webb, P., Kushner, P.J., et al.** (2002). p300 Modulates the BRCA1 inhibition of estrogen receptor activity. *Cancer Res.* **62**, 141-151.
- Farrelly, N., Lee, Y.J., Oliver, J., Dive, C., and Streuli, C.H.** (1999). Extracellular matrix regulates apoptosis in mammary epithelium through a control on insulin signaling. *J. Cell Biol.* **144**, 1337-1348.
- Folkman, J., and Moscona, A.** (1978). Role of cell shape in growth control. *Nature* **273**, 345-349.
- Giles, R.H., Petrij, F., Dauwerse, H.G., den Hollander, A.I., Lushnikova, T., van Ommen, G.J., Goodman, R.H., Deaven, L.L., Doggett, N.A., Peters, D.J., et al.** (1997). Construction of a 1.2-Mb

CBP Loss and Resistance to ECM-induced apoptosis

contig surrounding, and molecular analysis of, the human CREB-binding protein (CBP/CREBBP) gene on chromosome 16p13.3. *Genomics* **42**, 96-114.

Goodman, R.H., and Smolik, S. (2000). CBP/p300 in cell growth, transformation, and development. *Genes Devel.* **14**, 1553-1577.

Hao, J., Jackson, L., Calaluce, R., McDaniel, K., Dalkin, B.L., and Nagle, R.B. (2001). Investigation into the mechanism of the loss of laminin 5 ($\alpha 3\beta 3\gamma 2$) expression in prostate cancer. *Amer. J. Pathol.* **158**, 1129-1135.

Hashida, H., Takabayashi, A., Tokuhara, T., Taki, T., Kondo, K., Kohno, N., Yamaoka, Y., and Miyake, M. (2002). Integrin $\alpha 3$ expression as a prognostic factor in colon cancer: association with MRP-1/CD9 and KAI1/CD82. *Int. J. Cancer* **97**, 518-525.

Henning, K., Berndt, A., Katenkamp, D., and Kosmehl, H. (1999). Loss of laminin-5 in the epithelium-stroma interface: an immunohistochemical marker of malignancy in epithelial lesions of the breast. *Histopathol.* **34**, 305-309.

Hood, J.D., and Cheresch, D.A. (2002). Role of integrins in cell invasion and migration. *Nature Rev. Cancer* **2**, 91-100.

Horvai, A.E., Xu, L., Korzus, E., Brard, G., Kalafus, D., Mullen, T.M., Rose, D.W., Rosenfeld, M.G., and Glass, C.K. (1997) Nuclear integration of JAK/STAT and Ras/AP-1 signaling by CBP and p300. *Proc. Natl. Acad. Sci. USA* **94**, 1074-1079.

Howlett, A.R., Bailey, N., Damsky, C., Petersen, O.W., and Bissell, M.J. (1995). Cellular growth and survival are mediated by $\beta 1$ integrins in normal human breast epithelium but not in breast carcinoma. *J. Cell Sci.* **108**, 1945-1957.

Hsu, S.L., Cheng, C.C., Shi, Y.R., and Chiang, C.W. (2001). Proteolysis of integrin $\alpha 5$ and $\beta 1$ subunits involved in retinoic acid-induced apoptosis in human hepatoma Hep3B cells. *Cancer Lett.* **167**, 193-204.

CBP Loss and Resistance to ECM-induced apoptosis

- Ilic, D., Almeida, E.A., Schlaepfer, D.D., Dazin, P., Aizawa, S., and Damsky, C.H. (1998). Extracellular matrix survival signals transduced by focal adhesion kinase suppress p53-mediated apoptosis. *J. Cell Biol.* **143**, 547-560.
- Kamei, Y., Xu, L., Heinzl, T., Torchia, J., Kurokawa, R., Gloss, B., Lin, S.C., Heyman, R.A., Rose, D.W., Glass, C.K., et al. (1996). A CBP integrator complex mediates transcriptional activation and AP-1 inhibition by nuclear receptors. *Cell* **85**, 403-414.
- Kawasaki, H., Eckner, R., Yao, T.P., Taira, K., Chiu, R., Livingston, D.M., and Yokoyama, K.K. (1998). Distinct roles of the co-activators p300 and CBP in retinoic-acid-induced F9-cell differentiation. *Nature* **393**, 284-289.
- Klingelutz, A.J., Foster, S.A., and McDougall, J.K. (1996). Telomerase activation by the E6 gene product of human papillomavirus type 16. *Nature* **380**, 79-82.
- Kwok, R.P., Lundblad, J.R., Chrivia, J.C., Richards, J.P., Bachinger, H.P., Brennan, R.G., Roberts, S.G., Green, M.R., and Goodman, R.H. (1994). Nuclear protein CBP is a coactivator for the transcription factor CREB.[comment]. *Nature* **37**, 223-226.
- Lininger, R.A., Park, W.S., Man, Y.G., Pham, T., MacGrogan, G., Zhuang, Z., and Tavassoli, F.A. (1998). LOH at 16p13 is a novel chromosomal alteration detected in benign and malignant microdissected papillary neoplasms of the breast. *Human Pathol.* **29**, 1113-1118.
- Majno, G., and Joris, I. (1995). Apoptosis, oncosis, and necrosis. An overview of cell death. *American J. Pathol.* **146**, 3-15.
- Manda, R., Kohno, T., Niki, T., Yamada, T., Takenoshita, S., Kuwano, H., and Yokota, J. (2000). Differential expression of the LAMB3 and LAMC2 genes between small cell and non-small cell lung carcinomas. *Biochem. Biophys. Res. Commun.* **275**, 440-445.
- Martin, K.J., Kwan, C.P., Nagasaki, K., Zhang, X., O'Hare, M.J., Kaelin, C.M., Burgeson, R.E., Pardee, A.B., and Sager, R. (1998). Down-regulation of laminin-5 in breast carcinoma cells. *Mol. Med.* **4**, 602-613.

CBP Loss and Resistance to ECM-induced apoptosis

- Mercurio, A.M., Bachelder, R.E., Chung, J., O'Connor, K.L., Rabinovitz, I., Shaw, L.M., and Tani, T.** (2001). Integrin laminin receptors and breast carcinoma progression. *J. Mamm. Gland Biol. Neoplasia* **6**, 299-309.
- Miller, K.A., Chung, J., Lo, D., Jones, J.C., Thimmapaya, B., and Weitzman, S.A.** (2000). Inhibition of laminin-5 production in breast epithelial cells by overexpression of p300. *J. Biol. Chem.* **275**, 8176-8182.
- Miller, K.A., Eklund, E.A., Peddinghaus, M.L., Cao, Z., Fernandes, N., Turk, P.W., Thimmapaya, B., and Weitzman, S.A.** (2001). Kruppel-like factor 4 regulates laminin alpha 3A expression in mammary epithelial cells. *J. Biol. Chem.* **276**, 42863-42868.
- Mrozek, K., Karakousis, C.P., Perez-Mesa, C., and Bloomfield, C.D.** (1993). Translocation t(12;22)(q13;q12.2-12.3) in a clear cell sarcoma of tendons and aponeuroses. *Genes Chrom. Cancer* **6**, 249-252.
- Niki, T., Kohno, T., Iba, S., Moriya, Y., Takahashi, Y., Saito, M., Maeshima, A., Yamada, T., Matsuno, Y., Fukayama, M., et al.** (2002). Frequent co-localization of Cox-2 and laminin-5 gamma2 chain at the invasive front of early-stage lung adenocarcinomas. *Am. J. Pathol.* **160**, 1129-1141.
- O'Connor, M.J.** (2000). Targeting of transcriptional cofactors by the HPV E6 protein: another tale of David and Goliath. *Trends Microbiol.* **8**, 45-47.
- Patel, D., Huang, S.M., Baglia, L.A., and McCance, D.J.** (1999). The E6 protein of human papillomavirus type 16 binds to and inhibits co-activation by CBP and p300. *EMBO J.* **18**, 5061-5072.
- Petersen, O.W., Ronnov-Jessen, L., Howlett, A.R., and Bissell, M.J.** (1992). Interaction with basement membrane serves to rapidly distinguish growth and differentiation pattern of normal and malignant human breast epithelial cells. *Proceedings of the Natl. Acad. Sci. USA* **89**, 9064-9068.

CBP Loss and Resistance to ECM-induced apoptosis

Pyke, C., Romer, J., Kallunki, P., Lund, L.R., Ralfkiaer, E., Dano, K., and Tryggvason, K. (1994).

The gamma 2 chain of kalinin/laminin 5 is preferentially expressed in invading malignant cells in human cancers. *Am. J. Pathol.* **145**, 782-791.

Robyr, D., Wolffe, A.P., and Wahli, W. (2000). Nuclear hormone receptor coregulators in action: diversity for shared tasks. *Mol. Endocrinol.* **14**, 329-347.

Rohan, T.E., Hartwick, W., Miller, A.B., and Kandel, R.A. (1998). Immunohistochemical detection of c-erbB-2 and p53 in benign breast disease and breast cancer risk. [comment]. *J. Natl. Cancer Inst.* **90**, 1262-1269.

Ronco, L.V., Karpova, A.Y., Vidal, M., and Howley, P.M. (1998). Human papillomavirus 16 E6 oncoprotein binds to interferon regulatory factor-3 and inhibits its transcriptional activity. *Genes Devel.* **12**, 2061-2072.

Roskelley, C.D., Desprez, P.Y., and Bissell, M.J. (1994). Extracellular matrix-dependent tissue-specific gene expression in mammary epithelial cells requires both physical and biochemical signal transduction. *Proc. Natl. Acad. Sci. USA* **91**, 12378-12382.

Sathyanarayana, U.G., Toyooka, S., Padar, A., Takahashi, T., Brambilla, E., Minna, J.D., and Gazdar, A.F. (2003). Epigenetic inactivation of laminin-5-encoding genes in lung cancers. *Clin. Cancer Res.* **9**, 2665-2672.

Schenk, S., Hintermann, E., Bilban, M., Koshikawa, N., Hojilla, C., Khokha, R., and Quaranta, V. (2003). Binding to EGF receptor of a laminin-5 EGF-like fragment liberated during MMP-dependent mammary gland involution. *J. Cell Biol.* **161**, 197-209.

Schrock, E., du Manoir, S., Veldman, T., Schoell, B., Wienberg, J., Ferguson-Smith, M.A., Ning, Y., Ledbetter, D.H., Bar-Am, I., Soenksen, D., et al. (1996). Multicolor spectral karyotyping of human chromosomes. *Science* **273**, 494-497.

- Seewaldt, V.L., Johnson, B.S., Parker, M.B., Collins, S.J., and Swisshelm, K. (1995). Expression of retinoic acid receptor beta mediates retinoic acid-induced growth arrest and apoptosis in breast cancer cells. *Cell Growth Diff.* **6**, 1077-1088.
- Seewaldt, V.L., Caldwell, L.E., Johnson, B.S., Swisshelm, K., Collins, S.J., and Tsai, S. (1997a). Inhibition of retinoic acid receptor function in normal human mammary epithelial cells results in increased cellular proliferation and inhibits the formation of a polarized epithelium in vitro. *Exptl. Cell Res.* **236**, 16-28.
- Seewaldt, V.L., Kim, J.H., Caldwell, L.E., Johnson, B.S., Swisshelm, K., and Collins, S.J. (1997b). All-trans-retinoic acid mediates G1 arrest but not apoptosis of normal human mammary epithelial cells. *Cell Growth Diff.* **8**, 631-641.
- Seewaldt, V.L., Dietze, E.C., Johnson, B.S., Collins, S.J., and Parker, M.B. (1999a). Retinoic acid-mediated G1-S-phase arrest of normal human mammary epithelial cells is independent of the level of p53 protein expression. *Cell Growth Diff.* **10**, 49-59.
- Seewaldt, V.L., Kim, J.H., Parker, M.B., Dietze, E.C., Srinivasan, K.V., and Caldwell, L.E. (1999b). Dysregulated expression of cyclin D1 in normal human mammary epithelial cells inhibits all-trans-retinoic acid-mediated G0/G1-phase arrest and differentiation in vitro. *Exptl. Cell Res.* **249**, 70-85.
- Seewaldt, V.L., Mrozek, K., Sigle, R., Dietze, E.C., Heine, K., Hockenbery, D.M., Hobbs, K.B., and Caldwell, L.E. (2001a). Suppression of p53 function in normal human mammary epithelial cells increases sensitivity to extracellular matrix-induced apoptosis. *J. Cell Biol.* **155**, 471-486.
- Seewaldt, V.L., Mrozek, K., Dietze, E.C., Parker, M., and Caldwell, L.E. (2001b). Human papillomavirus type 16 E6 inactivation of p53 in normal human mammary epithelial cells promotes tamoxifen-mediated apoptosis. *Cancer Res.* **61**, 616-624.
- Seftor, R.E., Seftor, E.A., Koshikawa, N., Meltzer, P.S., Gardner, L.M., Bilban, M., Stetler-Stevenson, W.G., Quaranta, V., and Hendrix, M.J. (2001). Cooperative interactions of laminin 5

CBP Loss and Resistance to ECM-induced apoptosis

gamma2 chain, matrix metalloproteinase-2, and membrane type-1-matrix/metalloproteinase are required for mimicry of embryonic vasculogenesis by aggressive melanoma. *Cancer Res.* **61**, 6322-6327.

Shang, Y., Hu, X., DiRenzo, J., Lazar, M.A., and Brown, M. (2000). Cofactor dynamics and sufficiency in estrogen receptor-regulated transcription. *Cell* **103**, 843-852.

Shang, M., Koshikawa, N., Schenk, S., and Quaranta, V. (2001). The LG3 module of laminin-5 harbors a binding site for integrin alpha3beta1 that promotes cell adhesion, spreading, and migration. *J. Biol. Chem.* **276**, 33045-33053.

Shaulian, E., and Karin, M. (2002). AP-1 as a regulator of cell life and death. *Nature Cell Biol.* **4**, E131-136.

Steffgen, K., Dufraux, K., and Hathaway, H. (2002). Enhanced branching morphogenesis in mammary glands of mice lacking cell surface beta1,4-galactosyltransferase. *Devel. Biol.* **244**, 114-133.

Strange, R., Li, F., Saurer, S., Burkhardt, A., and Friis, R.R. (1992). Apoptotic cell death and tissue remodelling during mouse mammary gland involution. *Development* **115**, 49-58.

Stromblad, S., Fotedar, A., Brickner, H., Theesfeld, C., Aguilar de Diaz, E., Friedlander, M., and Cheresh, D.A. (2002). Loss of p53 compensates for alpha v-integrin function in retinal neovascularization. *J. Biol. Chem.* **277**, 13371-13374.

Stupack, D.G., and Cheresh, D.A. (2002). Get a ligand, get a life: integrins, signaling and cell survival. *J. of Cell Sci.* **115**, 3729-3738.

Thiery, J.P. (2003). Cell adhesion in cancer. *Comptes Rendus Phys.* **4**, 289-304.

Thomas, M., and Banks, L. (1999). Human papillomavirus (HPV) E6 interactions with Bak are conserved amongst E6 proteins from high and low risk HPV types. *J. Gen. Virol.* **80**, 1513-1517.

CBP Loss and Resistance to ECM-induced apoptosis

- Tsuda, H., Sakamaki, C., Tsugane, S., Fukutomi, T., and Hirohashi, S.** (1998). Prognostic significance of accumulation of gene and chromosome alterations and histological grade in node-negative breast carcinoma. *Jap. J. Clin. Oncol.* **28**, 5-11.
- Ugai, H., Uchida, K., Kawasaki, H., and Yokoyama, K.K.** (1999). The coactivators p300 and CBP have different functions during the differentiation of F9 cells. *J. Mol. Med.* **77**, 481-494.
- Virolle, T., Monthouel, M.N., Djabari, Z., Ortonne, J.P., Meneguzzi, G., and Aberdam, D.** (1998). Three activator protein-1-binding sites bound by the Fra-2/JunD complex cooperate for the regulation of murine laminin alpha3A (lama3A) promoter activity by transforming growth factor-beta. *J. Biol. Chem.* **273**, 17318-17325.
- Virolle, T., Coraux, C., Ferrigno, O., Cailleteau, L., Ortonne, J.P., Pognonec, P., and Aberdam, D.** (2002). Binding of USF to a non-canonical E-box following stress results in a cell-specific derepression of the lama3 gene. *Nucleic Acids Res.* **30**, 1789-1798.
- Wayner, E.A., and Carter, W.G.** (1987). Identification of multiple cell adhesion receptors for collagen and fibronectin in human fibrosarcoma cells possessing unique alpha and common beta subunits. *J. Cell Biol.* **105**, 1873-1884.
- Wayner, E.A., Carter, W.G., Piotrowicz, R.S., and Kunicki, T.J.** (1988). The function of multiple extracellular matrix receptors in mediating cell adhesion to extracellular matrix: preparation of monoclonal antibodies to the fibronectin receptor that specifically inhibit cell adhesion to fibronectin and react with platelet glycoproteins Ic-IIa. *J. Cell Biol.* **107**, 1881-1891.
- Yahata, T., Shao, W., Endoh, H., Hur, J., Coser, K.R., Sun, H., Ueda, Y., Kato, S., Isselbacher, K.J., Brown, M., et al.** (2001). Selective coactivation of estrogen-dependent transcription by CITED1 CBP/p300-binding protein. *Genes Devel.* **15**, 2598-2612.
- Yamamoto, H., Itoh, F., Iku, S., Hosokawa, M., and Imai, K.** (2001). Expression of the gamma(2) chain of laminin-5 at the invasive front is associated with recurrence and poor prognosis in human esophageal squamous cell carcinoma. *Clin. Cancer Res.* **7**, 896-900.

CBP Loss and Resistance to ECM-induced apoptosis

- Yao, T.P., Oh, S.P., Fuchs, M., Zhou, N.D., Ch'ng, L.E., Newsome, D., Bronson, R.T., Li, E., Livingston, D.M., and Eckner, R.** (1998). Gene dosage-dependent embryonic development and proliferation defects in mice lacking the transcriptional integrator p300. *Cell* **93**, 361-372.
- Yoon, D.S., Wersto, R.P., Zhou, W., Chrest, F.J., Garrett, E.S., Kwon, T.K., and Gabrielson, E.** (2002). Variable levels of chromosomal instability and mitotic spindle checkpoint defects in breast cancer. *Am. J Pathol.* **161**, 391-397.
- Zimmermann, H., Degenkolbe, R., Bernard, H.U., and O'Connor, M.J.** (1999). The human papillomavirus type 16 E6 oncoprotein can down-regulate p53 activity by targeting the transcriptional coactivator CBP/p300. *J. Virol.* **73**, 6209-6219.
- zur Hausen, H.** (2000). Papillomaviruses causing cancer: evasion from host-cell control in early events in carcinogenesis. *J. Natl. Cancer Inst.* **92**, 690-698.
- Zutter, M.M., Santoro, S.A., Staatz, W.D., and Tsung, Y.L.** (1995). Re-expression of the alpha 2 beta 1 integrin abrogates the malignant phenotype of breast carcinoma cells. *Proc. Natl. Acad. Sci. USA* **92**, 7411-7415.

CBP Loss and Resistance to ECM-induced apoptosis

CBP Loss and Resistance to ECM-induced apoptosis

Table 1: CBP-specific antisense ODN sequences

Target gene	Sequences	Size	Status
CBP			
A3342V	5'-CACTTCAGGTTTCTTTTCATCC -3'	22 bp	Active
scrA3342V	5'- ATTCTCATCATCGTCTTCGTTC-3'	22 bp	Inactive

The first and last three base pairs of each ODN sequence were phosphorothiolate modified.

Table 2: Laminin and integrin primers

Gene	Primer set	Cycle conditions	PCR cycle number
<i>ITGA3</i>	F: 5'-AAGCCAAGTCTGAGACT -3' R: 5'-GTAGTATTGGTCCCGAGTCT -3'	4°C 3 min. 4°C 30 sec. 0°C 1 min. 2°C 1 min. 2°C 7 min.	22
<i>ITGB1</i>	F: 5'-GCGAAGGCATCCCTGAAAGT -3' R: 5'-GGACACAGGATCAGGTTGGA -3'	4°C 3 min. 4°C 30 sec. 4°C 30 sec. 2°C 1 min. 2°C 7 min.	19
<i>LAMA3</i>	F: 5'-TGTGGATCTTTGGGGCAG-3' R: 5'-TTGCCATAGTAGCCCTCCTG -3'	4°C 3 min. 4°C 30 sec. 8°C 30 sec. 2°C 1 min. 2°C 7 min.	20
<i>LAMB3</i>	F: 5'-TGAGGTTTCAGCAGGTACTGC -3' R: 5'-TAACTGTCCCATTTGGCTCAG -3'	5°C 3 min. 5°C 1 min. 5°C 1 min. 2°C 1 min. 2°C 7 min.	23
<i>LAMC2</i>	F: 5'-CTGAGTATGGGCAATGCCAC -3' R: 5'-GCTCTGGTATCAACCTTCTG -3'	5°C 3 min. 5°C 1 min. 5°C 1 min. 2°C 1 min. 2°C 7 min.	22
Beta-actin	F: 5'-GCTCGTCGTCGACAACGGCTC-3' R: 5'-CAAACATGATCTGGGTCATCTTCTC-3' (Invitrogen)	4°C 2 min. 4°C 15 sec. 5°C 30 sec. 2°C 30 sec. 2°C 7 min.	18

CBP Loss and Resistance to ECM-induced apoptosis

Fig. 1. (a) Karyotype of late passage HMEC-E6 cells.(b) Partial karyotypes of a representative late passage HMEC-E6 (passage 20) mitotic cells demonstrate two copies of an unbalanced translocation between chromosomes 13 and 16 involving 16p13 (arrows). SKY in display (**SKY display**) colors (blue, chromosome 13 material; bluish gray, chromosome 16 material). SKY in classification (**SKY classification**) colors (red, chromosome 13 material; orange, chromosome 16 material). Inverted and contrast-enhanced DAPI (**DAPI**) image of the same metaphase cells.

Fig. 2. (a) Expression of endogenous p53 and exogenous HPV-16 E6 mRNA in HMECs. Passage 10 and 18 HMEC-P parental cells (**Parental**), HMEC-LXSN controls (**LXSN**), and HMEC-E6 cells (**E6**) were analyzed for p53 and HPV-16 E6 mRNA expression. Ten micrograms of RNA were loaded per lane. 36B4 served as a loading control.

(b) Expression of p53 protein is suppressed in HMEC-E6 cells. Passage 10 and 18 HMEC-P parental cells (**Parental**), p53(+) HMEC-LXSN controls (**LXSN**), and HMEC-E6 cells (**E6**) were analyzed for p53 protein expression as described in Materials and Methods. Equal amounts of protein lysate were loaded per lane. Actin was used as a loading control.

(c) CBP protein expression is decreased in apoptosis-resistant late passage HMEC-E6 cells. Early and late passage HMEC-LXSN vector controls (**LXSN**) (passages 11 and 16) and HMEC-E6 cells (**E6**) (passages 11 and 18) were analyzed for CBP protein expression as described in Materials and Methods. Equal amounts of protein lysate were loaded per lane. Actin was used as a loading control.

(d) CBP protein expression is suppressed by antisense ODNs. HMEC-LXSN vector controls (**LXSN**) (passage 12) and early passage HMEC-E6 cells (**E6**) (passage 12) were cultured in the presence of (1) no treatment, (2) active CBP-specific ODN (A3342V), and (3) inactive CBP ODN (scrA3342V). Resultant cells were analyzed for CBP protein expression as described in Materials and Methods. Equal amounts of protein lysate were loaded per lane. Actin was used as a loading control.

Fig. 3. Inhibition of CBP expression in HMECs by antisense ODNs results in enhanced proliferation in rECM. The mean diameter of spheres formed by early passage HMEC-LXSN vector controls (passage 10) (*a*) and early passage HMEC-E6 cells (passage 11) (*b*) treated with either CBP antisense ODN (A3342V) (**CBPAS**) or inactive CBP ODN (scrA3342V) (**CBPscr**) were plotted as a function of days in culture. Cells were plated in rECM on Day 0, and the diameter of growing spherical cell colonies was measured with an eye-piece equipped with a micrometer spindle. Ki-67 (*c*, *d*) staining indices in early passage HMEC-LXSN cells (passage 10) (*c*) and early passage HMEC-E6 cells (passage 11) (*d*). Two hundred cells were surveyed per time point and indices were calculated from an average of three independent experiments. *Error bars* show standard error.

Fig. 4. Inhibition of CBP in early passage HMECs by antisense ODNs blocks apoptosis in rECM culture. Electron micrographs of early passage HMEC-LXSN control cells (passage 11) (*a*) and early passage HMEC-E6 cells (passage 11) (*b*) treated with CBP antisense (A3342V) ODN and grown in rECM for 9 days. Cells formed large, dense, irregularly shaped multicellular colonies with no central lumen (*a*, *b*). In contrast, early passage HMEC-E6 cells (passage 10) treated with inactive CBP ODN (scrA3342V) (*c*) underwent apoptosis when grown in rECM for 7 days as evidenced by 1) nuclear condensation (**n**), 2) cell shrinkage and separation, and 3) margination of chromatin (**mr**). Percent of apoptotic cells in early passage HMEC-E6 cells (passage 11) (*d*) and early passage HMEC-LXSN controls (passage 11) (*e*) treated either with active (A3342V) or inactive (scrA3342V) CBP-specific ODNs. Apoptosis was measured by TUNEL-staining as described in Materials and Methods. Apoptotic index was measured by calculating the percentage of TUNEL-staining cells relative to the total number of cells surveyed. Data represents an average of three independent experiments. *Error bars* show standard error.

Fig. 5. Expression of CBP in late passage HMEC-E6 cells promotes apoptosis in rECM.

(a) CBP and laminin α -3 protein expression are compared in late passage HMEC-E6 cells (Φ) (passage 18), late passage HMEC-E6 cells (passage 18) transduced with the empty retroviral vector LXSXN ((-)CBP), late passage HMEC-E6 cells expressing exogenous CBP ((+)CBP) (passage 18), and HMEC-E6 cells (passage 10). Equal amounts of protein lysate were loaded per lane. Actin was used as a loading control.

(b) Exogenous expression of CBP in apoptosis-resistant late passage HMEC-E6 cells results in decreased proliferation in rECM. The mean diameter of spheres formed by late passage HMEC-E6 cells (passage 16) expressing exogenous CBP ((+)CBP) or transduced with the LXSXN control vector ((-)CBP). Cells were plated in rECM on Day 0, and the diameter of growing spherical cell colonies was measured with an eye-piece equipped with a micrometer spindle.

(c) Ki-67 staining indices in late passage HMEC-E6 cells (passage 17) expressing exogenous CBP ((+)CBP) or transduced with the LXSXN control vector ((-)CBP). Two hundred cells were surveyed per time point and indices were calculated from an average of three independent experiments. *Error bars* show standard error.

(d) Electron micrographs of late passage HMEC-E6 cells (passage 17) expressing exogenous CBP ((+)CBP) or transduced with the LXSXN control vector ((-)CBP) grown in rECM for 7 days. Late passage HMEC-E6 (-)CBP control cells formed large, dense, irregularly shaped multicellular colonies with no central lumen. In contrast, late passage HMEC-E6 (+)CBP cells underwent apoptosis when grown in rECM for 7 days as evidenced by 1) nuclear condensation (**n**), 2) cell shrinkage and separation, and 3) margination of chromatin (**mr**).

CBP Loss and Resistance to ECM-induced apoptosis

(e) Percent of apoptotic cells in late passage HMEC-E6 cells (passage 16) expressing exogenous CBP ((+) **CBP**) or transduced with the LXS control vector ((-) **CBP**). Apoptosis was measured by TUNEL-staining as described in Materials and Methods. Apoptotic index was measured by calculating the percentage of TUNEL-staining cells relative to the total number of cells surveyed. Data represents an average of three independent experiments. *Error bars* show standard error.

Fig. 6. Laminin-5 α 3-chain expression is decreased in rECM-resistant, CBP-“poor” late passage HMEC-E6 cells.

(a) Analysis of differential gene expression in early (**E6E**) and late (**E6L**) passage HMEC-E6 cells (passage 10 and 18) relative to early passage HMEC-LXS controls (passage 10) (**LXS**). Cells were grown in contact with rECM and harvested for differential gene expression as described in Materials and Methods. All RNA combinations used for array analysis were obtained from cells that were matched for passage number, cultured under the identical growth conditions, and harvested at identical confluency. Data was collected in triplicate using independent biological replicates. Array images were processed using Affymetrix MAS 5.0 software. Pair-wise “treatment vs control” comparisons were made employing CyberT, a Bayesian t-statistic algorithm derived for microarray analysis. Color-coding: green, downregulation of gene expression; red, induction; black, no significant change; grey, no data available.

(b) Semiquantitative RT-PCR analysis of integrin and laminin-5 mRNA expression in early and late passage HMEC-E6 cells (passage 10 and 18) and HMEC-LXS controls (passage 10 and 16). Expression was normalized to beta-actin. These data are representative of three separate experiments.

(c) Quantitation of RT-PCR expression data. Studies were performed in triplicate. The resulting film images were digitized and quantitated using Kodak 1D Image Analysis Software. Expression was normalized to beta-actin. * $p < 0.0001$

CBP Loss and Resistance to ECM-induced apoptosis

(d) Laminin-5 $\alpha 3$ -chain protein expression is decreased in rECM-resistant, late passage HMEC-E6 cells (passage 18) relative to rECM-sensitive, early passage HMEC-E6 cells (passage 10) and early and late passage HMEC-LXSN controls (passage 11 and 18). Western analysis was performed as described in Material and Methods. Equal amounts of protein lysate were loaded per lane. Actin serves as a loading control.

(e) Quantitation of processed and unprocessed laminin-5 $\alpha 3$ -chain protein expression. The resulting film images were digitized and quantitated using Kodak 1K Image Analysis Software. Expression was normalized to beta-actin. * $p < 0.0001$

Fig. 7. Immunofluorescence characterization of $\alpha 3$ -integrin and laminin-5 $\alpha 3$ -chain expression in rECM-sensitive and -resistant cells. Frozen section of early passage HMEC-LXSN controls (passage 10) (a, b), late passage HMEC-controls (passage 16) (c, d), early passage HMEC-E6 cells (passage 10) (e, f), and late passage HMEC-E6 cells (passage 18) (g, h) grown in rECM for 6 days, cryosectioned, and immunostained for localization of $\alpha 3$ -integrin (a, c, e, g) and laminin-5 $\alpha 3$ -chain expression (b, d, f, h). $\alpha 3$ -integrin and laminin-5 $\alpha 3$ -chain expression was primarily localized at the basal surface of early and late passage HMEC-LXSN and early passage HMEC-E6 cells (arrow heads) (a-f). In contrast, apoptosis-resistant, late passage HMEC-E6 cells showed dispersed membrane and intracellular staining of $\alpha 3$ -integrin (arrow) and qualitatively decreased laminin-5 $\alpha 3$ -chain expression.

Fig. 8. Immunofluorescent characterization of $\alpha 3\beta 1$ -integrin and laminin-5 $\alpha 3$ chain expression in HMECs treated with CBP antisense ODNs. Frozen section of early passage HMEC-LXSN vector controls (passage 11) and HMEC-E6 cells (passage 11) treated either with CBP antisense ODN (A3342V) or inactive CBP ODN (scrA3342V). Cells were grown in rECM for 6 days, cryosectioned, and immunostained for either $\alpha 3$ -integrin (a-d) or laminin-5 $\alpha 3$ -chain (e-h) as described in Materials

CBP Loss and Resistance to ECM-induced apoptosis

and Methods. $\alpha 3$ - and laminin-5 $\alpha 3$ -chain expression were primarily localized at the basolateral surface in HMEC-LXSN and HMEC-E6 cells treated with inactive CBP ODNs (*arrow heads*). In contrast, HMEC-LXSN and HMEC-E6 cells treated with antisense CBP ODNs demonstrated disorganized membrane and cytosolic staining of $\alpha 3$ -integrin (*arrows*) and markedly reduced levels of laminin-5 $\alpha 3$ -chain expression.

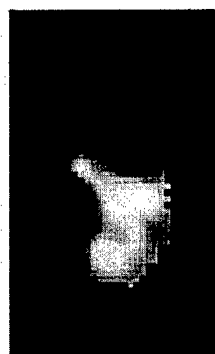
Fig. 9. Suppression of CBP expression results in a decrease in *LAMA3A* promoter activity in cells grown in contact with rECM. (a) *LAMA3A* promoter activity was measured in 1) early and late passage HMEC-LXSN controls (passage 11 and 16) and 2) early passage HMEC-E6 cells (passage 10) and compared to rECM-resistant, CBP-“poor” late passage HMEC-E6 cells (passage 18). (b) *LAMA3A* promoter activity is measured in early passage HMEC-LXSN controls (passage 11) or HMEC-E6 cells (passage 11) treated with either 1) CBP-specific antisense ODNs (A3342V) or 2) inactive ODNs (scrA3342V) and grown in rECM. *LAMA3A* promoter activity was measured as described in Materials and Methods. Data represent two independent experiments performed in triplicate. Error bars show standard error.

Fig. 10. Suppression of CBP in HMECs grown in rECM promotes decreased occupancy of the 277 bp AP-1-“rich” region of the *LAMA3A* promoter. (a) ChIP was performed in 1) early and HMEC-LXSN controls (passage 11 and 16) and 2) early passage HMEC-E6 cells (passage 11) and compared with rECM-resistant, CBP-“poor”, late passage HMEC-E6 cells (passage 18). (b) Early passage HMEC-E6 cells (passage 10) treated with CBP-specific ODNs, and grown in contact with rECM, were tested by ChIP to determine whether suppression of CBP expression resulted in a loss of CBP-binding AP-1-“rich” site of the *LAMA3A* promoter. ChIP was performed as described in Materials and Methods. Input controls test the integrity of the DNA samples. (c) Early passage HMEC-E6 cells (passage 11) treated with CBP-specific ODNs and grown in contact with rECM demonstrated markedly reduced levels of

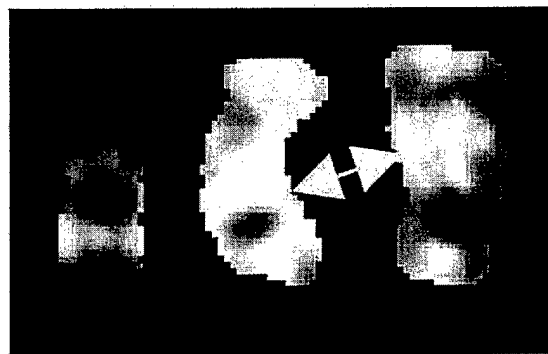
CBP Loss and Resistance to ECM-induced apoptosis

laminin-5 α 3-chain mRNA by RT-PCR. Beta-actin serves as a loading control. These data are representative of two separate experiments.

a



13

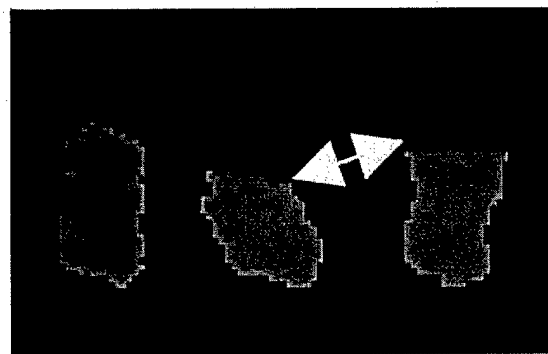


16

b

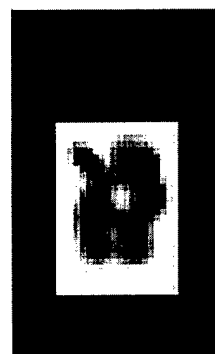


13

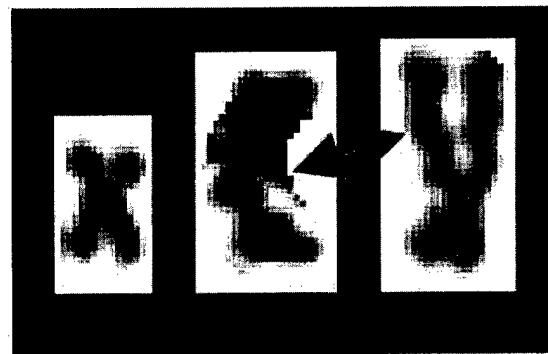


16

c



13



16

Figure 1

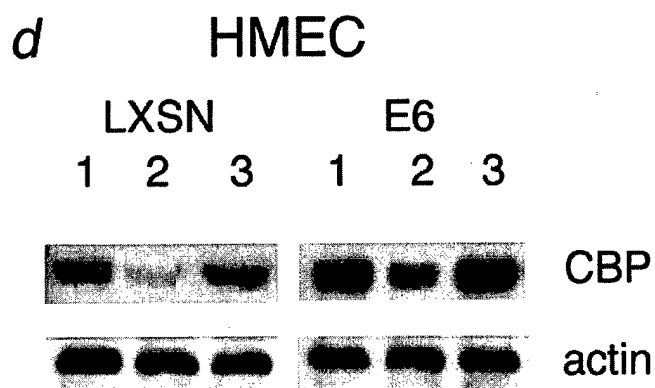
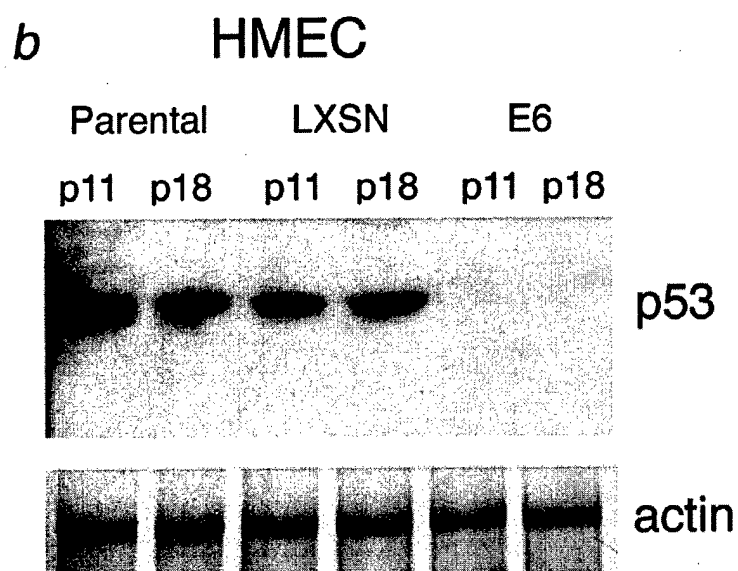
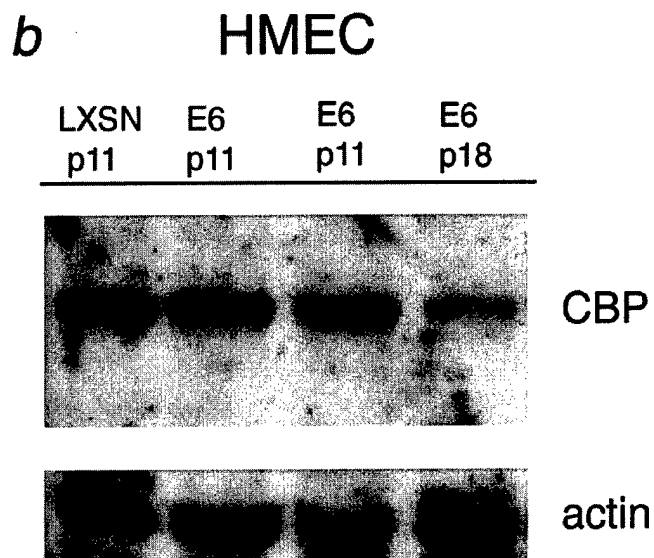
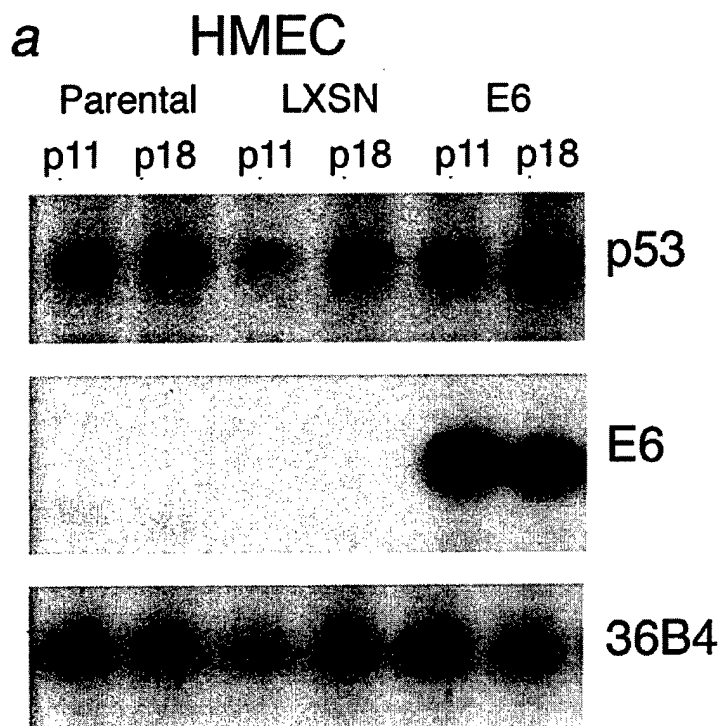


Figure 2

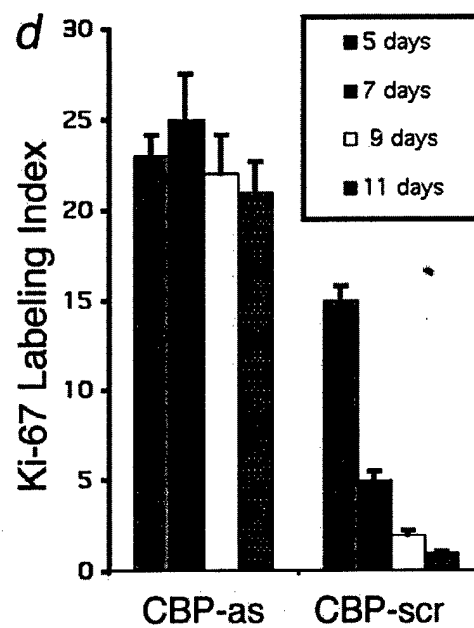
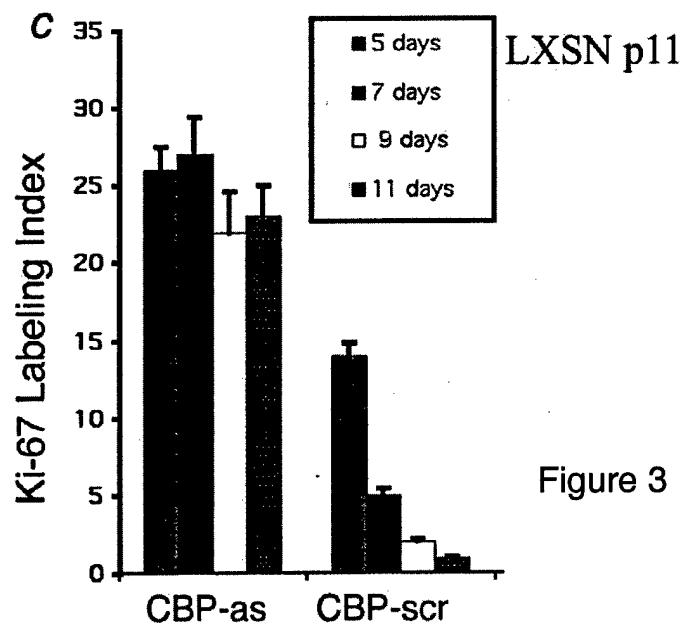
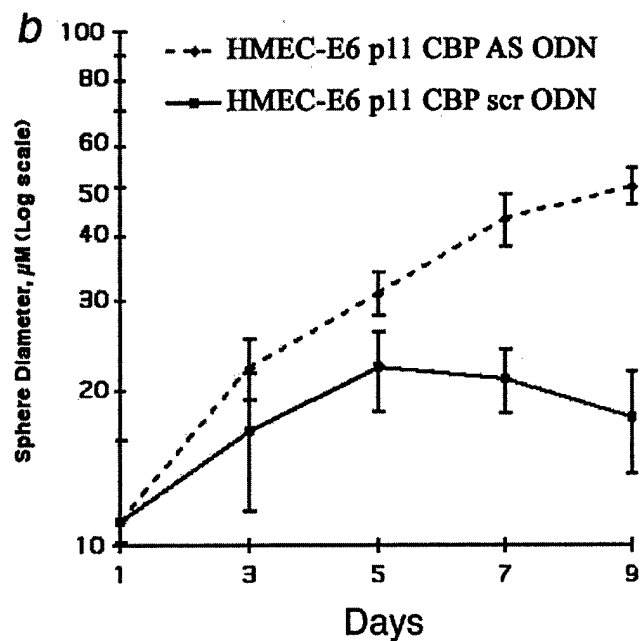
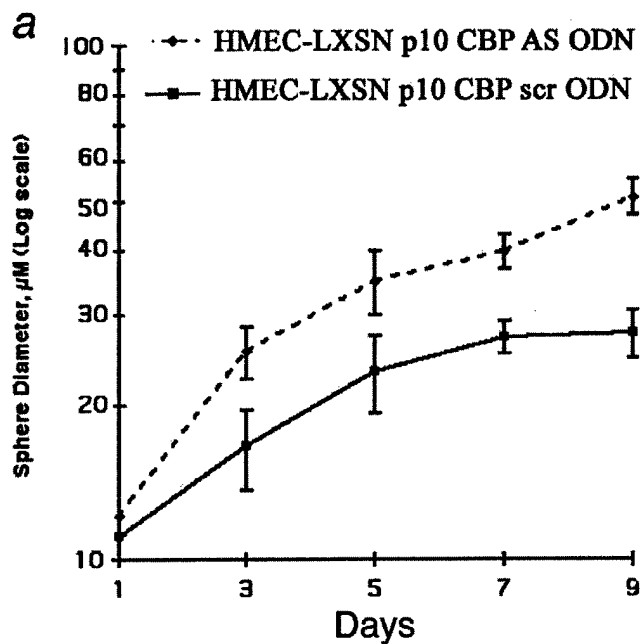
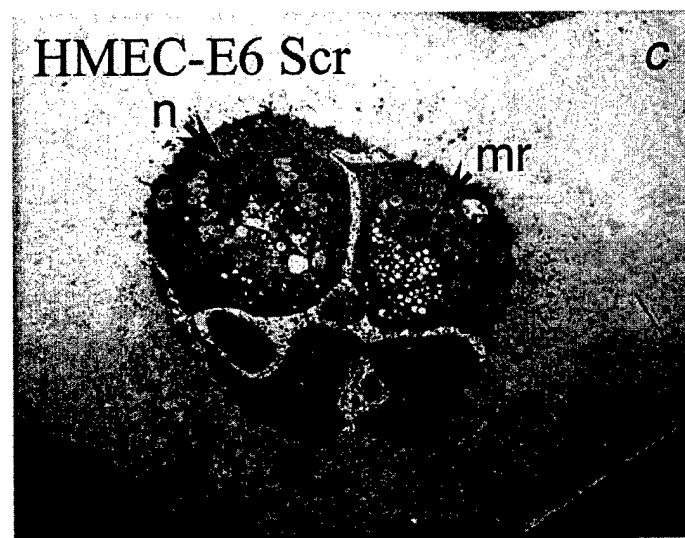
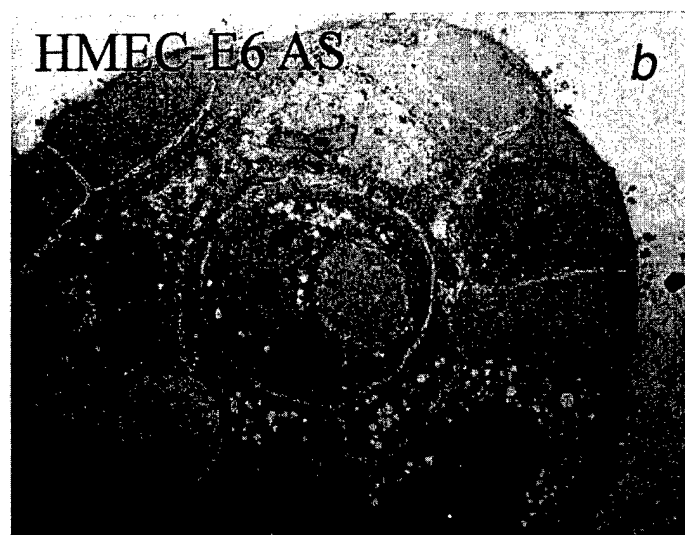


Figure 3



10 μ m

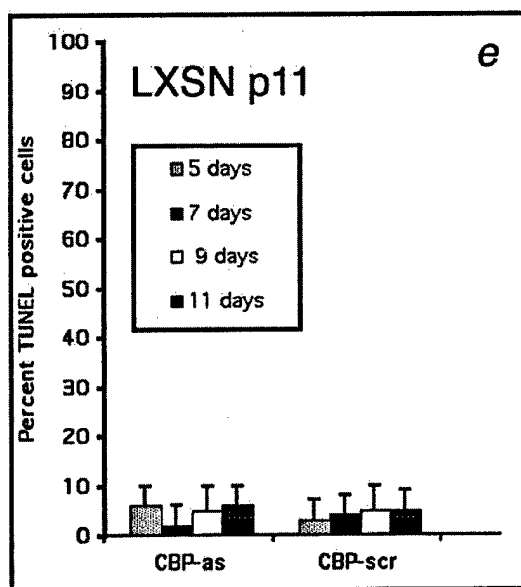
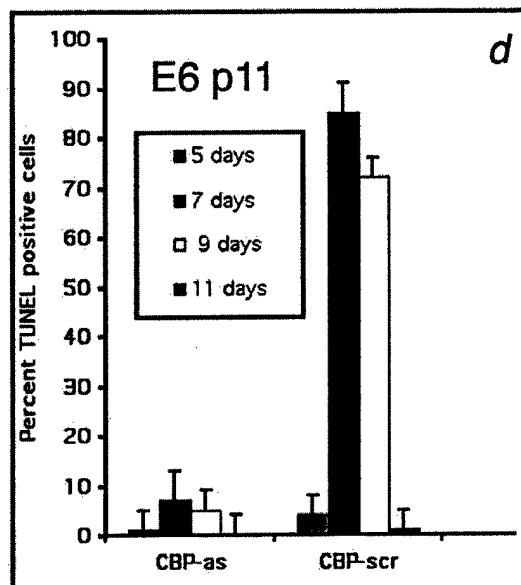


Figure 4

a.

LXSN+ECM
E6E+ECM
E6L+ECM

M10277. Human cytoplasmic beta-actin gene, complete cds
M35198. Human integrin B-6 mRNA, complete cds
U31201. Human laminin gamma2 chain gene (LAMC2). Human laminin gamma2 chain
L34155. Homo sapiens laminin-related protein (LamA3) mRNA, complete cds
X53587. Human mRNA for integrin beta 4
U17760. Human laminin S B3 chain (LAMB3) gene
U31201. Human laminin gamma2 chain gene (LAMC2). Human laminin gamma2 chain
M14648. Human cell adhesion protein (vitronectin) receptor alpha subunit
J03925. Human Mac-1 gene encoding complement receptor type 3, CD11b
X53002. Human mRNA for integrin beta-5 subunit
J05633. Human integrin beta-5 subunit mRNA, complete cds
U40279. Human beta-2 integrin alphaD subunit (ITGAD) gene, exons 25-30
S80335. Integrin beta 7 subunit [human, mRNA, 2798 nt]
X68742. H.sapiens mRNA for integrin, alpha subunit
X64072. H. sapiens CD18 exon 2
M34189. Integrin Beta 1
L25851. Homo sapiens integrin alpha E mRNA, complete cds
M34344. Human platelet glycoprotein IIb (GPIIb) gene
M14199. Human laminin receptor (2H5 epitope) mRNA, 5' end
X07979. Human mRNA for fibronectin receptor beta subunit
U40282. Human integrin-linked kinase (ILK) mRNA, complete cds
D25303. Human mRNA for integrin alpha subunit, complete cds
L36531. Homo sapiens integrin alpha 8 subunit mRNA, 3' end
Y00796. Human mRNA for leukocyte-associated molecule-1 alpha subunit
X16983. Human mRNA for integrin alpha-4 subunit
X02761. Human mRNA for fibronectin (FN precursor)
M61916. Human laminin B1 chain mRNA, complete cds
M59911. Human integrin alpha-3 chain mRNA, complete cds
S70348. Integrin beta 3 {alternatively spliced, clone beta 3C}
X79683. H.sapiens LAMB2 mRNA for beta2 laminin.
X74295. H.sapiens mRNA for alpha 7B integrin
M55210. Human laminin B2 chain (LAMB2) gene
Z26653. H.sapiens mRNA for laminin M chain (merosin)
M15395. Human leukocyte adhesion protein (LFA-1/Mac-1/p150,95 family)
J02963. Human platelet glycoprotein IIb mRNA, 3' end
X02761. Fibronectin. Alt. Splice 1
X06256. Human mRNA for fibronectin receptor alpha subunit
S78569. laminin alpha 4 chain [human, fetal lung, mRNA, 6204 nt]
U33880. Human beta 1 integrin isoform D (ITGB1) gene, partial cds.
X53586. Integrin alpha 6 (or alpha E) protein gene extracted from Human mRNA
U43901. Human 37 KD laminin receptor precursor/p40 ribosome associated protei
M73780. Human integrin beta-8 subunit mRNA, complete cds
M35999. Human platelet glycoprotein IIIa (GPIIIa) mRNA, complete cds

Figure 6a

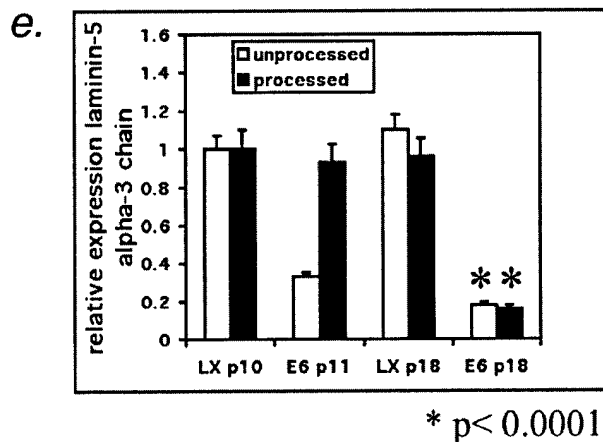
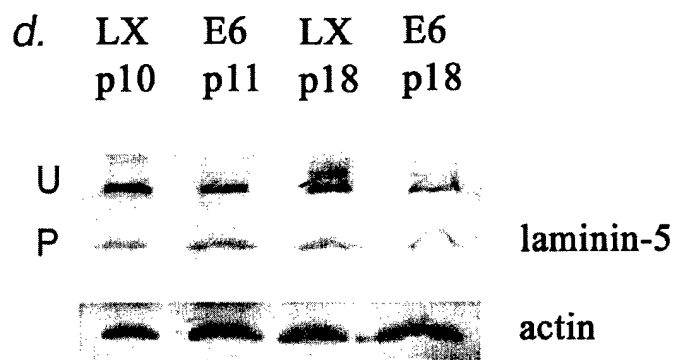
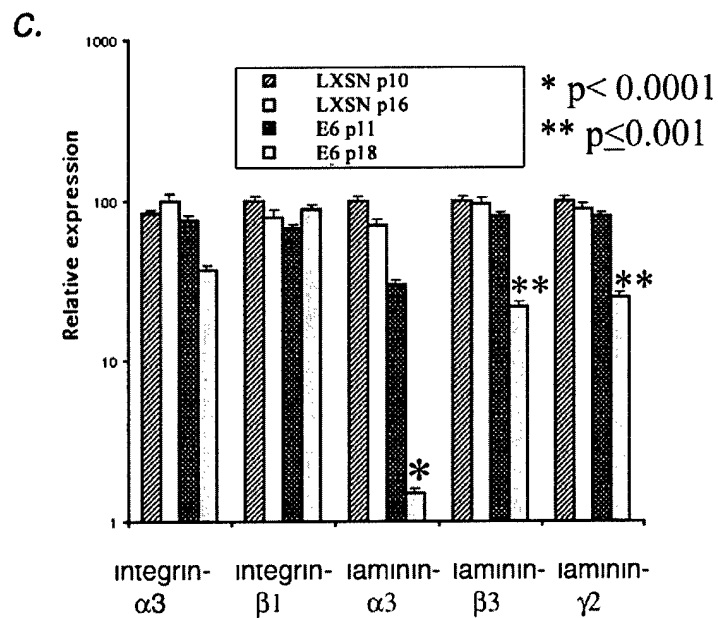
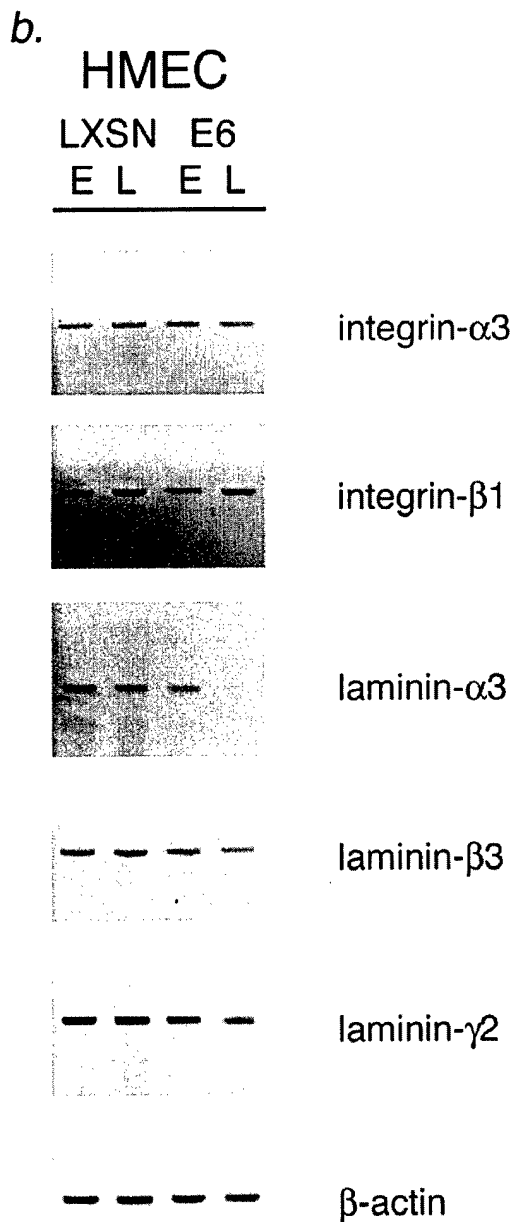


Figure 6bcde

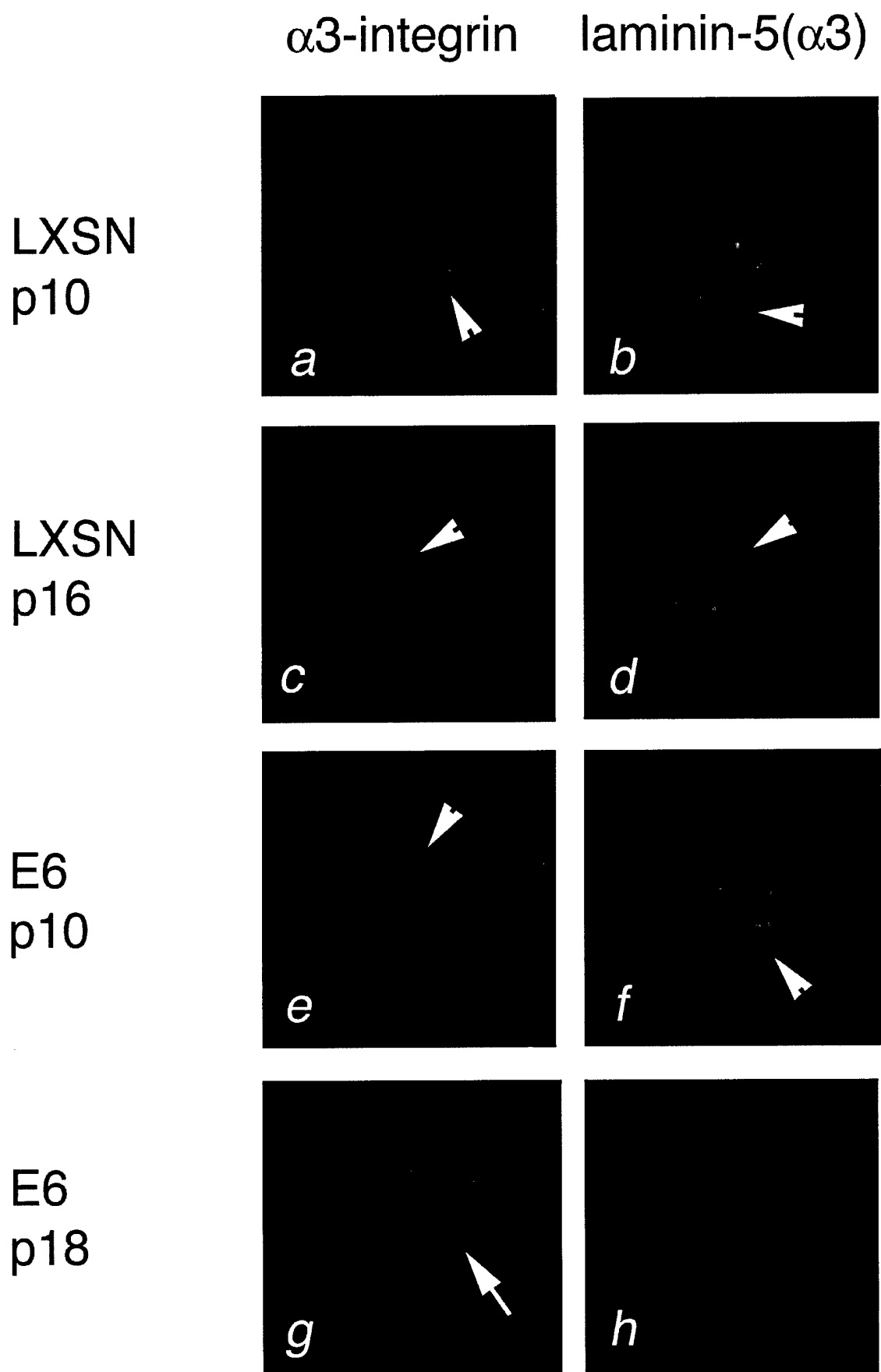



Figure 7


25 μ m

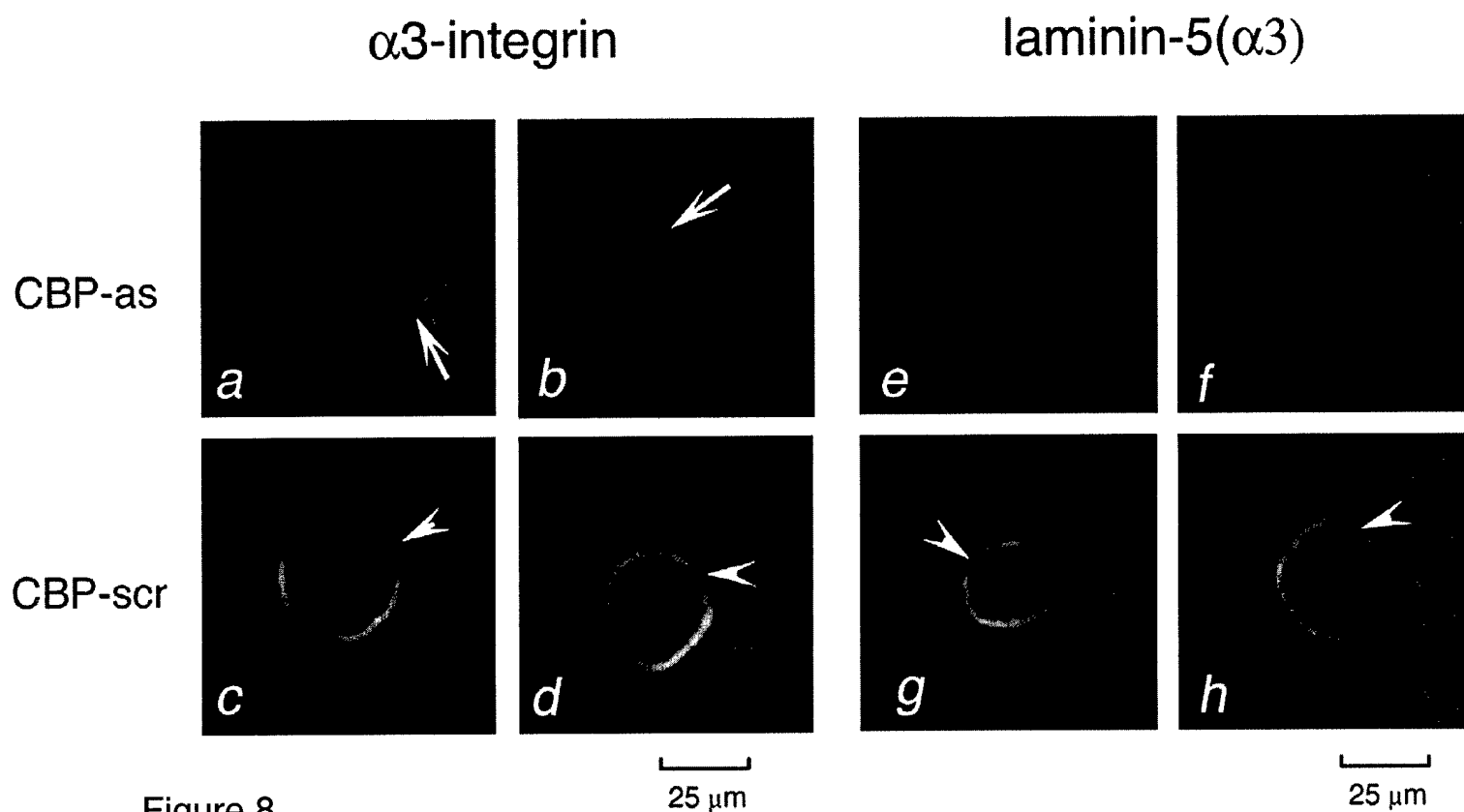


Figure 8

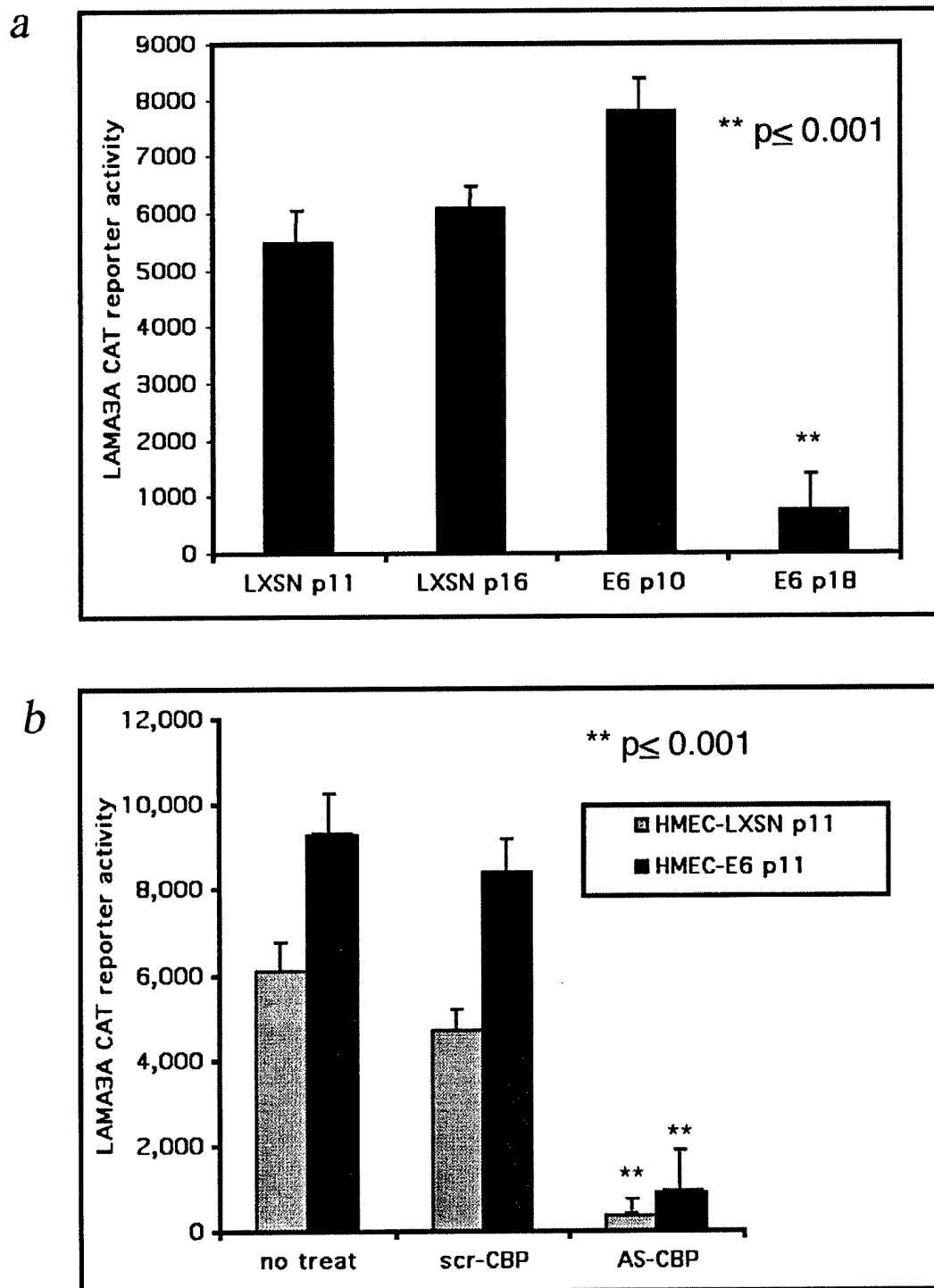


Figure 9

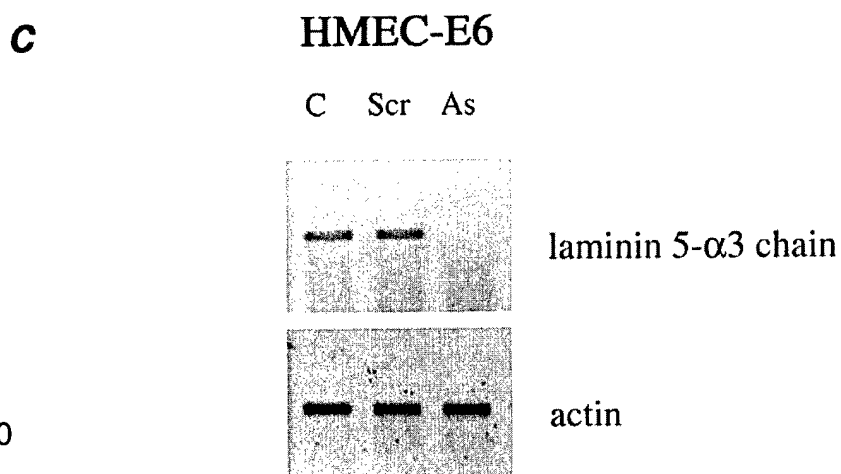
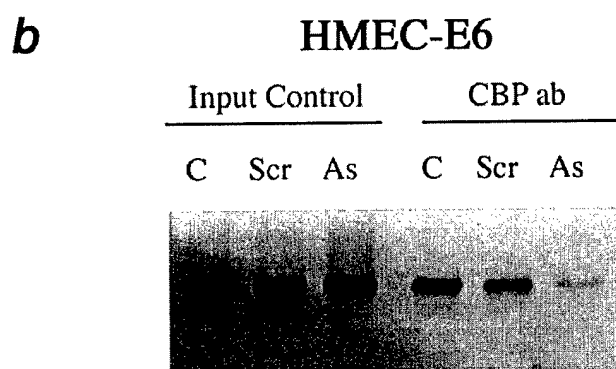
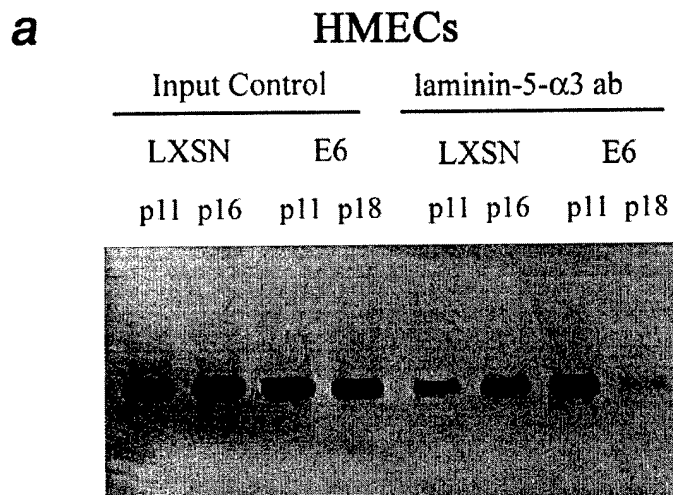


Figure 10

Tamoxifen and tamoxifen ethyl bromide induce apoptosis in acutely damaged mammary epithelial cells through modulation of AKT activity

Eric C Dietze¹, Michelle M Troch¹, Gregory R Bean¹, Joshua B Heffner¹, Michelle L Bowie¹, Paul Rosenberg², Brooke Ratliff¹ and Victoria L Seewaldt^{*1}

¹Division of Medical Oncology, Department of Medicine, Duke University Medical Center, Durham, NC 27710, USA; ²Division of Cardiology, Department of Medicine, Duke University Medical Center, Durham, NC 27710, USA

Normal human mammary epithelial cells (HMECs), unlike estrogen receptor-positive (ER+) breast cancers, typically express low nuclear levels of ER (ER-'poor'). We previously demonstrated that 1.0 μ M tamoxifen (Tam) induced apoptosis in ER-'poor' HMECs acutely transduced with human papillomavirus-16 E6 (HMEC-E6) through a rapid mitochondrial signaling pathway. Here, we show that plasma membrane-associated E2-binding sites initiate the rapid apoptotic effects of Tam in HMEC-E6 cells through modulation of AKT activity. At equimolar concentrations, Tam and tamoxifen ethyl bromide (QTam), a membrane impermeant analog of Tam, rapidly induced apoptosis in HMEC-E6 cells associated with an even more rapid decrease in phosphorylation of AKT at serine-473. Treatment of HMEC-E6 cells with 1.0 μ M QTam resulted in a 50% decrease in mitochondrial transmembrane potential, sequential activation of caspase-9 and -3, and a 90% decrease in AKT Ser-473 phosphorylation. The effects of both Tam and QTam were blocked by expression of constitutively active AKT (myristoylated AKT or AKT-Thr308Asp/Ser473-Asp). These data indicate that Tam and QTam induce apoptosis in HMEC-E6 cells through a plasma membrane-activated AKT-signaling pathway that results in (1) decreased AKT phosphorylation at Ser-473, (2) mitochondrial membrane depolarization, and (3) activated caspase-9 and -3.

Oncogene (2004) 23, 3851–3862. doi:10.1038/sj.onc.1207480
Published online 1 March 2004

Keywords: tamoxifen; apoptosis; AKT; plasma membrane; mammary epithelial cells

Introduction

The mechanism of both estrogen (E2) and tamoxifen (Tam) action in normal mammary epithelial cells (HMECs) and early proliferative breast lesions is poorly characterized. Typically, greater than 90% of normal HMECs express low levels of estrogen receptor (ER)

and are considered ER-'poor' (Anderson *et al.*, 1998). It has been observed that ER-'poor', but not ER-positive (ER+), HMECs proliferate in response to E2 (Anderson *et al.*, 1998). The National Surgical Adjuvant Breast and Bowel Project Breast Cancer Prevention Trial (BCPT) demonstrated that Tam markedly reduced the incidence of breast cancers in patients with atypical hyperplasia (Fisher *et al.*, 1998). While many of the benefits of Tam in the BCPT appear to be mediated through ER, it is unclear how Tam acted in ER-'poor' atypical mammary epithelial cells (Friedman, 1998).

We previously developed an *in vitro* model of Tam action in acutely damaged, ER-'poor' HMECs. In this model system, we demonstrated that 1.0 μ M Tam promotes apoptosis in ER-'poor' HMECs acutely transduced with HPV-16 E6 (HMEC-E6), but not in HMEC vector controls (HMEC-LX) (Dietze *et al.*, 2001; Seewaldt *et al.*, 2001a). Disruption of mitochondrial electron transport is an early feature of apoptosis. We observed in our model of acute cellular damage that Tam rapidly induced mitochondrial membrane depolarization and activation of caspase-9. Both the loss of mitochondrial membrane potential ($\Delta\Psi_m$) and caspase-9 induction occurred within 30–60 min (Dietze *et al.*, 2001). Effects observed at later times included mitochondrial condensation and caspase-3 activation at 6–12 h and morphologic and biochemical evidence of effector-phase apoptosis starting at 12 h.

Rapid signaling by E2, and E2 agonists/antagonists such as Tam, have been demonstrated in numerous cell types and are thought to be initiated by membrane-associated ER (Marquez and Pietras, 2001; Pietras *et al.*, 2001; Behl, 2002; Ho and Liao, 2002; Kousteni *et al.*, 2002; Levin, 2002; Ropero *et al.*, 2002; Segars and Driggers, 2002; Doolan and Harvey, 2003; Li *et al.*, 2003). Plasma-membrane association of ER α is ablated by mutation at Ser-522 (Razandi *et al.*, 2003a) and may require palmitoylation (Li *et al.*, 2003). ERs have also been shown to associate with caveolin-1, a major component of caveoli in the plasma membrane (Schlegel *et al.*, 1999; Chambliss *et al.*, 2002; Razandi *et al.*, 2002). Rapid, membrane-associated ER α -linked E2 signaling has been shown to activate signal-transduction pathways involving cAMP, Ca²⁺, NO, Ras, AKT, and mitogen-activated protein kinase (MAPK) (Aronica *et al.*, 1994; Improta-Brears *et al.*, 1999; Linford *et al.*,

*Correspondence: VL Seewaldt, DUMC, Box 2628, Durham, NC 27710, USA; E-mail: seewa001@mc.duke.edu

Received 3 October 2003; revised 23 December 2003; accepted 24 December 2003; Published online 1 March 2004

2000; Pietras *et al.*, 2001; Behl, 2002; Ho and Liao, 2002). In turn, some of these signaling pathways have been shown to activate ER α . For example, ER α is phosphorylated on Ser-118 and -167 by MAPK and AKT, respectively (Kato *et al.*, 1995; Campbell *et al.*, 2001).

AKT activity is critical for normal mammary gland homeostasis and overexpression of AKT is frequently observed in primary mammary tumors (Sun *et al.*, 2001). E2 promotes mammary epithelial cell survival through AKT activation; loss of AKT activity promotes apoptosis and mammary gland involution (Kandel and Hay, 1999; Okano *et al.*, 2000; Aoudjet and Vuori, 2001; Hutchinson *et al.*, 2001; Schwartzfeger *et al.*, 2001; Strange *et al.*, 2001; Sun *et al.*, 2001; Testa and Bellacosa, 2001). ER has been shown to directly interact with the regulatory subunit of phosphatidylinositol-3-OH kinase (PI3K) which results in the activation of AKT (Simoncini *et al.*, 2000). Association between the pleckstrin homology domain of AKT and the PI3K lipid product results in two events leading to AKT activation: (1) recruitment of AKT to the plasma membrane and (2) phosphorylation of Thr-308 in the kinase domain and of Ser-473 in the C-terminal hydrophobic motif domain by membrane bound kinases (Brazil and Hemmings, 2001; Whitehead *et al.*, 2001; Scheid and Woodgett, 2003). Overexpression of AKT and increased AKT-1 activity is frequently observed in primary breast cancer (Sun *et al.*, 2001) and dysregulation of AKT signaling appears to be an important event in mammary carcinogenesis.

Activation of AKT by plasma membrane-associated ER α has been recently shown to play an important role in proliferation, survival, and signal transduction in MCF-7 cells. E2 activation of AKT and MAPK in MCF-7 cells by plasma membrane-associated ER α has been shown to promote increased proliferation (Marquez and Pietras, 2001). Membrane-associated ER α has been shown to rapidly activate AKT following E2 treatment and thereby protect MCF-7 cells against proapoptotic stimuli (Razandi *et al.*, 2000; Marquez and Pietras, 2001; Stocia *et al.*, 2003a). Membrane-associated E2 activation of AKT also blocked both taxol- and UV-irradiation-induced apoptosis in MCF-7 cells (Razandi *et al.*, 2000). Rapid AKT activation appears to require ErbB2 activity (Stocia *et al.*, 2003a, b) and may be G-protein coupled (Razandi *et al.*, 2003b). In MCF-7 cells, E2 binding promotes ER α association with Shc which is then phosphorylated by Src and activates MAPK (Song *et al.*, 2002). An ER α construct targeted to the plasma membrane showed an increased ability to activate MAPK (Zhang *et al.*, 2002). Taken together, these observations suggest that activation of AKT through E2 binding to plasma membrane-associated ER α may play an important role in E2-related signal transduction in ER+ breast cancer cells.

The potential role of membrane-associated ER α regulation of AKT activity during Tam-induced apoptosis in ER-'poor' HMECs has not been studied. In our *in vitro* model of acute cellular damage, we tested the hypothesis that Tam rapidly induces a decrease in mitochondrial membrane potential ($\Delta\Psi_m$) and an increase in caspase-9 and -3 activities by a mechanism

that involves binding of Tam to plasma membrane-associated E2-binding sites and subsequent inactivation of AKT. We show that HMEC-E6 cells bound E2 on the cell surface and that this binding was blocked by either Tam or tamoxifen ethyl bromide (QTam), a membrane impermeant analog of Tam. Furthermore, both Tam and QTam induced a rapid decrease in $\Delta\Psi_m$ and rapid caspase-9 activation. These changes were preceded by loss of AKT phosphorylation at Ser-473 and followed by induction of apoptosis. Inhibition of AKT with SH-6 (Kozikowski *et al.*, 2003) mimicked and expression of constitutively active AKT blocked these events. These observations demonstrate an important role for plasma membrane-associated E2-binding sites in modulating AKT activity and apoptosis in ER-'poor' HMECs.

Results

Plasma membrane-association of tamoxifen aziridine (Taz) and tamoxifen in HMEC-E6 cells

[³H]Taz was found to distribute throughout HMEC-E6 cells (Figure 1). Of the Taz recovered, 43% was found in the nuclear fraction and 20, 18, 13, and 6% were

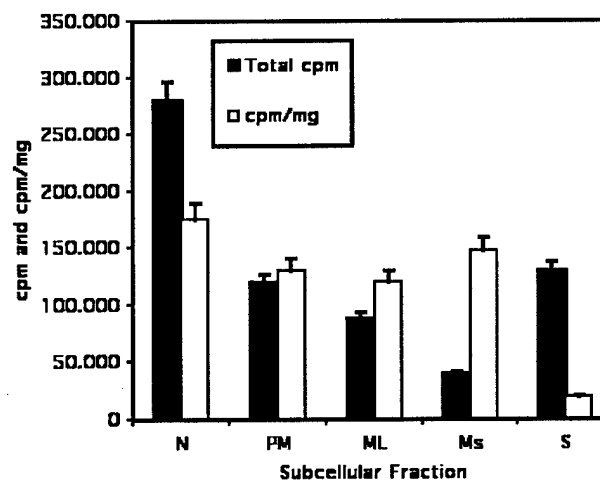


Figure 1 Distribution of [³H]Taz binding (c.p.m.) to HMEC-E6 subcellular fractions and the specific activity (c.p.m./mg protein) of [³H]Taz in each fraction. Cells were preincubated with 6.0 μ M unlabeled Tam and then incubated with 0.5 μ M [³H]Taz (Perkin-Elmer) for another 15 min. Next, the cells were washed with ice-cold PBS, trypsinized, pelleted, and resuspended in ice-cold homogenization buffer (50 mM Tris/10 mM sodium pyrophosphate/5 mM EDTA (pH 7.5), 150 mM NaCl, 1.0 mM Na orthovanadate, 10 mM NaF, 2 \times Complete protease inhibitor). The resuspended cells were homogenized at 4°C and the lysate, or respective supernatants, were centrifuged at 4°C for 10 min at 1000, 3000, and 20000g. The final supernatant was centrifuged for 60 min at 4°C and 100000g to produce microsomal and cytosolic fractions (N – nuclei; PM – plasma membrane; ML – mitochondria/lysosome; Ms – microsome; and S – soluble). All pellets were washed once by resuspending in homogenization buffer and repelleting. The washed pellets were resuspended in homogenization buffer and an aliquot counted. The crude nuclear fraction (1000g) was subfractionated into an enriched nuclear fraction and a plasma membrane fraction by discontinuous sucrose density gradient centrifugation. The mean of two experiments with s.d. is shown

found in the soluble, plasma membrane, mitochondrial/lysosomal, and microsomal fractions, respectively. The specific activity of Taz binding to the nuclear, enriched plasma membrane, mitochondrial/lysosomal, and microsomal fractions was similar, approximately 150 000 c.p.m./mg protein. The specific binding to the soluble fraction was much lower, 15 000 c.p.m./mg protein. The high percentage of Taz binding to the plasma membrane fraction at a specific activity of binding similar to subcellular compartments known to contain Taz-binding proteins was similar to observations made by Marquez and Pietras (2001) in Tam-treated MCF-7 cells. Taken together, these observations raised the possibilities that (1) the plasma membrane fraction of HMEC-E6 cells contained a Tam-binding protein and (2) Tam might, in part, induce apoptosis through a plasma membrane-associated binding site.

We tested for (1) the presence of E2-binding sites on the HMEC-E6 cell surface and (2) the ability of Tam to compete for potential plasma membrane-associated E2-binding sites using competitive binding with a membrane impermeable derivative of E2. Estradiol conjugated to BSA/fluorescence isothiocyanate (E2-BSA/FITC) does not cross the plasma membrane and has been extensively used to characterize plasma membrane binding of E2 (Razandi *et al.*, 2000; Marquez and Pietras, 2001; Segars and Driggers, 2002). Incubation of HMEC-E6 cells with 0.2 μ M E2-BSA/FITC resulted in ligand binding to the cell surface, predominantly at cell-cell interfaces (Figure 2a). This binding required the presence of E2 as BSA/FITC did not bind to HMEC-E6 cells (Figure 2b). Binding of E2-BSA/FITC to the cell surface of HMEC-E6 cells was blocked by 0.1 μ M E2 (Figure 2c). However, E2-BSA/FITC binding was not blocked by 1.0 μ M E2-17-hemisuccinate-BSA, a ligand that should not interfere with the specific binding of E2 (Figure 2d). These data clearly demonstrate the presence of specific binding sites for E2-BSA/FITC on the plasma membrane surface of HMEC-E6 cells.

We next tested whether Tam blocked the binding of E2-BSA/FITC to HMEC-E6 cells. Binding of E2-BSA/FITC to the cell surface of HMEC-E6 cells was specifically blocked by 1.0 μ M Tam (Figure 2e). These observations demonstrated that Tam competitively binds to cell surface-associated E2-binding sites in HMEC-E6 cells.

QTam blocks E2-BSA/FITC binding to and promotes apoptosis in HMEC-E6 cells

We observed that (1) a significant amount of Taz bound to the plasma membrane fraction of HMEC-E6 cells and (2) Tam blocked the E2-BSA/FITC binding to the cell surface. These observations raised the possibility that Tam might, in part, be inducing apoptosis through a plasma membrane-associated site. QTam, a quaternary ammonium derivative of Tam, does not cross the plasma membrane and has been extensively used to test for plasma membrane-mediated effects of Tam

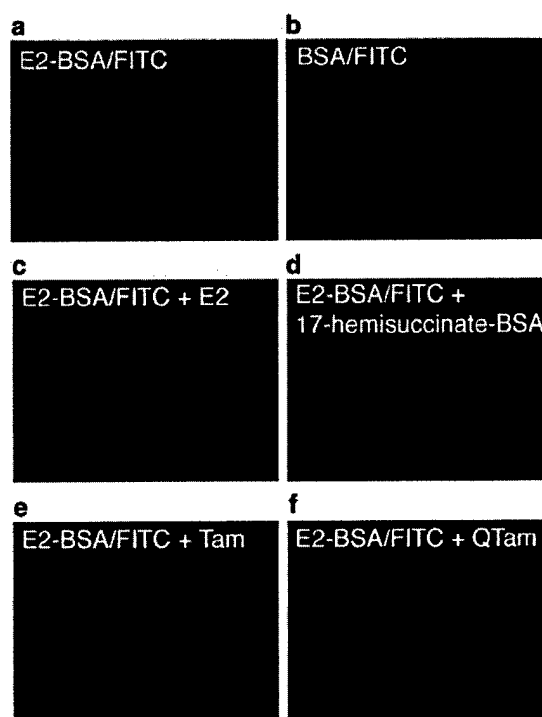


Figure 2 Binding of 200 nM E2-BSA/FITC to HMEC-E6 cells. (a) E2-BSA alone. (b) 1.0 μ M BSA/FITC alone. (c) E2-BSA/FITC with (0.1 μ M) E2. (d) E2-BSA/FITC with 1.0 μ M E2-17-hemisuccinate-BSA. (e) E2-BSA/FITC with 1.0 μ M Tam. (f) E2-BSA/FITC with 1.0 μ M QTam. The HMEC-E6 cells were plated and allowed to grow for 1 day, fixed for 10 min with 1% formaldehyde, washed with PBS, and incubated with the indicated ligand(s) for 15 min. The cells were then washed two times with ice-cold PBS and observed with a Nikon TE2000 microscope. Representative images are shown

(Fernandez *et al.*, 1993; Kirk *et al.*, 1994; Allen *et al.*, 2000; Dick *et al.*, 2002). Similar to observations with Tam (Figure 2e), 1.0 μ M QTam blocked the binding of E2-BSA/FITC to the cell surface of HMEC-E6 cells (Figure 2f). These observations demonstrated that QTam, similar to Tam, competitively binds to cell surface-associated E2-binding sites on HMEC-E6 cells.

We previously observed that 1.0 μ M Tam induced apoptosis in HMEC-E6 cells but promoted growth arrest alone in HMEC-LX controls (Dietze *et al.*, 2001). Similar to our observations in Tam-treated HMEC-E6 cells, apoptosis-sensitive HMEC-E6 cells treated with 1.0 μ M QTam for 18 h underwent apoptosis as evidenced by (1) Annexin V binding and (2) morphologic criteria demonstrated by electron microscopy (Figure 3a and data not shown). In contrast, a majority of HMEC-LX cells treated with 1.0 μ M QTam (similar to our prior observations utilizing Tam) underwent growth arrest but did not undergo apoptosis (Figure 3 and data not shown). HMEC-E6 cells treated with Tam or QTam had a 690 and 610% increase in the percentage of apoptotic cells, respectively. However, HMEC-LX cells demonstrated no change in the percentage of apoptotic cells.

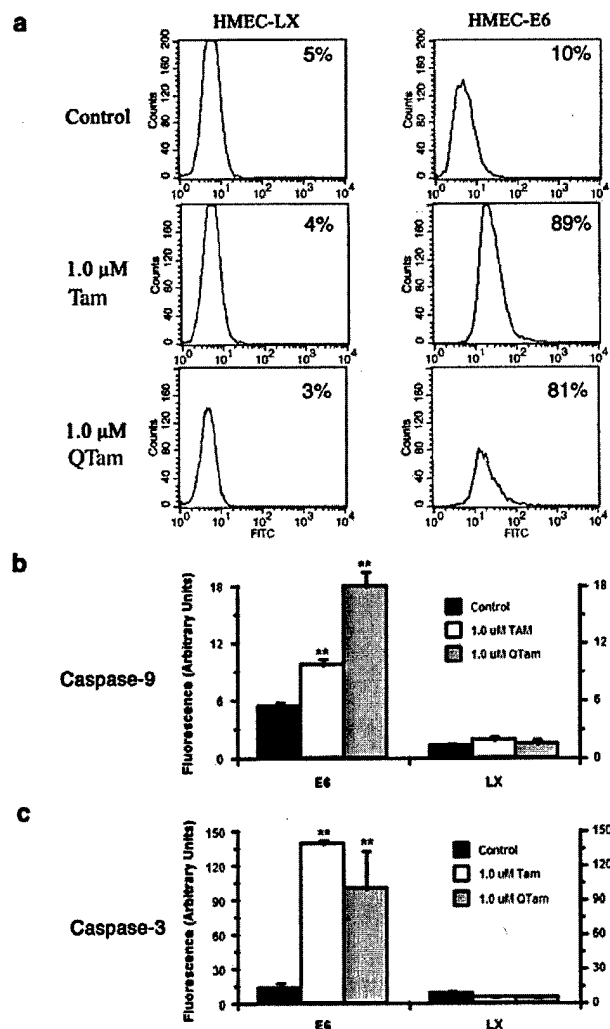


Figure 3 Tam and QTam induce apoptosis in HMEC-E6 cells and caspase-9 and -3 are activated. (a) HMEC-LX vector controls (passage 10) and HMEC-E6 cells (passage 10) treated with either 1.0 μ M Tam (Tam) or 1.0 μ M QTam (Q-Tam) for 18 h. Untreated control cells (Control) received an equivalent volume of ethanol. (b) Caspase-9 activity in apoptosis-sensitive HMEC-E6 cells (passage 11) and HMEC-LX controls (passage 11) treated with either 1.0 μ M Tam (Tam) or QTam (QTam) for 1 h. (c) Caspase-3 activity in HMEC-E6 cells and HMEC-LX controls (both passage 10) treated with either 1.0 μ M Tam (Tam) or 1.0 μ M QTam (QTam) for 18 h. Detection of apoptotic cells was with FITC-conjugated Annexin V as described in Materials and methods. These data are representative of three experiments. Cells for caspase assays were harvested by trypsinization, washed, and pelleted. The pellets were lysed and assayed according to the manufacturer's instructions (Clontech, Caspase 3 assay kit/K2026 and Caspase-9/6 assay kit/K2015). Assays were performed in duplicate. Data are the mean of three separate experiments with s.d. (**: $P < 0.025$)

QTam promotes mitochondrial membrane depolarization and activates caspase-9 and -3 in HMEC-E6 cells

Disruption of mitochondrial electron transport is an early feature of apoptosis. We previously observed that 1.0 μ M Tam promoted a decrease in $\Delta\Psi_m$ starting at 1 h in apoptosis-sensitive HMEC-E6 cells but not in HMEC-LX controls (Dietze *et al.*, 2001). The ability

of membrane impermeable QTam to induce a decrease in $\Delta\Psi_m$ in HMEC-E6 cells was tested by rhodamine 123 staining (Johnson *et al.*, 1980).

As previously observed (Dietze *et al.*, 2001), baseline $\Delta\Psi_m$ of apoptosis-sensitive HMEC-E6 cells was 25% lower than that of HMEC-LX controls (Table 1). Treatment of HMEC-E6 cells with either Tam or QTam for 6 h resulted in a dose-dependent decrease in $\Delta\Psi_m$. Treatment with 0.1 μ M Tam or QTam decreased $\Delta\Psi_m$ by 28 and 29%, respectively ($P < 0.02$) (Table 1). Treatment with 1.0 μ M Tam or QTam resulted in a 43 and 58%, respectively, decrease in $\Delta\Psi_m$ ($P < 0.01$) (Table 1). When HMEC-LX cells were treated with either 0.1 or 1.0 μ M Tam or QTam, there was no significant change in $\Delta\Psi_m$ ($P > 0.05$) (Table 1). Mitochondrial mass was measured by staining with nonyl-acridine orange (NAO), a fluorescent dye that specifically binds to the mitochondrial inner membrane independent of $\Delta\Psi_m$ (Boserma *et al.*, 1996). The mitochondrial mass of apoptosis-sensitive HMEC-E6 cells and HMEC-LX controls was the same as judged by NAO staining (Table 1). Thus, 1.0 μ M QTam, similar to 1.0 μ M Tam (Dietze *et al.*, 2001), promoted a decrease in $\Delta\Psi_m$ in apoptosis-sensitive HMEC-E6 cells but not in HMEC-LX controls.

Previously, we also observed that 1.0 μ M Tam promoted activation of caspase-9 and -3 in apoptosis-sensitive HMEC-E6 cells but not in HMEC-LX controls (Dietze *et al.*, 2001). Caspase-9 and -3 activations were maximal at 1 and 12–18 h, respectively. Here, we tested whether equimolar concentrations of Tam or membrane impermeable QTam similarly activated caspase-9 and -3 in HMEC-E6 cells at 1 and 18 h, respectively (Figure 3b, c). Caspase-9 activation was increased by 80 and 230% ($P < 0.01$) by Tam or QTam treatment, respectively, relative to untreated controls. Neither 1.0 μ M Tam nor QTam increased caspase-9 activity ($P > 0.05$) in HMEC-LX controls.

Caspase-3 activation gave similar results (Figure 3c). Activity was measured 18 h after treatment as above and was found to be significantly increased ($P < 0.01$) by 1000 and 670%, respectively, by treatment with either 1.0 μ M Tam or QTam. As observed with caspase-9 activity, caspase-3 activity was not increased

Table 1 Baseline mitochondrial membrane potential ($\Delta\Psi_m$) is decreased in HMEC-E6 cells relative to HMEC-LX vector control cells

	Treatment	E6	LX
NAO	0 h 1.0 μ M Tam	1.00 \pm 0.05	0.98 \pm 0.04
	6 h 1.0 μ M Tam	0.72 \pm 0.04	1.41 \pm 0.06
Rhodamine/NAO	0 h 1.0 μ M Tam	1.00 \pm 0.05	1.34 \pm 0.04
	6 h 0.1 μ M Tam	0.72 \pm 0.04	1.41 \pm 0.06
	6 h 1.0 μ M Tam	0.57 \pm 0.06	1.36 \pm 0.03
	6 h 0.1 μ M QTam	0.71 \pm 0.05	1.32 \pm 0.07
	6 h 1.0 μ M QTam	0.42 \pm 0.07	1.28 \pm 0.09

HMEC-E6 cells (passage 11, E6) and HMEC-LX cells (passage 11, LX) treated with 0.1 or 1.0 μ M tamoxifen (Tam) for 0 or 6 h. $\Delta\Psi_m$ is measured by rhodamine 123 staining and normalized to mitochondrial mass, measured by NAO staining. Fluorescence values are reported relative to ethanol-treated controls. Reported values represent the average of three separate experiments

in HMEC-LX controls after treatment for 18 h with either 1.0 μ M Tam or QTam. These observations showed that 1.0 μ M QTam, similar to Tam, activates caspase-3 in apoptosis-sensitive HMEC-E6 cells but not in HMEC-LX controls.

Tam and QTam reduce AKT phosphorylation at Ser-473 in HMEC-E6 cells

Phosphorylated AKT serves as a cell-survival signal that modulates mitochondrial depolarization and caspase-9 activation; decreased AKT-phosphorylation at Ser-473 is observed during apoptosis (Brazil and Hemmings, 2001; West et al., 2002). We hypothesized that membrane-associated effects of Tam might inhibit AKT activity in apoptosis-sensitive HMEC-E6 cells.

AKT Ser-473 phosphorylation showed a rapid, time-dependent loss of phosphorylation ($P < 0.01$) when HMEC-E6 cells were incubated with 1.0 μ M Tam (Figure 4a). Ser-473 phosphorylation was tested at 0, 5, 15, and 30 min. A 15 and 88% decrease was observed

at 5 and 15 min, respectively. At 30 min, the relative degree of phosphorylation was not significantly different ($P > 0.1$) than at 15 min. Identically treated HMEC-LX cells showed no significant decrease ($P > 0.1$). At baseline, passage-matched apoptosis-sensitive HMEC-E6 cells and HMEC-LX controls expressed similar levels of total AKT protein (Figure 4b). Treatment of HMEC-E6 cells with either 1.0 μ M Tam or QTam for 60 min resulted in a 98 and 90%, respectively, decrease in AKT phosphorylation at Ser-473 relative to untreated controls (Figure 4b, d). The loss of phosphorylation observed is similar to that seen after 30 min treatment with 1.0 μ M Tam. AKT activity was similarly decreased in HMEC-E6 cells treated with 1.0 μ M Tam or QTam by 93 and 91%, respectively (Figure 4c, e). Total AKT protein levels remained relatively constant and were not decreased by treatment with Tam or QTam in HMEC-E6 cells (Figure 4b, d). In contrast, treatment of HMEC-LX controls with either 1.0 μ M Tam or QTam had a much smaller decrease in levels of AKT Ser-473 phosphorylation, 20 and 54%, respectively, or in AKT activity, 0.0 and 8.0%, respectively (Figure 4b-e).

Inhibition of AKT activity promotes apoptosis and caspase-9/-3 activation in HMEC-E6 cells

As demonstrated above, we observed a temporal association between Tam/QTam-induced (1) induction of apoptosis, loss of $\Delta\Psi_m$, and caspase-9 and -3 activation and (2) loss of AKT-phosphorylation and AKT-activity (Figures 3 and 4). To test whether inhibition of AKT-activity could promote apoptosis and caspase-9 and -3 activation, apoptosis-sensitive HMEC-E6 cells were treated with SH-6, a specific inhibitor of AKT activity (Kozikowski et al., 2003). Treatment of HMEC-E6 cells with 12 μ M SH-6 resulted in apoptosis as evidenced by Annexin V-binding at 18 h (Figure 5a). In contrast, an equal volume of DMSO did not promote apoptosis. Treatment of apoptosis-sensitive HMEC-E6 cells with SH-6 also resulted in 780 and 1100% activation of caspase-9 at 1 h and caspase-3 at 12 h ($P < 0.025$), respectively (Figure 5b, c). As expected, treatment of HMEC-LX controls with SH-6 did not result in activation of caspase-9 or -3 (data not shown). Like Tam/QTam treatment, direct inhibition of AKT activity promotes apoptosis and activation of caspase-9 and -3 in HMEC-E6 cells but not in HMEC-LX controls.

Constitutively active AKT blocks Tam- and QTam-induced apoptosis in HMEC-E6 cells

To directly test whether a decrease in AKT activity was required for Tam- and QTam-induced apoptosis, constitutively active AKT constructs, AKT1-myr and AKT1-DD, were transduced into HMEC-E6 cells (Figure 6a). The resulting transduced cells were designated HMEC-Myr/E6 and HMEC-DD/E6, respectively. HPV-16 E6 and the empty retroviral vector LXS-N were also simultaneously expressed in

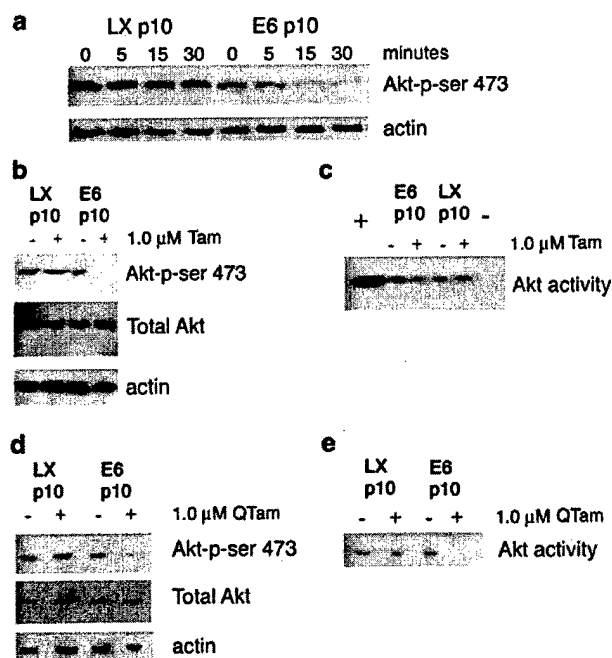


Figure 4 Loss of AKT Ser-473 phosphorylation and AKT activity were observed in Tam- and QTam-treated HMEC-E6 cells. (a, b, c) Equal amounts of protein lysate were loaded in each lane. Actin serves as a loading control. Membranes were incubated with antibody specific for AKT phosphoserine-473 (Akt-p-Ser 473) and AKT (Total Akt). HMEC-E6 cells were treated for the indicated time with (a) 1.0 μ M Tam (Tam). (b, d) HMEC-E6 cells were treated for the 1 h with (b) 1.0 μ M Tam (Tam) or (d) 1.0 μ M QTam (QTam). (c, e) AKT was immunoprecipitated from equal amounts of cell lysate and assayed. Lanes 1 and 6 of panel c show AKT-positive and -negative controls, respectively. AKT was assayed with a Cell Signaling Technology AKT assay kit according to the manufacturer's instructions. Bound antibodies were visualized using the appropriate secondary antibody-AP conjugate (Santa Cruz) and LumiPhos (Pierce). Luminescence was recorded using a Kodak Digital Science IS 440 system (Eastman Kodak)

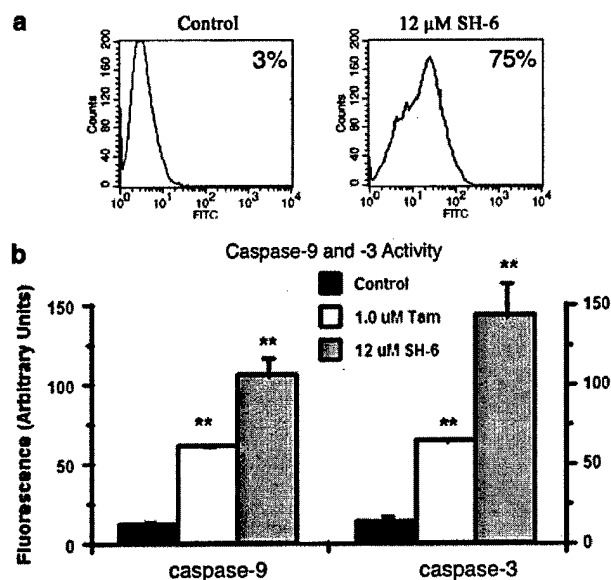


Figure 5 AKT inhibitor SH-6 promotes apoptosis and activation of both caspase-9 and -3 activity in HMEC-E6 cells. (a) Annexin V binding in HMEC-E6 cells treated with 12 μM SH-6 for 18 h (SH-6). Detection of apoptotic cells was with FITC-conjugated Annexin V as described in Materials and methods. Data are representative of two experiments. (b) Caspase-9 activity in HMEC-E6 cells (passage 11) treated with either 12 μM SH-6 (SH-6) or 1.0 μM Tam (Tam) for 1 h and caspase-3 activity in HMEC-E6 cells (passage 11) with identical treatment for 12 h. Experiments were performed in duplicate. Data are expressed as the mean of two separate experiments with s.d. (**: $P < 0.025$)

HMECs (HMEC-LX/E6) to ensure that apoptosis sensitivity was not abrogated by retroviral transduction or cell selection. All experiments were conducted within three passages of retroviral transduction. Expression of the constitutively active AKT constructs and HPV-16 E6 were confirmed by Western analysis using antibodies specific for each construct (Figure 6b).

HMEC-Myr/E6 and HMEC-DD/E6 cells had significantly ($P < 0.01$) increased AKT activity relative to HMEC-LX/E6 cells (Figure 6c). The modest, but significant in AKT activity seen in HMEC-LX/Myr and -LX/DD is due to the ability of the LXSN transduction system to stably insert one copy of the transduced gene into target cells. In untreated cells, AKT activity was 400% higher in HMEC-Myr/E6 and 300% higher in HMEC-LX/DD cells than HMEC-LX/E6 cells. As expected, neither 1.0 μM Tam or QTam treatment had a significant ($P > 0.1$) effect on AKT activity in either HMEC-LX/Myr or -LX/DD cells (Figure 6c, d). However, consistent with results obtained with HMEC-E6 cells (Figure 4c, e), treatment with either Tam or QTam resulted in, respectively, 93 and 87% decreases ($P < 0.01$) in the AKT activity of HMEC-LX/E6 cells. In addition, the expression of AKT was not decreased by treatment with either Tam (data not shown) or QTam for 1 h (Figure 6e).

Annexin V binding was utilized to test whether constitutive activation of AKT in HMEC-E6 cells

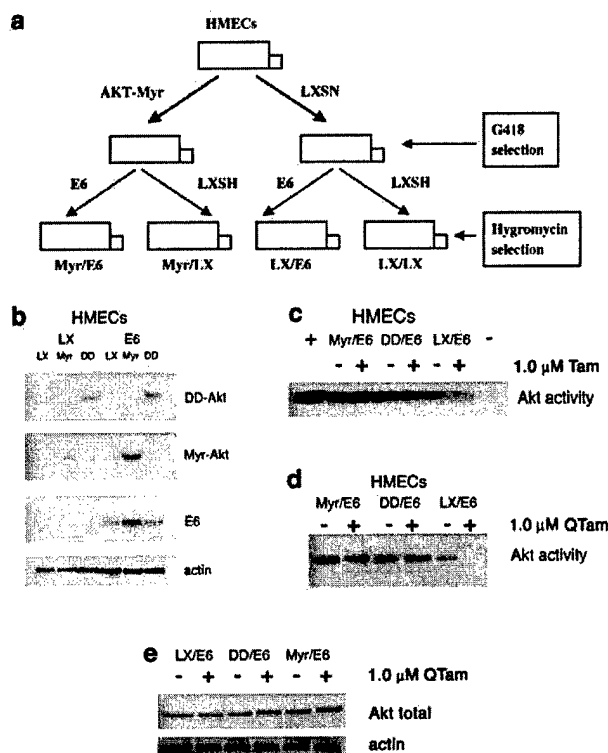


Figure 6 Constitutively active AKT expression in HMEC-E6 cells blocks loss of AKT activity on treatment with either Tam or QTam. (a) Illustration of the selection scheme used to produce the HMEC double transfectants, (b) Expression of the transfected gene products in the double transfectants as demonstrated by Western blotting, and the AKT activity of double transfectants (c) treated with 1.0 μM Tam or (d) treated with 1.0 μM QTam. For expression of gene products, cells were harvested, equal amounts of protein were loaded in each lane, and the proteins separated by SDS-PAGE. The membrane was sequentially probed with anti-HA, anti-Myc myristoylation sequence, anti-HPV16 E6, and anti-β-actin antibodies (first two antibodies from Cell Signaling Technology, second two antibodies from Santa Cruz). For AKT activity, cells were treated for 1 h and harvested by trypsinization. Equal amounts of cell lysate were immunoprecipitated and assayed using a Cell Signaling Technology AKT assay kit according to the manufacturer's instructions. Lanes 1 and 6 of panel a show AKT-positive and -negative controls, respectively. Bound antibodies were visualized using the appropriate secondary antibody-AP conjugate (Santa Cruz) and LumiPhos (Pierce). Luminescence was recorded using a Kodak Digital Science IS440 system (Eastman Kodak)

blocked Tam- or QTam-induced apoptosis. Similar to results obtained in apoptosis-sensitive HMEC-E6 cells (Figure 3a), Tam and QTam induced apoptosis in HMEC-LX/E6 cells (Figure 7a). Treatment of HMEC-LX/E6 cells with either 1.0 μM Tam or QTam for 18 h resulted in a majority of cells undergoing apoptosis, 85 and 53%, respectively, compared to 6% in untreated controls. In contrast, when HMEC-Myr/E6 or HMEC-DD/E6 cells were treated with either 1.0 μM Tam or QTam, there was no significant difference ($P > 0.05$) in the number of apoptotic cells, 13–18%, when compared to untreated controls, 5–8% (Figure 7a).

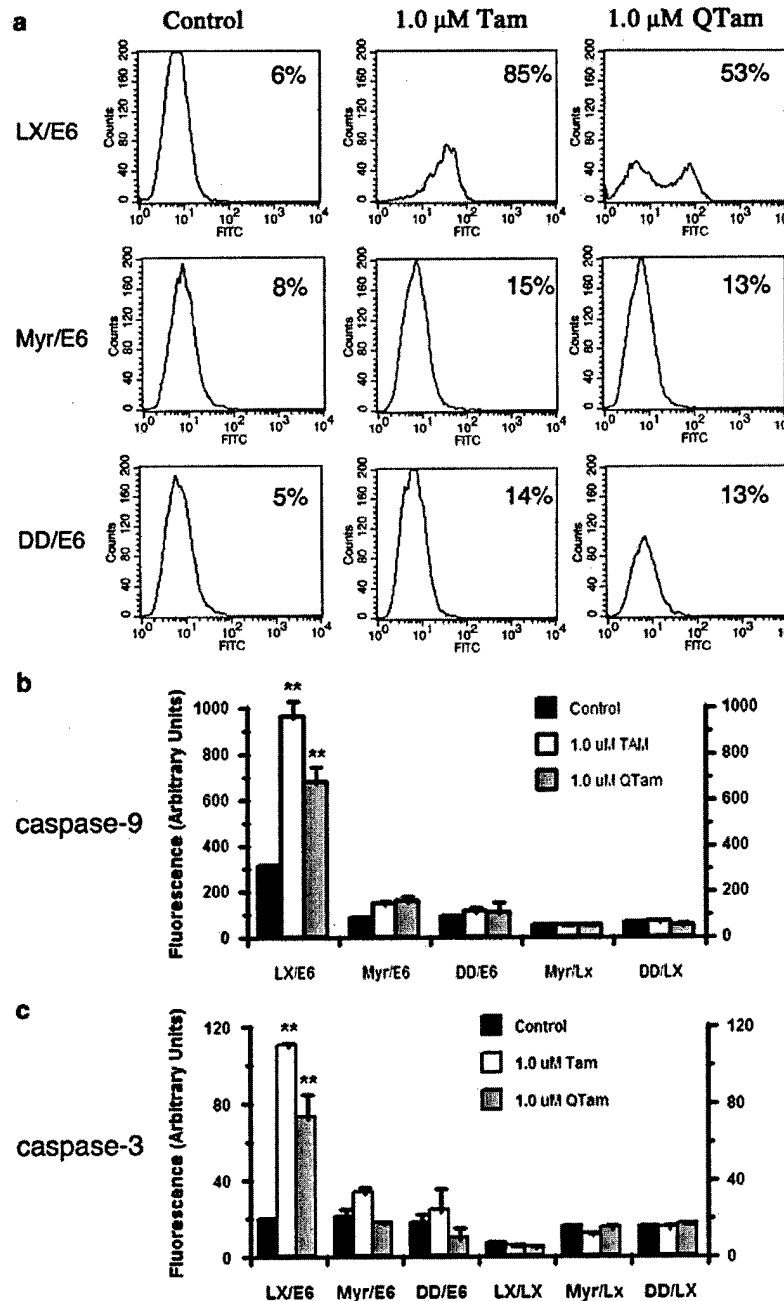


Figure 7 Tam- and QTam-induced apoptosis and caspase-9 and -3 activation in HMEC-LX/E6 cells but not in HMEC-Myr/E6 or -DD/E6 cells. (a) HMEC-LX/E6 controls (passage 11), HMEC-Myr/E6 cells (passage 11), and HMEC-DD/E6 cells (passage 11) treated with either 1.0 μ M Tam (Tam) or 1.0 μ M QTam (Q-Tam) for 18 h. Untreated control cells (Control) received an equivalent volume of ethanol. (b) Caspase-9 activity in apoptosis-sensitive HMEC-LX/E6 cells (passage 12) and apoptosis-insensitive HMEC-Myr/E6 and -DD/E6 cells (both passage 12) treated with either 1.0 μ M Tam (Tam) or QTam (QTam) for 1 h. (c) Caspase-3 activity in apoptosis-sensitive HMEC-LX/E6 cells (passage 12) and apoptosis-insensitive HMEC-Myr/E6 and -DD/E6 cells (both passage 12) treated with either 1.0 μ M Tam (Tam) or 1.0 μ M QTam (QTam) for 12 h. Detection of apoptotic cells was with FITC-conjugated Annexin V as described in Materials and methods. These data are representative of three experiments. Cells for caspase assays were harvested by trypsinization, washed, and pelleted. The pellets were lysed and assayed according to the manufacturer's instructions (Clontech, Caspase 3 assay kit/K2026 and Caspase9/6 assay kit/K2015). Assays were performed in duplicate. Data are the mean of three separate experiments with s.d. (**: $P < 0.025$)

Constitutively active AKT blocks Tam- and QTam-induced mitochondrial membrane depolarization and activation of caspase-9 and -3 in HMEC-E6 cells

Expression of the constitutively active AKT-Myr and AKT-DD constructs in HMEC-E6 cells blocked the ability of 1.0 μ M Tam or QTam to decrease $\Delta\Psi_m$. $\Delta\Psi_m$ remained unchanged in HMEC-Myr/E6 and HMEC-DD/E6 cells after treatment for 1 or 3 h with either Tam or QTam ($P>0.05$) (Table 2b, c). However, apoptosis-sensitive HMEC-LX/E6 cells showed a 20 and a 30% decrease in $\Delta\Psi_m$ when treated with 1.0 μ M Tam or QTam, respectively (Table 2b, c). The mitochondrial mass was similar in each untreated cell type (Table 2a). Interestingly, HMEC-Myr/E6 and HMEC-DD/E6 cells had 51 and 30% higher baseline levels of $\Delta\Psi_m$, respectively, than HMEC-LX/E6 cells.

Expression of the constitutively active AKT-Myr and AKT-DD constructs in HMEC-E6 cells also blocked the ability of Tam and QTam to activate caspase-9. Apoptosis-resistant HMEC-Myr/E6 and HMEC-DD/E6 cells treated with either 1.0 μ M Tam or QTam for 1 h exhibited only a slight increase (81–94 and 11–24%, respectively, $P>0.05$) in caspase-9 activation (Figure 7b). This was in marked contrast to HMEC-LX/E6 cells that, similar to HMEC-E6 cells, exhibited a significant increase ($P<0.01$) in caspase-9 activation after treatment with either Tam or QTam, 210 and 120%, respectively. As expected, treated HMEC-Myr/LX and HMEC-DD/LX controls did not exhibit an increase in caspase-9 activation. Baseline caspase-9 activity was significantly ($P<0.01$) lower in control HMEC-Myr/E6 and HMEC-DD/E6 cells when compared to control HMEC-LX/E6 cells (Figure 7b).

Similar to results obtained for caspase-9, expression of the constitutively active AKT-Myr and AKT-DD constructs in HMEC-E6 cells blocked the ability of Tam

and QTam to activate caspase-3. Apoptosis-resistant HMEC-Myr/E6 and HMEC-DD/E6 cells treated with either 1.0 μ M Tam or QTam for 12 h exhibited no significant change ($P>0.05$) in caspase-3 activation (Figure 7c). In contrast, HMEC-LX/E6 cells, similar to HMEC-E6 cells, exhibited a significant increase in caspase-3 activation after treatment with either 1.0 μ M Tam or QTam, 480 and 280%, respectively. As expected, Tam and QTam treated HMEC-Myr/LX and HMEC-DD/LX controls did not exhibit a significant ($P>0.05$) increase in caspase-3 activation. Unlike results obtained for caspase-9, baseline caspase-3 activity was similar in HMEC-Myr/E6, HMEC-DD/E6, and HMEC-LX/E6 cells (Figure 7c).

Discussion

The 'classic' or genomic mechanism of tamoxifen action requires the presence of ER and changes in both transcription and translation due to alteration(s) in promoter site occupancy. The interaction between Tam and nuclear ER has been well characterized (O'Regan and Jordan, 2002). However, there is evidence that E2, and perhaps antiestrogens, act through rapid, nongenomic signaling pathways that are initiated by ligand binding to plasma membrane-associated E2-binding sites (Marquez and Pietras, 2001; Pietras et al., 2001; Behl, 2002; Ho and Liao, 2002; Koustni et al., 2002; Levin, 2002; Ropero et al., 2002; Segars and Driggers, 2002; Doolan and Harvey, 2003; Li et al., 2003). Both E2 and Tam have been found to have specific binding sites on the plasma membrane. While there have been many reports of plasma membrane ER, there have been few reports of plasma membrane mediated effects of Tam in normal breast cells or breast cancer cell lines (Kirk et al., 1994).

Table 2 Baseline mitochondrial membrane potential ($\Delta\Psi_m$) is decreased in HMEC-Myr/E6 and -DD/E6 cells relative to HMEC-LX/E6, -Myr/LX, and -DD/LX control cells. (a) Baseline mitochondrial mass (NAO), potential (Rhodamine), and normalized potential (Rhodamine/NAO). (b) HMECs treated with 1.0 μ M Tam for 1 or 3 h. (c) HMECs treated with 1.0 μ M QTam for 1 or 3 h. $\Delta\Psi_m$ is measured by rhodamine 123 staining and normalized to mitochondrial mass, measured by NAO staining

	LX	LX/E6	Myr/LX	DD/LX	Myr/E6	DD/E6
(a)						
NAO	0.71 \pm 0.07	0.71 \pm 0.05	0.75 \pm 0.07	0.69 \pm 0.07	0.61 \pm 0.07	0.72 \pm 0.03
Rhodamine	0.88 \pm 0.05	0.76 \pm 0.04	0.98 \pm 0.06	1.01 \pm 0.06	0.85 \pm 0.06	0.87 \pm 0.09
Rhod/NAO	1.23 \pm 0.07	0.92 \pm 0.05	1.30 \pm 0.06	1.46 \pm 0.06	1.39 \pm 0.06	1.20 \pm 0.09
(b)						
	Treatment	LX/E6	Myr/LX	DD/LX	Myr/E6	DD/E6
Rhod/NAO	0 h TAM	1.00 \pm 0.05	1.83 \pm 0.06	1.98 \pm 0.06	1.76 \pm 0.06	2.23 \pm 0.09
	1 h TAM	0.83 \pm 0.04	1.78 \pm 0.03	2.11 \pm 0.05	1.69 \pm 0.07	2.39 \pm 0.07
	3 h TAM	0.80 \pm 0.03	1.79 \pm 0.04	1.93 \pm 0.05	1.75 \pm 0.06	2.27 \pm 0.08
(c)						
	Treatment	LX/E6	Myr/LX	DD/LX	Myr/E6	DD/E6
Rhod/NAO	0 h QTam	1.00 \pm 0.09	1.21 \pm 0.10	1.24 \pm 0.07	1.37 \pm 0.07	1.26 \pm 0.05
	1 h QTam	0.69 \pm 0.07	1.32 \pm 0.08	1.19 \pm 0.05	1.35 \pm 0.08	1.32 \pm 0.05
	3 h QTam	0.70 \pm 0.06	1.32 \pm 0.05	1.23 \pm 0.09	1.37 \pm 0.05	1.32 \pm 0.09

Fluorescence values are reported relative to ethanol-treated controls. Reported values represent the average of three separate experiments

The molecular mechanism(s) of Tam action in ER-'poor' HMECs is not well characterized. We previously developed an *in vitro* model of early mammary carcinogenesis and acute cellular damage of ER-'poor' HMECs. In this system, acute cellular damage was modeled by transduction with a retroviral vector coding for the HPV-16 E6 protein. We observed that Tam-treated HMEC-E6 cells rapidly underwent apoptosis, while HMEC-LX vector controls underwent growth arrest alone (Dietze *et al.*, 2001). Tam-induced apoptosis in HMEC-E6 cells was associated with a rapid decrease in $\Delta\Psi_m$ followed by sequential activation of caspase-9 and -3 (Dietze *et al.*, 2001). The rapidity of Tam's action in HMEC-E6 cells raised the possibility that Tam might act through a 'nonclassic', plasma membrane-associated signaling pathway.

Here, we provide evidence for (1) the presence of plasma membrane-associated E2-binding sites, (2) Tam initiation of apoptosis in HMEC-E6 cells by binding to plasma membrane-associated sites, and (3) the association of apoptosis with decreased AKT activity and Ser-473 phosphorylation. Initial experiments demonstrated that (1) Taz was enriched in a plasma membrane fraction prepared from Taz-treated HMEC-E6 cells (Figure 1) and (2) incubation of HMEC-E6 cells with 0.2 μM E2-BSA/FITC resulted in specific binding to the cell surface that was blocked by coinubation with 0.1 μM E2 (Figure 2c) but not by 1.0 μM E2-17-hemisuccinate-BSA (Figure 2d). These observations suggested the presence of plasma membrane-associated binding sites in HMEC-E6 cells for both Tam and E2. QTam (1) is a quaternized derivative of Tam which does not cross the plasma membrane (Fernandez *et al.*, 1993; Kirk *et al.*, 1994; Allen *et al.*, 2000; Dick *et al.*, 2002), (2) has similar binding characteristics to Tam (Jarman *et al.*, 1986; Allen *et al.*, 2000), and (3) like Tam, rapidly induced apoptosis in HMEC-E6 cells associated with mitochondrial membrane depolarization and caspase-9/-3 activation (Figure 3 and Table 1). Binding of E2-BSA/FITC to the plasma membrane surface of HMEC-E6 cells was specifically blocked by either 1.0 μM Tam or QTam (Figure 2e, f). These observations demonstrated that Tam and QTam competitively bound to cell surface-associated E2-binding sites on HMEC-E6 cells.

Phosphorylation of Thr-308 and Ser-473 activate AKT and serve as a cell-survival signal. Loss of AKT phosphorylation at Ser-473 is observed during apoptosis (Brazil and Hemmings, 2001; West *et al.*, 2002). Recently, plasma membrane-associated sites for E2 have been shown to modulate AKT activity and signaling (Marquez and Pietras, 2001). Here, we provide evidence that membrane-associated effects of Tam decrease AKT activity and promote apoptosis in HMEC-E6 cells. Tam treatment of HMEC-E6 cells, but not HMEC-LX cells, resulted in a rapid, time-dependent loss of Ser-473 phosphorylation (Figure 4a). Loss of Ser-473 phosphorylation was complete at approximately 15 min. Treatment of apoptosis-sensitive HMEC-E6 cells with either 1.0 μM Tam or QTam resulted in (1) a decrease in AKT Ser-473 phosphorylation and AKT activity at 1 h (Figure 4b-e) and (2)

biochemical and morphologic evidence of effector-phase apoptosis at 18 h (Figure 3 and data not shown).

SH-6 is a recently described specific inhibitor of AKT (Kozikowski *et al.*, 2003). AKT activity is blocked without inhibition of PI3K or PDK1. HMEC-E6 cells treated with SH-6 demonstrated both increased caspase-9 and -3 activities and apoptosis (Figure 5). This demonstrated that direct inhibition of AKT had the same effects on HMEC-E6 cells as treatment with either Tam or QTam. We next explored whether or not constitutively active AKT constructs were able to block Tam- or QTam-induced decrease in $\Delta\Psi_m$, activation of caspase-9 and -3, and apoptosis.

Two constitutively active AKT constructs were used to test whether active AKT blocked Tam- and QTam-induced apoptosis in HMEC-E6 cells (Figure 6). The first construct incorporates the Myc myristoylation sequence into AKT1 (AKT-Myr). The expressed protein is inserted into the plasma membrane and, as a result, resides in proximity to activator kinases, which by mass action phosphorylate and activate AKT without the need of elevated PI3K activity. The second construct, AKT308D/S473D (AKT-DD), was generated by mutating the wild-type AKT phosphorylation sites Thr-308 and Ser-473 to Asp (Hutchinson *et al.*, 2001). Expression of either AKT-Myr or AKT-DD in HMEC-E6 cells blocked the ability of Tam and QTam to induce apoptosis (Figure 7a). HMEC-Myr/E6 or HMEC-DD/E6 cells treated with either 1.0 μM Tam or QTam did not exhibit (1) a decrease in $\Delta\Psi_m$ (Table 2b) or (2) increased caspase-9/-3 activation (Figure 7b, c). Thus, both AKT-Myr and -DD were able to block the effects of either 1.0 μM Tam or QTam in apoptosis-sensitive HMEC-E6 cells.

Unexpectedly, HMEC-E6 and -LX/E6 cells showed a decrease in $\Delta\Psi_m$ and elevated caspase-9 activity without an accompanying increase in caspase-3 activity when compared to HMEC-LX cells (Tables 1 and 2; Figures 3b, c and 7b, c). The decrease in $\Delta\Psi_m$ was blocked by the expression of either of the constitutively active AKT constructs (Table 2). Increased caspase-9 activity was also blocked (Figure 7b). Thus, there appears to be an increase in the basal level of mitochondrial depolarization and caspase-9 activation in HMECs expressing E6 that is blocked by constitutively active AKT.

Taken together, these data indicate that Tam-induced apoptosis in HMEC-E6 cells is mediated through a plasma membrane-associated site and subsequent rapid inhibition of AKT activity. Tam did not directly inhibit AKT since QTam had the same effect on AKT. The results also indicate that a second, nongenomic pathway exists by which Tam might act as a chemoprevention/chemotherapeutic agent in breast cancer, possibly in ER-'poor' mammary epithelial cells. Membrane-bound ER has been shown to activate AKT when MCF-7 cells were stimulated with E2 (Marquez and Pietras, 2001; Razandi *et al.*, 2003b). However, we have previously shown that while Tam induced apoptosis in this system but 4-hydroxyTam did not (Dietze *et al.*, 2001). 4-HydroxyTam binds ER with higher affinity than Tam and would also be expected to induce apoptosis

mediated by ER binding. Thus, this AKT inhibition pathway may involve ER localized to the plasma membrane or an as yet uncharacterized receptor. We are now determining the properties of the receptor involved as well as the mechanism by which Tam or QTam inhibit AKT activity by binding a plasma membrane-associated receptor.

Materials and methods

Materials

All chemicals were obtained from Sigma-Aldrich (St Louis, MO, USA), DNA primers from GibcoBRL (Bethesda, MD, USA), and cell culture plasticware from Corning (Corning, NY, USA) unless otherwise noted. A 1.0 mM Tam stock solution was prepared in ethanol and stored in opaque tubes at -70°C . Tam was only used under reduced yellow lighting. AKT inhibitor SH-6 was obtained from CalBiochem (San Diego, CA, USA). Complete protease inhibitor was obtained from Roche (Indianapolis, IN, USA).

QTam was synthesized according to established methods (Allen *et al.*, 2000) and stored desiccated in amber vials at -20°C . Tam and QTam were resolved with a 25 cm \times 2.1 mm ID pkb100 column (Supelco, Bellefonte, PA, USA). The mobile phase was 40% aqueous 0.05% trifluoroacetic acid (TFA) and 60% aqueous 95% acetonitrile with 0.05% TFA. The flow rate was 1.0 ml/min and each run was 15 min with 5 min between injections. The column effluent was monitored at 280 nm and the retention time of Tam and QTam were 4.3 and 4.8 min, respectively. QTam was $>95\%$ pure by reverse phase HPLC. The high-resolution FAB-MS and ^1H NMR spectra were consistent with reported values (data not shown).

Construction of retroviral vectors

Two retroviral vectors containing the coding sequences for constitutively active AKT were generated. The pAkt1-Myr plasmid (Upstate Biotechnology, Lake Placid, New York, USA) was digested with Tsp509I; the AKT308D/S473D (AKT-DD) plasmid (generous gift of J Woodgett) was digested with *Xho*I and *Eco*R1 (Hutchinson *et al.*, 2001). The released inserts were inserted into the cloning site of the LXSN retrovirus as previously described (Seewaldt *et al.*, 1995; Seewaldt *et al.*, 1997b). Correct orientation and sequence were verified by direct sequencing. Transducing virions were derived as previously described (Seewaldt *et al.*, 1995).

Cell culture conditions and retroviral transduction

Cell culture Normal HMEC strain AG11132 (M Stampfer #172R/AA7) was purchased from the National Institute of Aging, Cell Culture Repository (Coriell Institute, Camden, NJ, USA; Stampfer, 1985). HMEC strain AG11132 was established from normal tissue obtained at reduction mammoplasty, had a limited life span in culture, and failed to divide after approximately 20–25 passages. HMECs exhibit a low level of ER staining characteristic of normal mammary epithelial cells. HMECs were grown and mycoplasma testing was performed as previously reported (Seewaldt *et al.*, 1997a, 1999b).

Single construct transduction The LXSN16E6 retroviral vector containing the HPV-16 E6 coding sequence was provided by D Galloway (Fred Hutchinson Cancer Research Center, Seattle, WA, USA) (Demers *et al.*, 1996). HMECs were transduced with PA317-LXSN16E6 and PA317-LXSN

and selected as described (Seewaldt *et al.*, 1995). Transduced HMECs expressing the HPV-16 E6 construct were designated HMEC-E6 and vector control clones were designated HMEC-LXSN. All cells were maintained in the absence of G418 selection to minimize exposure to G418. All experiments were performed on mass cultures.

Double retroviral transductions Expression and selection of two retroviral constructs are adapted from previously published methods (Seewaldt *et al.*, 2001b). Construction of retroviral vectors containing either the coding sequences for AKT1-Myr or AKT-DD was as described (Seewaldt *et al.*, 1995). Transducing virions from either PA317-AKT-Myr or PA317-AKT-DD or the control PA317-LXSN (without insert) and PA317-LXSHE6 or PA317-LXSH were used for the first and second rounds of transduction, respectively (Figure 6a). At the completion of selection, all cells were removed from selection and used within three passages of the second transduction. Double transduced HMECs expressing the (1) LXSN/LXSH constructs were designated HMEC-LX/LX, (2) LXSN/HPV-16E6 constructs were designated HMEC-LX/E6, (3) LAKT-MyrSN/LXSH constructs were designated HMEC-Myr/LX, and (4) LAKT-MyrSN/HPV-16E6 constructs were designated HMEC-Myr/E6. Cells expressing the AKT-DD construct were designated either HMEC-DD/LX or HMEC-DD/E6.

Plasma membrane association of Tam and E2-BSA/FITC

Acutely transduced HMEC-E6s were plated in phenol-red-free media on glass Petri dishes. The cells were grown to 50% confluency and preincubated with $6.0\text{ }\mu\text{M}$ unlabeled Tam at 37°C for 10 min. After addition of $0.5\text{ }\mu\text{M}$ [^3H]Taz (B Katzenellenbogen, University of Illinois, Urbana, IL, USA), the incubation was continued for another 15 min. Next, the cells were washed with ice-cold PBS, trypsinized, pelleted, and resuspended in ice-cold homogenization buffer (50 mM Tris/10 mM sodium pyrophosphate/5 mM EDTA (pH 7.5), 150 mM NaCl, 1.0 mM Na orthovanadate, 10 mM NaF, $2\times$ Complete protease inhibitor). The resuspended cells were homogenized at 4°C with a Dounce homogenizer and the lysate, or respective supernatants, were centrifuged at 4°C for 10 min at 1000, 3000, and 20 000 g. The final supernatant was centrifuged for 60 min at 4°C and 100 000 g to produce microsomal and cytosolic fractions. All pellets were washed once by resuspending in homogenization buffer and repelleting. The washed pellets were resuspended in homogenization buffer, $5\text{ }\mu\text{l}$ of each fraction was counted in a scintillation counter, and the remainder was stored at -70°C . The crude nuclear fraction (1000 g) was subfractionated into an enriched nuclear fraction and a plasma membrane fraction by discontinuous sucrose density gradient centrifugation (Marquez and Pietras, 2001). The resulting fractions were assayed for the presence of DNA, 5'-nucleotidase activity, and LDH activity (Marquez and Pietras, 2001).

For binding of E2-BSA/FITC, cells were seeded in glass-bottomed microwell plates (MatTek, Ashland, MA, USA) at low density and allowed to attach for 1 day. The cells were fixed for 10 min in 1% formaldehyde in PBS at room temperature and then incubated for 15 min in room temperature PBS containing $10\text{ }\mu\text{M}$ BSA/FITC (Molecular Probes, Eugene, OR, USA), $0.2\text{ }\mu\text{M}$ E2-BSA/FITC, or $0.2\text{ }\mu\text{M}$ E2-BSA/FITC in the presence of either (1) $0.1\text{ }\mu\text{M}$ E2, (2) $1.0\text{ }\mu\text{M}$ Tam, $1.0\text{ }\mu\text{M}$ QTam, or (3) $1.0\text{ }\mu\text{M}$ E2-17-hemisuccinate-BSA as competitors. The cells were then washed rapidly twice with ice-cold PBS and observed at room temperature with a Nikon TE2000 fluorescence microscope (Nikon USA, Melville, NY,

USA) coupled to a Photometrics cooled CCD camera (Roper Scientific, Trenton, NJ, USA), using Metamorph software (Universal Imaging, Downingtown, PA, USA) and the preprogrammed settings for FITC.

SDS-PAGE and Western analysis

Three T-75 flasks of each cell type were grown to 50% confluency, treated for 1 h with 1.0 μ M Tam, harvested as previously described (Seewaldt et al., 2001b), resuspended in immunoprecipitation buffer (homogenization buffer with 1.0% Triton X-100, 0.1 mM PMSF, 0.1 mM TLCK, 0.1 mM TPCK, 1 μ g/ml pepstatin, 1 μ g/ml leupeptin, 15 μ g/ml calpain inhibitor I, 1 μ g/ml aprotinin, 50 μ g/ml bestatin), aliquoted, and stored at -70°C until use. The lysate was separated by 10% SDS-PAGE and transferred to a PVDF membrane that was blocked overnight with 10% BSA (w/v) dissolved in Tris-buffered saline with 0.1% Tween-20 (TTBS). The blocked membrane was incubated with antibodies directed against AKT (#9272, Cell Signaling Technology, Beverly, MA, USA), AKT phosphoserine-473 (#9271, Cell Signaling Technology), or actin (sc-1616, Santa Cruz Biotechnology, Santa Cruz, CA, USA) in TTBS. To detect protein expression of the AKT-DD and AKT-Myr, the blocked membrane was incubated with anti-HA tag antibody (#2362, Cell Signaling Technology) and anti-Myc tag antibody (#2276, Cell Signaling Technology), respectively. Anti-HPV16 E6 antibody was used to detect HPV16 E6 protein (Santa Cruz, sc-1583). The membrane was washed in TTBS, incubated with a 1:6000 dilution of the appropriate secondary antibody conjugated to alkaline phosphatase (Santa Cruz Biotechnology), washed, and developed with LumiPhos WB (Pierce Chemical, Rockford, IL, USA). The image was digitized with a Kodak Digital Science IS 440

and quantitated using Kodak 1D™ software (Eastman Kodak, Rochester, NY, USA).

Measurement of apoptosis, caspase-9/-3 activity, and mitochondria depolarization

Apoptosis was measured by Annexin V binding and FACS after treatment with 1.0 μ M Tam or 1.0 μ M QTam for 18 h as previously described (Seewaldt et al., 1999a; Dietze et al., 2001). Caspase-9 was measured after 1 h treatment and caspase-3 was measured after 12–18 h treatment, as noted, with either 1.0 μ M Tam or 1.0 μ M QTam. Cells were harvested by trypsinization. The cells were washed once with 100 volumes of ice-cold PBS and pelleted. Caspase-9 and -3 activities were then assayed according to the manufacturer's instructions using a Caspase 9/6 (K2015) or Caspase 3 (K2026) assay kit (Clontech, Palo Alto, CA, USA). Mitochondrial depolarization was also measured as previously described (Dietze et al., 2001) on cells treated for 1–6 h, as noted, with 0.10 or 1.0 μ M of either Tam or QTam.

Acknowledgements

We acknowledge the generous gifts of (1) J Woodgett for the AKT308D/S473D plasmid, (2) D Galloway for the LXSN16E6 retroviral vector containing the HPV-16 E6 coding sequence, and (3) B Katzenellenbogen for the [^3H]tamoxifen aziridine. This work is supported by NIH/NCI Grants 2P30CA14236-26 (VLS, ECD), R01CA88799 (VLS), R01CA98441 (VLS), NIH/NIDDK Grant 2P30DK 35816-11 (VLS), DAMD-98-1-851 and DAMD-010919 (VLS), American Cancer Society Award CCE-99898 (VLS), a V-Foundation Award (VLS), a Susan G Komen Breast Cancer Award (VLS, ECD), and a Charlotte Geyer Award (VLS).

References

- Allen MC, Gale PA, Hunter AC, Lloyd A and Hardy SP. (2000). *Biochim. Biophys. Acta*, **1509**, 229–236.
- Anderson E, Clarke RB and Howell A. (1998). *J. Mamm. Gland Biol. Neoplasia*, **3**, 23–35.
- Aoudjet F and Vuori K. (2001). *Oncogene*, **20**, 4995–5004.
- Aronica SM, Kraus WL and Katzenellenbogen BS. (1994). *Proc. Natl. Acad. Sci. USA*, **91**, 8517–8521.
- Behl C. (2002). *Nat. Rev. Neurosci.*, **3**, 433–442.
- Boserma AWM, Nooter K, Oostrum RG and Stoter G. (1996). *Cytometry*, **24**, 123–130.
- Brazil DP and Hemmings BA. (2001). *Trends Biochem. Sci.*, **26**, 657–664.
- Campbell RA, Baht-Nakshatri P, Patel NM, Constantinidou D, Ali S and Naksahtri H. (2001). *J. Biol. Chem.*, **276**, 9817–9824.
- Chambliss KL, Yuhanna IS, Anderson RGW, Mendelsohn ME and Shaul PW. (2002). *Mol. Endocrinol.*, **16**, 938–946.
- Demers GW, Espling E, Harry JB, Etscheid BG and Galloway DA. (1996). *J. Virol.*, **70**, 6862–6869.
- Dick GM, Hunter AC and Sanders KM. (2002). *Mol. Pharmacol.*, **61**, 1105–1113.
- Dietze EC, Caldwell LE, Grupin SL, Mancini M and Seewaldt VL. (2001). *J. Biol. Chem.*, **276**, 5384–5394.
- Doolan CM and Harvey BJ. (2003). *Mol. Cell. Endocrinol.*, **199**, 87–103.
- Fernandez A, Cantabrana B and Hildago A. (1993). *Gen. Pharmacol.*, **24**, 391–395.
- Fisher B, Constantino JP, Wickerham CDL, Redmond CK, Kavanah M, Cronin WM, Vogel V, Robidoux A, Dimitrov N, Atkins J, Daly M, Wieand S, Tan-Chiu E, Ford L and Wolmark N. (1998). *J. Natl. Cancer Inst.*, **90**, 1371–1388.
- Friedman ZY. (1998). *Cancer Invest.*, **16**, 391–396.
- Ho KJ and Liao JK. (2002). *Arterioscler. Thromb. Vasc. Biol.*, **22**, 1952–1961.
- Hutchinson J, Jin J, Cardiff RD, Woodgett JR and Muller WJ. (2001). *Mol. Cell. Biol.*, **21**, 2203–2212.
- Improta-Brears T, Whorton AR, Codazzi F, York JD, Meyer T and McDonnell DP. (1999). *Proc. Natl. Acad. Sci. USA*, **96**, 4686–4691.
- Jarman M, Leung OT, LeClerc G, Devleeschouwer N, Stossel S, Coombes RC and Skilton RA. (1986). *Anti-Cancer Drug Des.*, **1**, 259–268.
- Johnson LV, Walsh ML and Chen LB. (1980). *Proc. Natl. Acad. Sci. USA*, **77**, 990–994.
- Kandel ES and Hay N. (1999). *Exp. Cell Res.*, **253**, 210–229.
- Kato S, Endoh H, Masuhiro Y, Kitamoto T, Uchiyama S, Sasaki H, Masushige S, Gotoh Y, Nishida E, Kawashima H, Metzger D and Chambon P. (1995). *Science*, **270**, 1491–1494.
- Kirk J, Syed SK, Harris AL, Jarman M, Roufogalis BD, Stratford IJ and Carmichael J. (1994). *Biochem. Pharmacol.*, **48**, 277–285.
- Kousteni S, Chen JR, Bellido T, Han L, Ali AA, O'Brien CA, Plotkin L, Fu Q, Mancino AT, Wien Y, Vertino AM, Powers CC, Stewart SA, Ebert R, Parfitt AM, Weinstein RS, Jilka RL and Manolagas SC. (2002). *Science*, **298**, 843–846.
- Kozikowski AP, Sun H, Brognard J and Dennis PA. (2003). *J. Am. Chem. Soc.*, **125**, 1144–1145.
- Levin ER. (2002). *Steroids*, **67**, 471–475.

- Li L, Haynes MP and Bender JR. (2003). *Proc. Natl. Acad. Sci. USA*, **100**, 4607–4812.
- Linford N, Wade C and Dorsa D. (2000). *J. Neurocytol.*, **29**, 367–374.
- Marquez DC and Pietras RJ. (2001). *Oncogene*, **20**, 5420–5430.
- Okano J, Gaslightwala I, Birnbaum MJ, Rustgi AK and Nakagawa H. (2000). *J. Biol. Chem.*, **275**, 30934–30942.
- O'Regan RM and Jordan VC. (2002). *Lancet Oncol.*, **3**, 207–214.
- Pietras RJ, Nemere I and Szego CM. (2001). *Endocrine*, **14**, 417–427.
- Razandi M, Alton G, Pedram A, Ghonshani S, Webb P and Levin ER. (2003a). *Mol. Cell. Biol.*, **23**, 1633–1646.
- Razandi M, Oh P, Pedram A, Schnitzer J and Levin ER. (2002). *Mol. Endocrinol.*, **16**, 100–115.
- Razandi M, Pedram A and Levin ER. (2000). *Mol. Endocrinol.*, **14**, 1434–1447.
- Razandi M, Pedram A, Park ST and Levin ER. (2003b). *J. Biol. Chem.*, **278**, 2701–2712.
- Ropero AB, Soria B and Nadal A. (2002). *Mol. Endocrinol.*, **16**, 497–505.
- Scheid MP and Woodgett JR. (2003). *FEBS Lett.*, **546**, 108–112.
- Schlegel A, Wang C, Katzenellenbogen BS, Pestell RG and Lisanti MP. (1999). *J. Biol. Chem.*, **274**, 33551–33556.
- Schwartzfeger KL, Richert MM and Anderson SM. (2001). *Mol. Endocrinol.*, **15**, 867–881.
- Seewaldt VL, Caldwell LE, Johnson BS, Swisshelm K and Collins SJ. (1997a). *Cell Growth Diff.*, **8**, 631–641.
- Seewaldt VL, Caldwell LE, Johnson BS, Swisshelm K, Collins SJ and Tsai S. (1997b). *Exp. Cell Res.*, **236**, 16–28.
- Seewaldt VL, Dietze EC, Johnson BS, Collins SJ and Parker MB. (1999a). *Cell Growth Diff.*, **10**, 49–59.
- Seewaldt VL, Johnson BS, Parker MB, Collins SJ and Swisshelm K. (1995). *Cell Growth Diff.*, **6**, 1077–1088.
- Seewaldt VL, Kim J-H, Parker MB, Dietze EC, Srinivasan KV and Caldwell LE. (1999b). *Exp. Cell Res.*, **249**, 70–85.
- Seewaldt VL, Mrózek K, Dietze EC, Parker MB and Caldwell LE. (2001a). *Cancer Res.*, **61**, 616–624.
- Seewaldt VL, Mrózek K, Sigle R, Dietze EC, Heine K, Hockenbery DM, Hobbs KB and Caldwell LE. (2001b). *J. Cell Biol.*, **155**, 471–486.
- Segars JH and Driggers PH. (2002). *Trends Endocrinol. Metab.*, **13**, 349–354.
- Simoncini T, Hafezi-Moghandam A, Brazil DP, Ley K, Chin WW and Liao KJ. (2000). *Nature*, **407**, 538–541.
- Song RX-D, Mcpherson RA, Adam L, Bao Y, Shupnik M, Kumar R and Santen RJ. (2002). *Mol. Endocrinol.*, **16**, 116–127.
- Stampfer M. (1985). *J. Tissue Cult. Method*, **9**, 107–121.
- Stocia GE, Franke TF, Wellstein A, Czubyko F, List HJ, Reiter R, Morgan E, Martin MB and Stoica A. (2003a). *Mol. Endocrinol.*, **17**, 818–830.
- Stocia GE, Franke TF, Wellstein A, Morgan E, Czubyko F, List HJ, Reiter R, Martin MB and Stocia A. (2003b). *Oncogene*, **22**, 2073–2087.
- Strange R, Netcalfe T, Thackeray L and Dang M. (2001). *Microsc. Res. Tech.*, **52**, 171–181.
- Sun M, Wang G, Paciga JE, Feldman RI, Yuan ZQ, Ma XL, Shelley SA, Jove R, Tschlis PN, Nicosia SV and Cheng JQ. (2001). *Am. J. Path.*, **159**, 431–437.
- Testa JR and Bellacosa A. (2001). *Proc. Natl. Acad. Sci. USA*, **98**, 10983–10985.
- West KA, Castillo SS and Dennis PA. (2002). *Drug Resist. Updates*, **5**, 234–248.
- Whitehead JP, Molero JC, Clark S, Martin S, Meneilly G and James DE. (2001). *J. Biol. Chem.*, **276**, 27816–27824.
- Zhang Z, Maier B, Santen RJ and Song RX-D. (2002). *Biochem. Biophys. Res. Commun.*, **294**, 926–933.

IRF-1 and tamoxifen-induced apoptosis

Interferon Regulatory Factor-1 Is Critical for Tamoxifen-Mediated Apoptosis in Human Mammary Epithelial Cells

Michelle L. Bowie, Eric C. Dietze, Jeffery Delrow, Gregory R. Bean, Michelle M. Troch, Robin J. Marjoram, and Victoria L. Seewaldt

Division of Medical Oncology [M.L.B., E.C.D., G.R.B., M.M.T., R.M., and V.L.S.] and
Department of Pharmacology and Cancer Biology [V.L.S.], Duke University, Durham, N.C.
27710, Fred Hutchinson Cancer Research Center, Seattle, W.A. 98120 [J.D.]

Correspondence should be addressed to:

Victoria Seewaldt
Box 2628
Duke University Medical Center
Durham, NC 27710
Telephone: (919) 668-2455
Fax: (919) 668-2458
email: seewa001@mc.duke.edu

Abstract

Unlike estrogen receptor-positive (ER+) breast cancers, normal human mammary epithelial cells (HMECs) typically express low nuclear levels of ER (ER-“poor”). We previously demonstrated that 1.0 μ M tamoxifen (Tam) promotes apoptosis in acutely damaged ER-“poor” HMECs through a rapid, “non-classic” signaling pathway (Dietze *et al.*, 2001; Dietze *et al.*, 2004). IRF-1, a target of STAT1 transcriptional regulation, has been shown to promote apoptosis following DNA damage. Here we show that 1.0 μ M Tam promotes apoptosis in acutely damaged ER-“poor” HMECs through IRF-1 induction and caspase-1/3 activation. Treatment of acutely damaged HMEC-E6 cells with 1.0 μ M Tam resulted in recruitment of CBP to the GAS element of the *IRF-1* promoter, induction of IRF-1, and sequential activation of caspases-1 and -3. The effects of Tam were blocked by expression of siRNA directed against IRF-1 and caspase-1 inhibitors. These data indicate that Tam induces apoptosis in HMEC-E6 cells through a novel IRF-1-mediated signaling pathway that results in activated caspases-1 and -3.

Introduction

The “classic” or genomic mechanism of beta-estradiol (E2) action requires the presence of the estrogen receptor (ER), the E2/ER complex binding to an ERE, and changes in both transcription and translation. However, recent evidence suggests that estrogen and perhaps anti-estrogens may also act through rapid, “non-classic” signaling pathways in mammary epithelial cells (Kelly and Levin, 2001). Tamoxifen (Tam) is an ER agonist/antagonist that has been characterized as an inhibitor of the classic E2 pathway. The Breast Cancer Prevention Trial demonstrated a decreased incidence of *in situ* and ER(+) breast cancer in the high risk participants who were prescribed Tam for five years (Fisher *et al.*, 1998). However, the molecular mechanism of Tam action in normal breast tissue is poorly understood. Normal human mammary epithelial cells (HMECs), unlike estrogen receptor-positive (ER(+)) breast cancers, typically express low nuclear levels of estrogen receptor (ER-“poor”) (Anderson *et al.*, 1998). As a result, it is uncertain whether Tam is able to target the elimination of acutely damaged, ER-“poor” cells or whether Tam’s action is restricted to mammary epithelial cells that express high levels of ER. We have previously shown that 1.0 μ M Tam rapidly promotes apoptosis in acutely damaged, ER-“poor” HMECs but only induces growth arrest in HMEC controls (Dietze *et al.*, 2001; Seewaldt *et al.*, 2001). Here we further investigated the molecular mechanism of Tam-induced apoptosis in acutely damaged HMECs. Acute cellular damage was modeled via expression of the human papilloma virus E6 protein (E6) which results in dysregulation of multiple signaling pathways crucial for cellular homeostasis. E6 protein affects these pathways by interacting with proteins such as p53, p300/CBP, Bak, IRF-3, and paxillin and provides a convenient model of acute cellular damage (Mantovani and Banks, 2001).

Interferons (IFNs) are a family of cytokines that have multiple biological effects including immunodulatory, anti-viral, anti-proliferative, antigen modulation, cell differentiation, and apoptotic effects (Chawla-Sarkar *et al.*, 2003; Pestka *et al.*, 1987; Stark *et al.*, 1998). Upon secretion from cells, interferons bind to specific cell membrane receptors and activate the JAK-STAT pathway, which results in up-regulation of interferon-stimulated genes (ISGs) (Darnell *et al.*, 1994; Stark *et al.*, 1998). Many of the biological effects from interferons are mediated by these ISGs.

IFNs have also been shown to enhance the growth inhibitory actions of tamoxifen (Coradini *et al.*, 1997; Gibson *et al.*, 1993; Iacopino *et al.*, 1997). In studies by Lindner *et al.*, treatment with Tam (1.0 μ M) and IFN-beta (100 IU/ml) resulted in growth inhibition in both ER(+) and ER(-) breast cancer cell lines. In ER(-) cell lines, Tam in combination with IFN-beta treatment was significantly more effective in inhibiting cell growth than Tam alone. In addition, in MCF-7 cells resistant to IFN-beta treatment pre-incubation with Tam followed by IFN-beta treatment, resulted in growth inhibition and up-regulation of the ISGs 2'-5'-oligoadenylate synthetase, PKR, and interferon-induced protein 56 (IFI56). Furthermore, *in vivo* studies using nude mice with established 6-week-old MCF-7 (ER(+)) and OVCAR-3 (ER(-)) breast tumors showed tumor regression only with combined Tam/IFN therapy (Lindner and Borden, 1997; Lindner *et al.*, 1997). This synergistic cytotoxicity, combined with the observed induction of interferon genes in IFN resistant cells, suggests possible cross-talk between the two pathways. Cross-talk with the IFN pathway has also been shown with other steroid/thyroid and death receptor modulators including retinoic acid (Kolla *et al.*, 1996) and TRAIL/APO-2L (Kumar-Sinha *et al.*, 2002).

ISGs exert their effects in many different ways, including promoting apoptosis. Signal transducer and activator of transcription-1 (STAT1) is activated upon interferon ligand binding to its receptor, and acts either in a complex with STAT2/p48 (ISGF3), or as a homodimer, to induce transcription of ISGs (Horvath, 2000). Interferon regulatory factor-1 (IRF-1) is a target of STAT1 transcriptional regulation (Pine *et al.*, 1994). IRF-1 itself transcriptionally regulates additional ISGs and has been shown to promote apoptosis following DNA damage (Henderson *et al.*, 1997; Tamura *et al.*, 1995; Tanaka *et al.*, 1994). Specifically, IRF-1 promotes apoptosis associated with caspase-1 activation (Romeo *et al.*, 2002; Tamura *et al.*, 1995). More recently, IRF-1 has been shown to be a tumor suppressor and critical for mammary gland involution (Hoshiya *et al.*, 2003; Kim *et al.*, 2004; Nozawa *et al.*, 1999; Yim *et al.*, 1997). Studies have also shown that IRF-1 expression is lowered or the gene is mutated in multiple cancers, including breast cancer (Doherty *et al.*, 2001; Tzoanopoulos *et al.*, 2002).

CREB-binding protein (CBP) has been shown to be a critical co-activator in IFN signaling (Horvai *et al.*, 1997; Merika *et al.*, 1998). CBP, located at chromosome band 16p13.3, is a transcriptional cofactor that regulates proliferation, differentiation, and apoptosis (Giles *et al.*, 1997b; Yao *et al.*, 1998). Chromosomal loss at 16p13 has been reported to occur in a majority of benign and malignant papillary neoplasms of the breast and loss or amplification of 16p is frequently observed in premalignant breast lesions (Aubele *et al.*, 2000; Lininger *et al.*, 1998; Tsuda *et al.*, 1998). CBP acts as a key integrator of diverse signaling pathways including those regulated by retinoids, p53, and estrogen, and has been hypothesized to play a role in BRCA1-mediated DNA repair (Kawasaki *et al.*, 1998; Robyr *et al.*, 2000). CBP levels are tightly controlled and CBP is thought to be present in limiting amounts. It has been theorized that the

many transcription factors requiring CBP compete for its binding (Giles *et al.*, 1997a; Kawasaki *et al.*, 1998; Robyr *et al.*, 2000; Yao *et al.*, 1998). Recent evidence indicates that CBP activity is also regulated by both phosphorylation and expression (Guo *et al.*, 2001).

In this study, we aimed to identify potential mediators of Tam-induced apoptosis in acutely damaged HMEC apoptosis-sensitive cells expressing E6. Here we show that Tam promotes apoptosis in acutely damaged HMEC-E6 cells through IRF-1 induction and caspase-1 activation. These results provide evidence for a novel role for IRG-signaling in targeting the elimination of acutely damaged HMECs.

Results

cDNA microarray analysis of Tam-induced gene transcripts

To investigate the molecular mechanism of Tam-induced apoptosis, we analyzed the expression profiles of acutely damaged HMEC-E6 cells and passage matched HMEC-LX controls treated with or without 1.0 μ M Tam for 6 hr. Analysis was performed using Hu6800 cDNA microarrays (Affymetrix™). As shown in Table 2, twenty interferon-stimulated genes (ISGs) were significantly up-regulated in Tam-treated HMEC-E6 cells but not in HMEC-LX controls. The up-regulated genes included interferon induced (IFI) 9-27, IRF-1, ISG15, ISG-54, MX-A, interferon gamma inducible protein 16, STAT1 alpha, STAT1 beta, IFI 6-16, and ISG12. Differential expression was confirmed by semi-quantitative RT-PCR in triplicate, and normalized to beta-actin (Figure 1). Based on these observations, we hypothesized that ISGs may 1) participate in or 2) be a marker for Tam-induced apoptosis in acutely damaged HMEC-E6 cells.

Interferon-alpha, -beta, and -gamma are not induced by Tam-treatment

The subset of interferon-stimulated genes induced by 1.0 μ M Tam are only a few of the more than 300 genes shown to be up-regulated by Type I (IFN- α and IFN- β) and Type II (IFN- γ) Interferons (de Veer *et al.*, 2001; Der *et al.*, 1998). Our differential gene expression data indicated that interferon transcripts - α , - β , and - γ were not induced by 6 hr Tam treatment (data not shown). ELISA assays were performed in Tam-treated HMECs to test whether interferons were released following Tam treatment. Passage matched apoptosis-sensitive HMEC-E6 cells and HMEC-LX controls were treated with 1.0 μ M Tam for 24 hr. Release of IFN- α , - β , and - γ was not detected following Tam treatment (data not shown). These data show that Tam

promotes apoptosis and ISG induction in HMEC-E6 cells in the absence of INF- α , - β , and - γ induction or release.

IRF-1 is induced by Tam

IRF-1 is a transcriptional regulator that has been shown to promote apoptosis following DNA damage and is critical for mammary gland involution (Hoshiya *et al.*, 2003; Kroger *et al.*, 2002). Differential gene expression studies demonstrated that IRF-1 mRNA was induced by Tam in acutely damaged HMEC-E6 cells at 6 hr. Semi-quantitative RT-PCR and western analysis were performed to determine the kinetics of IRF-1 mRNA and protein induction. We observed that IRF-1 mRNA and protein were induced by 1.0 μ M Tam in acutely damaged HMEC-E6 cells but not in HMEC-LX controls. IRF-1 mRNA induction in HMEC-E6 cells was first observed at 30 min (5.1-fold, p-value < 0.01) and was maximally induced at 3 hr (8.8-fold, p-value < 0.0001) (Figure 2a, b). IRF-1 protein induction was first observed at 30 min (1.5-fold, p-value < 0.025) and was maximally induced at 3 hr (2.3-fold, p-value < 0.001) (Figure 2c, d). These observations demonstrate that IRF-1 mRNA and protein are induced by Tam in acutely damaged HMEC-E6 cells starting at 30 min.

Tam promotes recruitment of CBP to the ICS2/GAS element of the IRF-1 promoter

Chromatin immunoprecipitation (ChIP) and immunoprecipitation studies were performed to identify co-activators that might participate in IRF-1 mRNA induction in apoptosis-sensitive HMEC-E6 cells. CBP is a known regulator of apoptosis and a co-activator for steroid/thyroid- and Type II interferon signaling (Hiroi and Ohmori, 2003; Horvai *et al.*, 1997). STAT1 is a transcriptional regulator of IRF-1 and has been shown to interact with CBP through the 1)

CREB-binding domain and 2) CH3 domain (Zhang *et al.*, 1996). Recently, an IFN-inducible gamma-interferon-activated sequence (GAS) element was identified in the *IRF-1* promoter that serves to activate IRF-1 transcription (Harada *et al.*, 1994; Sims *et al.*, 1993). Using ChIP and immunoprecipitation studies, we tested whether Tam treatment of HMEC-E6 cells may promote 1) CBP or STAT1 recruitment to this *IRF-1* promoter GAS element and 2) induction of IRF-1 mRNA expression at 0, 2, and 6 hr. We observed that STAT1 was constitutively associated with the GAS element of the *IRF-1* promoter in HMEC-E6 cells and Tam treatment did not alter this association (Figure 3a). In contrast, CBP was recruited to the *IRF-1* promoter 2 hr following treatment of HMEC-E6 cells with 1.0 μ M Tam (Figure 3a). Neither STAT1 nor CBP were recruited to the GAS element of the *IRF-1* promoter in HMEC-LX controls with Tam treatment (data not shown). The observation that STAT1 was constitutively bound to the IRF-1 GAS element in the HMEC-E6 cells, suggested that it may be active at baseline. There are two known phosphorylation sites within STAT1, Tyr701 and Ser727. It has been shown that phosphorylation of Ser727 induces the highest transcriptional activation for STAT1 (Wen *et al.*, 1995). Western analysis was performed to determine the phosphorylation status of STAT1 in the untreated acutely damaged HMEC-E6 cells. We observed that STAT1 is phosphorylated at Ser727 in the HMEC-E6 cells at baseline (Figure 4d). The activation of STAT1 in the HMEC-E6 cells at baseline may be a response to the expression of E6 in these cells.

An immunoprecipitation time course using a biotin-labeled oligo, containing the *IRF-1* GAS promoter element, was performed to precisely pinpoint the temporal correlation between 1) CBP recruitment to the *IRF-1* promoter and 2) IRF-1 mRNA induction in Tam-treated HMEC-E6 cells. CBP was recruited to the GAS element of the *IRF-1* promoter at 30 min after 1.0 μ M Tam

treatment (Figure 3b). STAT1 was again shown to be constitutively associated with the *IRF-1* promoter GAS element between 0 and 60 min (data not shown). CBP recruitment correlated with IRF-1 mRNA induction at 30 min (Figure 2). These observations demonstrate that Tam-mediated recruitment of CBP to the GAS element of the *IRF-1* promoter in acutely damaged HMEC-E6 cells is temporally concurrent with IRF-1 mRNA and protein induction.

IFI 6-16 is induced by Tam

Interferons have been shown to regulate the expression of the IFI 6-16 gene (Gjermandsen *et al.*, 2000). Specifically, IRF-1 expression induces transcription of IFI 6-16 (Henderson *et al.*, 1997). Our differential gene expression studies demonstrate that IFI 6-16 mRNA is induced by treatment of acutely damaged HMEC-E6 cells with 1.0 μ M Tam for 6 hr. Semi-quantitative RT-PCR was performed to determine the kinetics of IFI 6-16 mRNA induction. IFI 6-16 mRNA was induced by 1.0 μ M Tam in acutely damaged HMEC-E6 cells but not in HMEC-LX controls (Figure 4). Induction of IFI 6-16 mRNA was 1) first observed in HMEC-E6 cells by 2 hr, 2) statistically significant by 3 hr (2.2-fold), and 3) maximally induced at 6 hr (3.1-fold) (Figure 4a). These observations demonstrate that Tam induces ISG IFI 6-16 mRNA in acutely damaged HMEC-E6 cells starting at 3 hr.

Tam promotes recruitment of IRF-1, STAT1, and CBP to the IFI 6-16 promoter ISRE element

IRF-1 has been shown to complex with STAT1 and to induce ISG expression through binding to the interferon consensus sequence 2/gamma-interferon-activated sequence (ICS2/GAS) element (Chatterjee-Kishore *et al.*, 1998). In addition, IRF-1 has been shown to directly bind to the interferon-stimulated response element (ISRE) within the *IFI 6-16* promoter and induce

transcription (Parrington *et al.*, 1993). We observe induction of IFI 6-16 mRNA in HMEC-E6 cells by 3 hr after treatment with 1.0 μ M Tam. ChIP was performed to test whether recruitment of IRF-1, STAT1, and the co-activator CBP to the ISRE element of the *IFI 6-16* promoter temporally correlated with IFI 6-16 mRNA induction. We observed that IRF-1, STAT1, and CBP are simultaneously recruited to the ISRE element of the *IFI 6-16* promoter in acutely damaged HMEC-E6 cells after 2 hr treatment with 1.0 μ M Tam (Figure 4c). These observations demonstrate that Tam treatment of acutely damaged HMEC-E6 cells promotes recruitment of IRF-1, STAT1, and CBP to the *IFI 6-16* promoter at 2 hr, followed by induction of IFI 6-16 mRNA by 3 hr.

Caspase-1 and caspase-3 are induced by Tam

IRF-1 is thought to mediate apoptosis through activation of caspase-1 (Karlsen *et al.*, 2000; Kim *et al.*, 2002). Recently, overexpression of IRF-1 in two mouse breast cancer cell lines has also shown to activate caspase-3 (Kim *et al.*, 2004). We have previously shown that caspase-3 is activated by 1.0 μ M Tam in acutely damaged HMEC-E6 cells starting at 6 hr, maximally at 24 hr, and precedes the appearance of marginated chromatin (early effector-phase apoptosis), first observed at 12 hr (Dietze *et al.*, 2001). In contrast, we observed that caspase-3 was not activated by Tam in HMEC-LX controls (Dietze *et al.*, 2001).

Here we tested for caspase-1 activation in Tam-treated acutely damaged HMEC-E6 cells and HMEC-LX controls. Our gene chip data showed no increase in caspase-1 mRNA at 6 hr, in either the HMEC-LX controls or the HMEC-E6 cells (data not shown). In HMEC-E6 cells, however, caspase-1 was activated by 1.0 μ M Tam starting at 3 hr (Figure 5a). This activation

temporally correlated with maximal IRF-1 mRNA and protein induction observed at 2-3 hr (Figure 2). In contrast, caspase-1 was not activated in passage matched HMEC-LX controls (Figure 5a).

Caspase-1 inhibitor IV blocks Tam-induced apoptosis

HMEC-E6 cells were pretreated with caspase-1 inhibitor IV to test whether caspase-1 activation was required for Tam-induced apoptosis. HMEC-E6 cells treated with 15 nM caspase-1 inhibitor and 1.0 μ M Tam for 4 hr failed to show a significant increase in caspase-1 activation (Figure 5b). As previously observed, HMEC-E6 cells treated with 1.0 μ M Tam showed activation of caspase-3 at 12 hr, and underwent apoptosis as demonstrated by Annexin V binding at 18 hr (Figure 5c,d) (Dietze *et al.*, 2001). Pretreatment with 15 mM caspase-1 inhibitor IV 3 hr prior to treatment with 1.0 μ M Tam for 12 hr and 18 hr inhibited both the induction of caspase-3 activity (Figure 5c) and apoptosis as evidenced by a lack of Annexin V binding (Figure 5d). Caspase-1 inhibitor IV treatment alone did not alter the proliferation rate of HMEC-E6 cells and did not induce apoptosis (Figure 5d and data not shown). These data demonstrate that caspase-1 activation is required for Tam-induced apoptosis in acutely damaged HMEC-E6 cells.

siRNA directed against IRF-1 blocks Tam-induced activation of caspase-1/3 and apoptosis

siRNA was used to test whether suppression of IRF-1 expression blocked Tam-mediated caspase activation and apoptosis in acutely damaged HMEC-E6 cells. Treatment of HMEC-E6 cells with siRNAs IRF-1 #1 and IRF-1 #4 sequences for 12 hr resulted in suppression of IRF-1 protein and mRNA (Figure 6a and data not shown). We observed that 1.0 μ M Tam activated caspase-1 at 3-4 hr (Figure 5a). Suppression of IRF-1 expression in HMEC-E6 cells by IRF-1-specific

siRNA blocked Tam-mediated caspase-1 activation at 3 and 4 hr (Figures 6b). We previously demonstrated that caspase-3 is activated by 1.0 μ M Tam in acutely damaged HMEC-E6 cells starting at 6 hr and maximally at 24 hr (Dietze *et al.*, 2001). Suppression of IRF-1 expression in HMEC-E6 cells by IRF-1-specific siRNA blocked Tam-mediated caspase-3 activation at 12 hr (Figures 6c). In previously published data, we showed that 1.0 μ M Tam induced apoptosis in acutely damaged HMEC-E6 cells as demonstrated by Annexin V binding at 18 hr (Dietze *et al.*, 2001). Here we show that two siRNA sequences directed against IRF-1 blocked Tam-mediated apoptosis in HMEC-E6 cells (Figure 6d). These observations demonstrate that IRF-1 expression is required for Tam-induced caspase-1/3 activation and apoptosis in acutely damaged HMEC-E6 cells.

Discussion

While IFN signaling is important for eliminating cells that are damaged by viral infection, evidence suggests that IFN signaling, through STAT1, IRF-1, and other ISGs, may play a more comprehensive role in mammary gland homeostasis and response to DNA damage. Recently, a similar subset of interferon-regulated genes was induced by overexpression of BRCA1, in the absence of further interferon production (Andrews *et al.*, 2002). This observation suggests that the loss of BRCA1 may facilitate the disruption of the interferon response. IFN-regulatory proteins such as IRF-1, STAT1, and ISG12 are dysregulated during breast carcinogenesis (Doherty *et al.*, 2001; Rasmussen *et al.*, 1993; Watson and Miller, 1995) and IFN exhibits cross-talk with estrogen and retinoid signaling (Bjornstrom and Sjoberg, 2002; Kolla *et al.*, 1996; Widschwendter *et al.*, 1996).

Here we report a novel role for the ISG, IRF-1, in regulating Tam-mediated apoptosis in acutely damaged HMEC-E6 cells. This finding is not completely unexpected. Recent reports have highlighted the ability of IRF-1 to mediate growth arrest and apoptosis in breast cancer cell lines (Hoshiya *et al.*, 2003; Kim *et al.*, 2002; Kim *et al.*, 2004). In addition, evidence suggests that IRF-1 plays a role in mammary homeostasis, as IRF-1 is critical for mammary gland involution and loss of expression of IRF-1 is an early event in mammary carcinogenesis (Doherty *et al.*, 2001). In this study, IRF-1 expression was induced by 60 min treatment with 1.0 μ M Tam (Figure 2). IRF-1 was induced by Tam in acutely damaged HMEC-E6 cells 1-3 hr prior to subsequent ISG induction, 9 hr prior to caspase-3 induction, and 21 hr prior to late effector-phase apoptosis (detection of apoptotic bodies) (Figure 2 and data not shown). Suppression of IRF-1 expression by siRNA sequences blocked the induction of apoptosis by Tam (Figure 6).

Taken together these results suggest a critical role for IRF-1 expression in mediating Tam-induced apoptosis in acutely damaged HMEC-E6 cells.

Recently, an IFN-inducible GAS element has been identified in the IRF-1 promoter (Harada *et al.*, 1994; Sims *et al.*, 1993). STAT1 homodimers bind to this GAS element and induce transcription. At a similar interferon response element, called γ RE element, a STAT1 dimer binds and recruits CBP to the promoter complex (Hiroi and Ohmori, 2003). STAT1 has been shown to interact with CBP through both the CREB-binding domain and CH3 domain (Zhang *et al.*, 1996). IRF-1 in turn has been reported to complex with STAT1 to induce ISG expression by binding to the interferon consensus sequence-2/gamma-interferon-activated sequence (ICS2/GAS) element (Chatterjee-Kishore *et al.*, 1998). Based on these observations we hypothesized that 1) STAT1 and CBP may play a role in IRF-1 induction and 2) IRF-1/STAT1/CBP, in turn, may cooperatively promote induction of further ISGs.

ChIP and immunoprecipitation experiments demonstrated that STAT1 was constitutively bound to the GAS element of the *IRF-1* promoter in HMEC-E6 cells (Figure 3). In contrast, CBP was not associated with the *IRF-1* GAS element at baseline. ChIP and immunoprecipitation experiments demonstrated that CBP was recruited to the GAS element of the *IRF-1* promoter by 30 min after Tam treatment (Figure 3). Neither STAT1 nor CBP were associated at baseline or recruited to the *IRF-1* GAS element in HMEC-LX vector controls cells. Based on these observations, we hypothesize that CBP recruitment to the *IRF-1* GAS element may be the crucial step in up-regulation of IRF-1 mRNA following Tam treatment.

Induction of IRF-1 was closely followed by induction of a small set of ISGs (Table 2). IRF-1 has previously been shown to participate in the induction of the ISG, IFI 6-16, through recruitment of IRF-1 to the *IFI 6-16* promoter ISRE sequence (Parrington *et al.*, 1993). Here we report that induction of IFI 6-16 mRNA temporally correlated with recruitment of STAT1, IRF-1, and CBP to the ISRE of the *IFI 6-16* promoter region (Figure 4). Tam induced IFI 6-16 mRNA expression at 3 hr in acutely damaged HMEC-E6 cells but not in HMEC-LX controls (Table 2, Figures 1, 4). ChIP analysis of untreated HMEC-E6 cells showed that IRF-1, STAT1, and CBP were not bound to the *IFI 6-16* ISRE at baseline (Figure 4c). However, when acutely damaged HMEC-E6 cells were treated with 1.0 μ M Tam for 2 hr, IRF-1, CBP, and STAT1 were recruited to the ISRE sequence in the *IFI 6-16* promoter (Figure 4) and this recruitment was followed by the induction of IFI 6-16 mRNA at 3 hr. These observations demonstrate a potential role for Tam 1) in promoting IRF-1 recruitment to the *IFI 6-16* promoter and 2) perhaps in promoting IFI 6-16 mRNA expression. Work is on-going in our laboratory to define 1) the requirement for IRF-1/STAT1/CBP in modulating IFI 6-16 expression and 2) whether IFI 6-16 directly participates in Tam-induced apoptosis in acutely damaged HMEC-E6 cells or whether it serves only as a marker of IRF-1 induction.

Caspase-1 and caspase-3 have previously been shown to participate in IRF-1-mediated apoptosis (Kim *et al.*, 2002; Kim *et al.*, 2004). IRF-1 has been shown to be critical for caspase-1 mRNA induction from cytokine treatment (Karlsen *et al.*, 2000). While caspase-3 is clearly an effector-caspase, the role of caspase-1 in promoting effector-phase apoptosis is controversial. Caspase-1/ICE is traditionally considered an initiator caspase, well known for its inflammatory actions in activating both IL-1 β and IL-18 cytokines (Creagh *et al.*, 2003). Some earlier studies, however,

suggest that it is also involved in apoptosis (Miura *et al.*, 1993; Wang *et al.*, 1994). There have also been several reports of sequential activation of caspases-1 and -3 (Kamada *et al.*, 1997; Dai and Krantz, 1999; Pasinelli *et al.*, 2000; Aiba-Masago *et al.*, 2001; Zhang *et al.*, 2003; Jiang *et al.*, 2004). While the phenotype of the caspase-1 knock-out mouse did not show major dysregulation of apoptosis, ICE-/- thymocytes were resistant to Fas-mediated apoptosis (Kuida *et al.*, 1995). More recently, studies with IFN-gamma have shown that caspase-1 is induced and activated in cells sensitive to apoptosis (Detjen *et al.*, 2001; Detjen *et al.*, 2002; Kim *et al.*, 2002).

Here we observed that caspase-1/3 are activated by Tam in acutely damaged HMEC-E6 cells by 3 and 12 hr (Figure 5, Dietze *et al.*, 2001), respectively, in the absence of IFN secretion (data not shown). Microarray analysis for both HMEC-LX and HMEC-E6 cells showed no induction of caspase-1 mRNA at 6 hr (data not shown), however, caspase-1 was activated 2 hr after the observed increase in IRF-1 protein levels (Figure 5a). Inhibition of caspase-1 activity with 15 nM caspase-1 inhibitor IV blocked Tam-induced 1) activation of caspase-1 and caspase-3 and 2) effector-phase apoptosis (Figure 5). siRNA directed against IRF-1 also blocked Tam-mediated activation of caspase-1/3 and apoptosis (Figure 6). Taken together these data indicate that Tam-induced apoptosis in acutely damaged HMEC-E6 cells requires both induction of IRF-1 and a subsequent increase in caspase-1 activity.

We have previously shown that caspase-9 was induced by Tam treatment of HMEC-E6 cells (Dietze *et al.*, 2001; Dietze *et al.*, 2004). Caspase-9 induction occurred within 1 hr of Tam treatment and returned to baseline by 12 hr after Tam treatment (Dietze *et al.*, 2001). Caspase-9

has not been shown to process procaspase-1. Thus it is unlikely that caspase-9 is involved in the observed activation of caspase-1. Also, *IRF-1*(-/-) cells were still able to induce caspase-9 activity (Oda *et al.*, 2000). Taken together with the kinetics of ISG IFI 6-16 induction (Figure 4), it is unlikely that IRF-1 participates in caspase-9 activation. The exact relationship of caspases-9, -1, and -3 to each other and to the execution phase of apoptosis is under study in our laboratory.

In previously published studies, we have recently shown that Tam treatment of acutely damaged HMEC-E6 cells results in rapid loss of AKT Ser-473 phosphorylation and activity (Dietze *et al.*, 2004). In this report we demonstrate that 1) Tam promotes recruitment of CBP to the GAS element of the *IRF-1* promoter and 2) this recruitment is temporally associated with induction of IRF-1. It is known that CBP and its related co-activator, p300, are present in limiting amounts. The current paradigm of CBP/p300 action suggests that CBP/p300 activity is mediated by competition of various promoter elements for limited quantities of CBP/p300. However, recent studies suggest that the activity of CBP may also be controlled by phosphorylation, although correlation between specific sites of phosphorylation and alteration of function has been rare (Kovacs *et al.*, 2003). Given our recent observations regarding 1) the role of AKT in regulating Tam-induced apoptosis and 2) Tam-modulated CBP recruitment to the *IRF-1* GAS element, we are currently investigating the potential role of AKT in promoting CBP recruitment and IRF-1 induction. AKT has been shown to phosphorylate the CBP analog p300 in the CH3 domain and block the transcriptional activity of C/EBP β which binds that domain (Guo *et al.*, 2001). We are currently investigating the possibility that AKT functions in a similar fashion to promote CBP binding to the STAT1-bound IRF-1 GAS element and thereby promote IRF-1 transcription in

acutely damaged HMEC-E6 cells.

Materials and Methods

Materials

All chemicals and cell culture reagents were obtained from Sigma-Aldrich (St. Louis, MO, USA), DNA primers from Invitrogen (Carlsbad, CA, USA) or Qiagen Operon (Alameda, CA, USA), and cell culture plasticware from Corning (Corning, NY, USA) unless otherwise noted. A 1.0 mM stock solution of tamoxifen was prepared in 100% ethanol and stored in opaque tubes at -70°C. Control cultures received equivalent volumes of the ethanol solvent. Stocks were used under reduced light. Caspase-1 inhibitor IV was obtained from EMD Biosciences Inc. (San Diego, CA, USA). IFN- γ was obtained from R&D Systems (Minneapolis, MN, USA), reconstituted to a 10 μ g/ml stock with 1x PBS (0.1% BSA), and stored at -70°C.

Cell Culture and Media

Normal human mammary epithelial cell strain AG11132 (M. Stampfer #172R/AA7) was purchased from the National Institute of Aging, Cell Culture Repository (Coriell Institute, Camden, NJ, USA; Stampfer, 1985). HMEC strain AG11132 was established from normal tissue obtained at reduction mammoplasty, has a limited life span in culture, and fails to divide after approximately 20 to 25 passages. HMECs exhibit a low level of estrogen receptor staining characteristic of normal mammary epithelial cells. HMECs were grown in Mammary Epithelial Cell Basal Medium (Clonetics, San Diego, CA, USA) supplemented with 4 μ l/ml bovine pituitary extract (Clonetics #CC4009), 5 μ g/ml insulin (UBI, Lake Placid, NY, USA), 10 ng/ml epidermal growth factor (UBI), 0.5 μ g/ml hydrocortisone, 10^{-5} M isoproterenol, and 10 mM HEPES buffer [Standard Media]. G418 containing Standard Media was prepared by the addition

of 300 µg/ml of G418 (Gibco, Grand Island, NY, USA) to Standard Media. Cells were cultured at 37°C in a humidified incubator with 5% CO₂/95% air. Mycoplasma testing was performed as previously reported (Seewaldt *et al.*, 1997a).

Retroviral Transduction

The LXSNI6E6 retroviral vector containing the human papillomavirus-16 (HPV-16) E6 coding sequence was provided by D. Galloway (Fred Hutchinson Cancer Research Center, Seattle, WA, USA) (Demers *et al.*, 1996). HMECs (passage 9) were plated in four T-75 tissue culture flasks in Standard Medium and grown to 50% confluency. Transducing virions from either the PA317-LXSNI6E6 or the control PA317-LXSN (without insert) retroviral producer line were added at a multiplicity of infection at 1:1 in the presence of 4 µg/ml Polybrene to log-phase cells grown in T-75 flasks. The two remaining T-75 flasks were not infected with virus. After 48 hr two flasks containing transduced cells and one flask with untransduced cells were passaged 1:3 (passage 10) and selected with Standard Media containing 300 µg/ml G418. Cells were grown in G418 containing Standard Media for four to seven days, until 100% of control untransduced cells were dead. The transduction efficiency was high during selection, cells were passaged 1:3 at the completion of selection (passage 11), and cells were maintained in the absence of selection before immediately proceeding to apoptosis experiments. The fourth flask of unselected, untransduced parental control cells was passaged in parallel with the selected, transduced experimental and vector control cells. Parental AG11132 cells were designated HMEC-P. Transduced AG11132 cells expressing the HPV-16 E6 construct were designated HMEC-E6 and vector control clones were designated HMEC-LX. All cells were maintained in Standard Media after transfection in the absence of G418 selection to ensure that any observed chromosomal

abnormalities or apoptosis resistance was not due to continued exposure to G418. All experiments were performed on mass cultures.

Differential Gene Expression Studies

Total RNA isolation was as previously described (Seewaldt *et al.*, 1995). RNA integrity was confirmed by electrophoresis, and samples were stored at -70°C until used. All RNA combinations used for array analysis were obtained from cells that were matched for passage number, cultured under the identical growth conditions, and harvested at identical confluency. cDNA synthesis and probe generation for cDNA array hybridization were obtained by following the standardized protocols provided by Affymetrix (Affymetrix, Santa Clara, CA, USA).

Expression data for approximately 5,600 full-length human genes were collected using Affymetrix GeneChip HuGeneFL™ arrays, and following the standardized protocols provided by the manufacturer. Data were collected in triplicate using independent biological replicates. Array images were processed using Affymetrix™ MAS 5.0 software, where we filtered for probe saturation, employed a global array scaling target intensity of 1000, and collected the signal intensity value (i.e., the “average difference”) for each gene. Pair-wise “treatment vs control” comparisons were made employing CyberT (Baldi and Long, 2001), a Bayesian t-statistic algorithm derived for microarray analysis. We employed a window size of 101 and used a confidence value of 10 in our CyberT analysis. Significant changes in expression were determined by ranking the assigned Bayesian p-values and applying a false discovery rate correction (FDR = 0.05) to account for multiple testing (Benjamini, *et al.*, 1995).

Semi-quantitative RT-PCR

To confirm the microarray data, relative transcript levels were analyzed by semi-quantitative reverse transcriptase-polymerase chain reaction (RT-PCR). Five micrograms of total RNA was used in first-strand cDNA synthesis with Superscript™ II reverse transcriptase (Invitrogen). PCR reaction conditions were optimized for each gene product to determine the PCR cycle number of linear amplification for each primer set. The primer sets, cycling conditions, and cycle numbers used are indicated in Table 1. All PCR reactions were in 50 µl total volume. For ISG15, IFI56, and IFI 9-27, a reaction was set up containing 100 nM of each primer, 1.0 mM dNTPs, 10 mM Tris-HCl (pH 8.3), 1.5 mM MgCl₂, 50 mM KCl, 2.5 units Taq polymerase (Roche Applied Science, Indianapolis, IN, USA), and 2.0 µl cDNA. IFI 6-16 was amplified with 100 nM of each primer, 1.0 mM dNTPs, 1x Expand High Fidelity Buffer (-MgCl₂) (Roche Applied Science), 0.5 mM MgCl₂, 10% DMSO, 2.0 units Taq polymerase, and 4.0 µl cDNA. Amplification of ISG12 was carried out with 100 nM of each primer, 1.0 mM dNTPs, 10 mM Tris-HCl (pH 8.3), 1.5 mM MgCl₂, 50 mM KCl, 2.0 units Taq polymerase, and 4.0 µl cDNA. IRF-1 cDNA was amplified with 200 nM of each primer, 1.0 mM dNTPs, 20 mM Tris-HCl (pH 8.4), 50 mM KCl, 1.0 mM MgCl₂, 2.5 units Taq polymerase, and 2.0 µl cDNA. Reaction conditions for beta-actin were 300 nM of each primer (sequences obtained from Invitrogen), 1.0 mM dNTPs, 10 mM Tris-HCl (pH 8.3), 1.5 mM MgCl₂, 50 mM KCl, 2.5 units Taq polymerase, and 2.0 µl cDNA. Products were amplified with GeneAmp PCR Systems 2400 and 9700 (Applied Biosystems, Foster City, CA, USA). Ten microliters of PCR product was analyzed by electrophoresis in 1.2-1.5% agarose (Invitrogen) gels containing ethidium bromide and visualized under UV light. All samples were performed in triplicate and normalized to beta-actin control. Band quantitation was done using Kodak 1D™ Image Analysis Software (Eastman Kodak, Rochester, NY, USA).

ChIP (Chromatin Immunoprecipitation Assay)

ChIP was performed by published methods with some modifications (Yahata *et al.*, 2001). Preliminary experiments were run to determine optimal sonication and formaldehyde cross-linking time. Once optimized, cells were harvested, pelleted, and treated with 1% formaldehyde for 15 min to cross-link cellular proteins. Cells were then rinsed twice in ice cold PBS containing protease inhibitors, pelleted, and resuspended in Lysis Buffer [1% SDS, 10 mM EDTA, 50 mM Tris-HCl at pH 8.1, 1x Protease Inhibitor Cocktail (4 µg/ml epibestatin hydrochloride, 2 µg/ml calpain inhibitor II, 2 µg/ml pepstatin A, 4 µg/ml mastoparan, 4 µg/ml leupeptin hydrochloride, 4 µg/ml aprotinin, 1 mM TPCK, 1 mM phenylmethylsulfonyl fluoride, and 100 µM TLCK)]. Samples were then sonicated 3 x 15 seconds each with a 1 min incubation on ice in between pulses on a Branson sonifier model 250 at 50% duty and maximum mini probe power. A 20 µl aliquot of lysate was saved and used to determine the input DNA for each sample. Supernatants were diluted (1:10) in Dilution Buffer [1% Triton X-100, 2 mM EDTA, 150 mM NaCl, 20 mM Tris-HCl at pH 8.1, 1x Protease Inhibitor Cocktail], and precleared with 2 µg of sheared salmon sperm DNA (Gibco), 20 µl normal human serum, and 45 µl of protein A-sepharose [50% slurry in 10 mM Tris-HCl at pH 8.1, 1.0 mM EDTA]. To precleared chromatin, 10 µl of either anti-CBP (A22, Santa Cruz Biotechnology, Santa Cruz, CA, USA), anti-STAT1 (E23, Santa Cruz Biotechnology), or anti-IRF-1 (H205, Santa Cruz Biotechnology) was added, and the reaction was incubated overnight, followed by an addition of 45 µl of protein A-sepharose and 2.0 µg sheared salmon sperm and an additional 1 hr incubation. Sepharose beads were then collected and washed sequentially for 10 min each in TSE I [0.1% SDS, 1% Triton X-100, 2 mM EDTA, 20 mM Tris-HCl at pH 8.1, 150 mM NaCl], TSE II [0.1% SDS, 1% Triton X-

100, 2 mM EDTA, 20 mM Tris-HCl at pH 8.1, 500 mM NaCl], and buffer III [0.25 M LiCl, 1% NP-40, 1% deoxycholate, 1 mM EDTA, 10 mM Tris-HCl at pH 8.1]. Beads were washed once with TE buffer and DNA eluted with 100 μ l of 1% SDS-0.1 M NaHCO₃. Eluate was heated at 65°C overnight to reverse the formaldehyde cross-linking. DNA fragments were cleaned-up with the QIAquick PCR purification kit (Qiagen, Valencia, CA, USA) and amplified in a PCR reaction. Primers for the *IRF-1* and *IFI 6-16* promoters were 1) IRF-1 forward 5'-GTA CTT CCC CTT CGC CG-3' and IRF-1 reverse 5'-GCG TAC TCA CCT CTG CTG C-3' and 2) IFI 6-16 forward 5'-ATA CCC TTA GCG GCT CCA AA-3' and IFI 6-16 reverse 5'-GCT GAA GGC TGG CTT TTT ATC-3'. Thirty microliters of PCR product was analyzed by electrophoresis in 1.5% agarose gels containing ethidium bromide and visualized under UV light using Kodak 1D™ Image Analysis Software. All reactions were performed in triplicate.

Western Blotting

Preparation of cellular lysates and immunoblotting were performed as previously described (Seewaldt *et al.*, 1997b; Seewaldt *et al.* 1999b). For IRF-1 expression, the membrane was incubated with a 1:100 dilution of mouse anti-human IRF-1 (C-20, Santa Cruz Biotechnology). For CBP expression, the blocked membrane was incubated with a 1:200 dilution of the CBP antibody (C-20, Santa Cruz Biotechnology). For STAT1 expression the membrane was incubated with a 1:100 dilution of antibody to STAT1 (E-23, Santa Cruz Biotechnology). For STAT1 phosphoserine-727 detection the membrane was incubated with a 1:400 dilution of the Phospho-STAT1-Ser727 antibody (Cell Signaling Technology, Beverly, MA, USA). Loading control was provided by a 1:200 dilution of antibody to β -actin (I-19, Santa Cruz Biotechnology). The resulting film images were digitized and quantitated using Kodak 1D™

Image Analysis Software.

Suppression of IRF-1 with siRNA

Two double-stranded siRNA oligos were designed using Ambion, Inc. software (Austin, TX, USA). Oligos were synthesized and annealed by Qiagen. IRF-1 #1 targets sequence: 5'-AACTTTCGCTGTGCCATGAAC-3', and IRF-1 #4 targets sequence: 5'-AAGTGTGAGCGCCTTGGTATG-3'. Control non-silencing siRNA was provided by Qiagen. Early passage HMEC-E6 cells were transfected with IRF-1 #1 and #4 siRNAs (167mM-600nM) and Cellfectin™ (Invitrogen). Twelve hours after transfection, RNA was harvested using the Aurum™ Total RNA kit (Bio-Rad Laboratories, Hercules, CA, USA) and protein was harvested as previously described (Seewaldt *et al.*, 1999a; Seewaldt *et al.*, 1997b). Western analysis (as described above) and RT-PCR were performed to confirm suppression of IRF-1 expression. cDNA was prepared for RT-PCR from 50 ng total RNA with Superscript™ II reverse transcriptase (Invitrogen). Beta-actin PCR reaction conditions were performed as described above except product was amplified for 24 cycles. IRF-1 amplification was re-optimized for lower input. The changes made to the reaction were as follows: 1) HotStarTaq™ polymerase (Qiagen) was used, 2) annealing temperature was increased to 57°C, and 3) amplification was carried out for 38 cycles. Twenty-five microliters of PCR product was ran on either 2.0% or 1.2% agarose gels stained with ethidium bromide and visualized with Kodak 1D™ Image Analysis Software.

ELISA

Aliquots of tissue culture media were withdrawn from flasks at 0, 30 min, 1, 2, and 4 hr and stored at -70°C. Manufacturer protocols for the commercial IFN-alpha, IFN-beta (Biosource International, Camarillo, CA, USA), and IFN-gamma (BD Biosciences Pharmingen, San Diego, CA, USA) ELISA kits were followed. Duplicate standard curves were run on each plate, and media samples were assayed in triplicate.

IRF-1 Promoter Immunoprecipitation

HMEC-E6 cells and HMEC-LX controls were treated with 1.0 μ M tamoxifen and harvested at 0, 30, and 60 min. Preparation of cellular lysates and immunoblotting were performed as previously described (Seewaldt *et al.*, 1997b; Seewaldt *et al.*, 1999b). A 25 bp section of the *IRF-1* promoter region, encompassing the GAS element (-134 to -109 bp upstream), was used to design biotin-labeled oligos. The complimentary oligos (Qiagen) were annealed in equal molar concentrations, heated to 95°C for 5 min, and allowed to cool to room temperature. Then 890 μ g of total protein lysate was precleared with Strep-avidin beads. The supernatant was subsequently incubated with IRF-1 GAS-annealed oligos and Strep-avidin beads for 2 hr at 4°C. The beads were washed 3x with lysis buffer with protease inhibitors, boiled, and ran on an SDS-PAGE gel. Antibodies to CBP (C-20, Santa Cruz Biotechnology) and STAT1 (E-23, Santa Cruz Biotechnology) were used to detect bound protein.

Measurement of Apoptosis and Caspase-1/3 Activity

Apoptosis was measured by Annexin V binding and FACS after treatment with 1.0 μ M Tam for 18 hr as previously described (Dietze *et al.*, 2001; Seewaldt *et al.*, 1999a). Caspase-1/3 assays were performed as follows: cells were harvested by trypsinization, washed once with 100 volumes of ice cold PBS and pelleted. Caspase-1 and -3 activities were then assayed according to the manufacturer's instructions using a caspase-1 (EMD Biosciences Inc.) or caspase-3 (Clontech, Palo Alto, CA, USA) assay kit. For IRF-1 suppression studies, early passage HMEC-E6 cells were transfected with IRF-1 siRNAs 12 hr prior to treatment with 1.0 μ M Tam. Caspase-1 and caspase-3 levels were measured at 4 hr and 18 hr, respectively, after Tam treatment.

Intentionally left blank.

Acknowledgments

This work is supported by NIH/NCI grants 2P30CA14236-26 [V.L.S., E.C.D.], R01CA88799 [to V.L.S.], R01984441 [V.L.S.], NIH/NIDDK grant 2P30DK 35816-11 [V.L.S.], DAMD17-98-1-8351 [to V.L.S.], American Cancer Society Award CCE-99898 [to V.L.S.], a V-Foundation Award [to V.L.S.], a Susan G. Komen Breast Cancer Award [to V.L.S., E.C.D.], and a Charlotte Geyer Award [V.L.S.]. The authors gratefully acknowledge Martha Stamfer's gift of normal human mammary epithelial cells.

References

- Aiba-Masago, S., Masago, R., Vela-Roch, N., Talal, N. and Dang, H. (2001). *Cell Signal.*, **13**, 617-24.
- Anderson, E., Clarke, R.B. and Howell, A. (1998). *J. Mamm. Gland Biol. Neoplasia*, **3**, 23-35.
- Andrews, H.N., Mullan, P.B., McWilliams, S., Sebelova, S., Quinn, J.E., Gilmore, P.M., McCabe, N., Pace, A., Koller, B., Johnston, P.G., Haber, D.A. and Harkin, D.P. (2002). *J. Biol. Chem.*, **277**, 26225-32.
- Aubele, M.M., Cummings, M.C., Mattis, A.E., Zitzelsberger, H.F., Walch, A.K., Kremer, M., Hofler, H. and Werner, M. (2000). *Diagn. Mol. Pathol.*, **9**, 14-9.
- Baldi, P. and Long, A.D. (2001). *Bioinformatics*, **17**, 509-19.
- Benjamini, Y. and Hochberg, Y. (1995). *J. R. Stat. Soc. Ser. B - Methodological*, **57**, 289-300.
- Bjornstrom, L. and Sjoberg, M. (2002). *Mol. Endocrinol.*, **16**, 2202-14.
- Chatterjee-Kishore, M., Kishore, R., Hicklin, D.J., Marincola, F.M. and Ferrone, S. (1998). *J. Biol. Chem.*, **273**, 16177-83.
- Chawla-Sarkar, M., Lindner, D.J., Liu, Y.F., Williams, B.R., Sen, G.C., Silverman, R.H. and Borden, E.C. (2003). *Apoptosis*, **8**, 237-49.
- Coradini, D., Biffi, A., Pellizzaro, C., Pirronello, E. and Di Fronzo, G. (1997). *Tumor Biol.*, **18**, 22-9.
- Creagh, E.M., Conroy, H. and Martin, S.J. (2003). *Immunol. Rev.*, **193**, 10-21.
- Dai, C. and Krantz, S.B. (1999). *Blood*, **93**, 3309-16.
- Darnell, J.E., Jr., Kerr, I.M. and Stark, G.R. (1994). *Science*, **264**, 1415-21.
- de Veer, M.J., Holko, M., Frevel, M., Walker, E., Der, S., Paranjape, J.M., Silverman, R.H. and Williams, B.R. (2001). *J. Leukoc. Biol.*, **69**, 912-20.
- Demers, G.W., Espling, E., Harry, J.B., Etscheid, B.G. and Galloway, D.A. (1996). *J. Virol.*, **70**, 6862-9.
- Der, S.D., Zhou, A., Williams, B.R. and Silverman, R.H. (1998). *Proc. Natl. Acad. Sci. USA*, **95**, 15623-8.
- Detjen, K.M., Farwig, K., Welzel, M., Wiedenmann, B. and Rosewicz, S. (2001). *Gut*, **49**, 251-62.
- Detjen, K.M., Kehrberger, J.P., Drost, A., Rabien, A., Welzel, M., Wiedenmann, B. and Rosewicz, S. (2002). *Int. J. Oncol.*, **21**, 1133-40.
- Dietze, E.C., Caldwell, L.E., Grupin, S.L., Mancini, M. and Seewaldt, V.L. (2001). *J Biol Chem*, **276**, 5384-94.
- Dietze, E.C., Troch, M.M., Bean, G.R., Heffner, J.B., Bowie, M.L., Rosenberg, P., Ratliff, B. and Seewaldt, V.L. (2004). *Oncogene*, **23**, 3851-62.
- Doherty, G.M., Boucher, L., Sorenson, K. and Lowney, J. (2001). *Ann. Surg.*, **233**, 623-9.
- Fisher, B., Costantino, J.P., Wickerham, D.L., Redmond, C.K., Kavanah, M., Cronin, W.M., Vogel, V., Robidoux, A., Dimitrov, N., Atkins, J., Daly, M., Wieand, S., Tan-Chiu, E., Ford, L. and Wolmark, N. (1998). *J. Natl. Cancer Inst.*, **90**, 1371-88.

- Gibson, D.F., Johnson, D.A., Goldstein, D., Langan-Fahey, S.M., Borden, E.C. and Jordan, V.C. (1993). *Breast Cancer Res. Treat.*, **25**, 141-50.
- Giles, R.H., Dauwerse, J.G., Higgins, C., Petrij, F., Wessels, J.W., Beverstock, G.C., Dohner, H., Jotterand-Bellomo, M., Falkenburg, J.H., Slater, R.M., van Ommen, G.J., Hagemeijer, A., van der Reijden, B.A. and Breuning, M.H. (1997a). *Leukemia*, **11**, 2087-96.
- Giles, R.H., Petrij, F., Dauwerse, H.G., den Hollander, A.I., Lushnikova, T., van Ommen, G.J., Goodman, R.H., Deaven, L.L., Doggett, N.A., Peters, D.J. and Breuning, M.H. (1997b). *Genomics*, **42**, 96-114.
- Gjermansen, I.M., Justesen, J. and Martensen, P.M. (2000). *Cytokine*, **12**, 233-8.
- Guo, S., Cichy, S.B., He, X., Yang, Q., Ragland, M., Ghosh, A.K., Johnson, P.F. and Unterman, T.G. (2001). *J. Biol. Chem.*, **276**, 8516-23.
- Harada, H., Takahashi, E., Itoh, S., Harada, K., Hori, T.A. and Taniguchi, T. (1994). *Mol. Cell Biol.*, **14**, 1500-9.
- Henderson, Y.C., Chou, M. and Deisseroth, A.B. (1997). *Br. J. Haematol.*, **96**, 566-75.
- Hiroi, M. and Ohmori, Y. (2003). *J. Biol. Chem.*, **278**, 651-60.
- Horvai, A.E., Xu, L., Korzus, E., Brard, G., Kalafus, D., Mullen, T.M., Rose, D.W., Rosenfeld, M.G. and Glass, C.K. (1997). *Proc. Natl. Acad. Sci. USA*, **94**, 1074-9.
- Horvath, C.M. (2000). *Trends Biochem. Sci.*, **25**, 496-502.
- Hoshiya, Y., Gupta, V., Kawakubo, H., Brachtel, E., Carey, J.L., Sasur, L., Scott, A., Donahoe, P.K. and Maheswaran, S. (2003). *J. Biol. Chem.*, **278**, 51703-12.
- Iacopino, F., Robustelli della Cuna, G. and Sica, G. (1997). *Int. J. Cancer*, **71**, 1103-8.
- Jiang, B., Liu, J.H., Bao, Y.M. and An, L.J. (2004). *Toxicol.*, **43**, 53-9.
- Kamada, S., Washida, M., Hasegawa, J., Kusano, H., Funahashi, Y. and Tsujimoto, Y. (1997). *Oncogene*, **15**, 285-90.
- Karlsen, A.E., Pavlovic, D., Nielsen, K., Jensen, J., Andersen, H.U., Pociot, F., Mandrup-Poulsen, T., Eizirik, D.L. and Nerup, J. (2000). *J. Clin. Endocrinol. Metab.*, **85**, 830-6.
- Kawasaki, H., Eckner, R., Yao, T.P., Taira, K., Chiu, R., Livingston, D.M. and Yokoyama, K.K. (1998). *Nature*, **393**, 284-9.
- Kelly, M.J. and Levin, E.R. (2001). *Trends Endocrinol. Metab.*, **12**, 152-6.
- Kim, E.J., Lee, J.M., Namkoong, S.E., Um, S.J. and Park, J.S. (2002). *J. Cell Biochem.*, **85**, 369-80.
- Kim, P.K., Armstrong, M., Liu, Y., Yan, P., Bucher, B., Zuckerbraun, B.S., Gambotto, A., Billiar, T.R. and Yim, J.H. (2004). *Oncogene*, **23**, 1125-35.
- Kolla, V., Lindner, D.J., Xiao, W., Borden, E.C. and Kalvakolanu, D.V. (1996). *J. Biol. Chem.*, **271**, 10508-14.
- Kovacs, K.A., Steinmann, M., Magistretti, P.J., Halfon, O., Cardinaux, J.R. (2003). *J. Biol. Chem.*, **278**, 36959-65.
- Kroger, A., Koster, M., Schroeder, K., Hauser, H. and Mueller, P.P. (2002). *J. Interferon Cytokine Res.*, **22**, 5-14.

- Kuida, K., Lippke, J.A., Ku, G., Harding, M.W., Livingston, D.J., Su, M.S. and Flavell, R.A. (1995). *Science*, **267**, 2000-3.
- Kumar-Sinha, C., Varambally, S., Sreekumar, A. and Chinnaiyan, A.M. (2002). *J. Biol. Chem.*, **277**, 575-85.
- Lindner, D.J. and Borden, E.C. (1997). *J. Interferon Cytokine Res.*, **17**, 681-93.
- Lindner, D.J., Kolla, V., Kalvakolanu, D.V. and Borden, E.C. (1997). *Mol. Cell Biochem.*, **167**, 169-77.
- Lininger, R.A., Park, W.S., Man, Y.G., Pham, T., MacGrogan, G., Zhuang, Z. and Tavassoli, F.A. (1998). *Hum. Pathol.*, **29**, 1113-8.
- Mantovani, F. and Banks, L. (2001). *Oncogene*, **20**, 7874-87.
- Merika, M., Williams, A.J., Chen, G., Collins, T. and Thanos, D. (1998). *Mol. Cell*, **1**, 277-87.
- Miller, K.A., Chung, J., Lo, D., Jones, J.C., Thimmapaya, B. and Weitzman, S.A. (2000). *J. Biol. Chem.*, **275**, 8176-82.
- Miura, M., Zhu, H., Rotello, R., Hartwig, E.A. and Yuan, J. (1993). *Cell*, **75**, 653-60.
- Nozawa, H., Oda, E., Nakao, K., Ishihara, M., Ueda, S., Yokochi, T., Ogasawara, K., Nakatsuru, Y., Shimizu, S., Ohira, Y., Hioki, K., Aizawa, S., Ishikawa, T., Katsuki, M., Muto, T., Taniguchi, T. and Tanaka, N. (1999). *Genes Dev.*, **13**, 1240-5.
- Oda, E., Ohki, R., Murasawa, H., Nemoto, J., Shibue, T., Yamashita, T., Tokino, T., Taniguchi, T. and Tanaka, N. (2000). *Science*, **288**, 1053-8.
- Parrington, J., Rogers, N.C., Gewert, D.R., Pine, R., Veals, S.A., Levy, D.E., Stark, G.R. and Kerr, I.M. (1993). *Eur. J. Biochem.*, **214**, 617-26.
- Pasinelli, P., Houseweart, M.K., Brown, R.H. Jr. and Cleveland, D.W. (2000). *Proc. Natl. Acad. Sci. USA*, **97**, 13901-6.
- Pestka, S., Langer, J.A., Zoon, K.C. and Samuel, C.E. (1987). *Annu. Rev. Biochem.*, **56**, 727-77.
- Pine, R., Canova, A., and Schindler, C. (1994). *EMBO J.*, **16**, 406-16.
- Rasmussen, U.B., Wolf, C., Mattei, M.G., Chenard, M.P., Bellocq, J.P., Chambon, P., Rio, M.C. and Basset, P. (1993). *Cancer Res.*, **53**, 4096-101.
- Robyr, D., Wolffe, A.P. and Wahli, W. (2000). *Mol. Endocrinol.*, **14**, 329-47.
- Romeo, G., Fiorucci, G., Chiantore, M.V., Percario, Z.A., Vannucchi, S. and Affabris, E. (2002). *J. Interferon Cytokine Res.*, **22**, 39-47.
- Seewaldt, V.L., Caldwell, L.E., Johnson, B.S., Swisshelm, K., Collins, S.J. and Tsai, S. (1997a). *Exp. Cell Res.*, **236**, 16-28.
- Seewaldt, V.L., Dietze, E.C., Johnson, B.S., Collins, S.J. and Parker, M.B. (1999a). *Cell Growth Differ.*, **10**, 49-59.
- Seewaldt, V.L., Johnson, B.S., Parker, M.B., Collins, S.J. and Swisshelm, K. (1995). *Cell Growth Differ.*, **6**, 1077-88.
- Seewaldt, V.L., Kim, J.H., Caldwell, L.E., Johnson, B.S., Swisshelm, K. and Collins, S.J. (1997b). *Cell Growth Differ.*, **8**, 631-41.
- Seewaldt, V.L., Kim, J.H., Parker, M.B., Dietze, E.C., Srinivasan, K.V. and Caldwell, L.E. (1999b). *Exp. Cell Res.*, **249**, 70-85.
- Seewaldt, V.L., Mrozek, K., Dietze, E.C., Parker, M. and Caldwell, L.E. (2001). *Cancer Res.*, **61**, 616-24.

- Sims, S.H., Cha, Y., Romine, M.F., Gao, P.Q., Gottlieb, K. and Deisseroth, A.B. (1993). *Mol. Cell Biol.*, **13**, 690-702.
- Stampfer, M. (1985). *J. Tissue Cult. Methods*, **9**, 109-21.
- Stark, G.R., Kerr, I.M., Williams, B.R., Silverman, R.H. and Schreiber, R.D. (1998). *Annu. Rev. Biochem.*, **67**, 227-64.
- Tamura, T., Ishihara, M., Lamphier, M.S., Tanaka, N., Oishi, I., Aizawa, S., Matsuyama, T., Mak, T.W., Taki, S. and Taniguchi, T. (1995). *Nature*, **376**, 596-9.
- Tanaka, N., Ishihara, M., Kitagawa, M., Harada, H., Kimura, T., Matsuyama, T., Lamphier, M.S., Aizawa, S., Mak, T.W. and Taniguchi, T. (1994). *Cell*, **77**, 829-39.
- Tsuda, H., Sakamaki, C., Tsugane, S., Fukutomi, T. and Hirohashi, S. (1998). *Jpn J Clin Oncol*, **28**, 5-11.
- Tzoanopoulos, D., Speletas, M., Arvanitidis, K., Veiopoulou, C., Kyriaki, S., Thyphronitis, G., Sideras, P., Kartalis, G. and Ritis, K. (2002). *Br. J. Haematol.*, **119**, 46-53.
- Wang, L., Miura, M., Bergeron, L., Zhu, H. and Yuan, J. (1994). *Cell*, **78**, 739-50.
- Watson, C.J. and Miller, W.R. (1995). *Br. J. Cancer*, **71**, 840-4.
- Wen, Z., Zhong, Z., Darnell, J.E. Jr. (1995). *Cell*, **82**, 241-50.
- Widschwendter, M., Daxenbichler, G., Bachmair, F., Muller, E., Zeimet, A.G., Windbichler, G., Uhl-Steidl, M., Lang, T. and Marth, C. (1996). *Anticancer Res.*, **16**, 369-74.
- Yahata, T., Shao, W., Endoh, H., Hur, J., Coser, K.R., Sun, H., Ueda, Y., Kato, S., Isselbacher, K.J., Brown, M. and Shioda, T. (2001). *Genes Dev.*, **15**, 2598-612.
- Yao, T.P., Oh, S.P., Fuchs, M., Zhou, N.D., Ch'ng, L.E., Newsome, D., Bronson, R.T., Li, E., Livingston, D.M. and Eckner, R. (1998). *Cell*, **93**, 361-72.
- Yim, J.H., Wu, S.J., Casey, M.J., Norton, J.A. and Doherty, G.M. (1997). *J. Immunol.*, **158**, 1284-92.
- Zhang, J.J., Vinkemeier, U., Gu, W., Chakravarti, D., Horvath, C.M. and Darnell, J.E., Jr. (1996). *Proc. Natl. Acad. Sci. USA*, **93**, 15092-6.
- Zhang, S., Liu, J., Dragunow, M. and Cooper, G.J.S. (2003). *J. Biol. Chem.*, **278**, 52810-19.

Table 1: ISG primers

Gene Name	Primer set	Cycle conditions	PCR cycle number
ISG15	F: 5'-AGTACAGGAGCTTGTGCCGT-3' R: 5'-GAAGGTCAGCCAGAACAGGT-3'	94°C 2 min. 94°C 30 sec. 58°C 30 sec. 72°C 1 min. 72°C 7 min.	22
ISG12	F: 5'-GAATTAACCCGAGCAGGCAT-3' R: 5'-CTCTGGAGATGCAGAATTGG-3'	94°C 2 min. 94°C 30 sec. 58°C 30 sec. 72°C 1 min. 72°C 7 min.	27
IFI-56	F: 5'-GGTCAAGGATAGTCTGGAGCA-3' R: 5'-AGTGGCTGATATCTGGGTGC-3'	94°C 2 min. 94°C 30 sec. 58°C 30 sec. 72°C 2 min. 72°C 7 min.	23
IFI 9-27	F: 5'-GAAACTGAAACGACAGGGGA-3' R: 5'-TGTATCTAGGGGCAGGACCA-3'	94°C 2 min. 94°C 30 sec. 58°C 30 sec. 72°C 1 min. 72°C 7 min.	24
IFI 6-16	F: 5'-CAAGGTCTAGTGACGGAGCC-3' R: 5'-CTGCTGGCTACTCCTCATCC-3'	94°C 2 min. 94°C 30 sec. 58°C 30 sec. 72°C 1 min. 72°C 7 min.	25
IRF-1	F: 5'-ACCCTGGCTAGAGATGCAGA-3' R: 5'-TTTTCCCCTGCTTGTATCG-3'	94°C 5 min. 94°C 30 sec. 51°C 30 sec. 72°C 45 sec. 72°C 7 min.	28
Beta-actin	F: 5'-GCTCGTCGTCGACAACGGCTC-3' R: 5'-AAACATGATCTGGGTCATCTTCTC-3'	94°C 2 min. 94°C 15 sec. 55°C 30 sec. 72°C 30 sec. 72°C 7 min.	18

Table 2: Tamoxifen gene changes

Gene Name	Genbank™	Fold change	
		HMEC-LX	HMEC-E6
IFI 9-27	J04164	----	4.5
IRF-1	L05072	----	4.0
ISG15	M13755	----	4.4
ISG-54	M14660	----	5.2
RANTES	M21121	----	1.9
IFI-56	M24594	----	2.3
MX-A	M33882	----	20.0
Interferon gamma-inducible protein 16	M63838	----	2.0
2'-5'-oligoadenylate synthetase 2, isoform p69	M87284	----	3.8
2'-5'-oligoadenylate synthetase 2, isoform p71	M87434	----	3.6
IRF-9	M87503	----	2.6
STAT1 alpha	M97935	----	2.0
STAT1 beta	M97936	-3.1	12.7
Interferon gamma receptor 1	U19247	----	2.1
IFI 6-16	U22970	----	17.5
RIG-G	U52513	----	2.1
IRF-7	U53830	----	9.7
Interferon-induced protein 35	U72882	----	2.6
2',5'-oligoadenylate synthetase 1 (1.6kb RNA)	X02874	----	4.5
2',5'-oligoadenylate synthetase 1 (1.8kb RNA)	X02875	----	4.2
Interleukin 6 (interferon, beta 2)	X04602	----	----
Interferon induced transmembrane protein 2 (1-8D)	X57351	----	----
ISG12	X67325	----	7.6
proteasome subunit, beta type 10	X71874	-1.6	----
proteasome subunit, beta type 8; LMP8	Z14982	-2.6	----

Figure 1: Semi-quantitative RT-PCR analysis of ISG mRNA expression in early passage acutely damaged HMEC-E6 cells (passage 10) and HMEC-LX vector controls (passage 10). Treated with 1.0 μ M Tam for 0 hr (Φ) and 6 hr (T-6). Beta-actin serves as a normalization control. These data are representative of three separate experiments.

Figure 2: Tam induces expression of IRF-1 mRNA and protein in acutely damaged HMEC-E6 cells.

(A) Semi-quantitative RT-PCR analysis of IRF-1 mRNA expression in early passage acutely damaged HMEC-E6 cells (passage 10) and HMEC-LX vector controls (passage 10). Treated with 1.0 μ M Tam for 0, 30 min, 2, 3, and 6 hr. Beta-actin serves as a normalization control. The negative sample (-) contained no cDNA. These data are representative of three separate experiments.

(B) Quantitation of IRF-1 mRNA expression in early passage HMEC-E6 cells and HMEC-LX vector controls treated with 1.0 μ M Tam. Expression is normalized to beta-actin. These data are the average of three separate determinations. (*: p-value < 0.01)

(C) Expression of IRF-1 protein in early passage HMEC-E6 cells (passage 11) treated with 1.0 μ M Tam for 0, 30 min, 2, 3, and 6 hr. Equal amounts of protein lysate were added in each lane. Beta-actin serves as a loading control.

(D) Quantitation of IRF-1 protein expression in early passage HMEC-E6 cells treated with 1.0 μ M Tam. Expression is normalized to beta-actin. These data are the average of three separate determinations. (*: p-value < 0.025; **: p-value < 0.001)

Figure 3: Tam promotes recruitment of CBP to the IRF-1 promoter GAS element in acutely damaged HMEC-E6 cells.

(A) ChIP was performed to test for STAT1 and CBP recruitment to the *IRF-1* GAS element as a function of Tam treatment. Early passage acutely damaged HMEC-E6 cells (passage 11) were treated with 1.0 μ M Tam for 0, 2, and 6 hr as described in Materials and Methods. Input controls tested the integrity of the DNA samples. These data represent three separate experiments.

(B) An immunoprecipitation time course using a biotin-labeled oligo, containing the *IRF-1* GAS promoter element, was performed to investigate the temporal correlation between CBP recruitment to the *IRF-1* promoter and IRF-1 mRNA induction in Tam-treated early passage HMEC-E6 cells (passage 12) as described in Materials and Methods. CBP-input controls are provided to assess the CBP content of protein lysates subjected to immunoprecipitation. CBP-bound assesses the amount of CBP bound to the *IRF-1* GAS promoter element oligo. These data are representative of three separate experiments.

Figure 4: Tam promotes induction of ISG IFI 6-16 mRNA and recruitment of STAT1, CBP, and IRF-1 to the ISRE element of the IFI 6-16 promoter.

(A) Semi-quantitative RT-PCR analysis of IFI 6-16 mRNA expression in early passage acutely damaged HMEC-E6 cells (passage 10) and HMEC-LX vector controls (passage 10). Treated with 1.0 μ M Tam for 0, 30 min, 2, 3, and 6 hr. Beta-actin serves as a normalization control. The negative control (-) contained no cDNA. These data are representative of three separate experiments.

(B) Quantitation of IFI 6-16 mRNA expression in early passage HMEC-E6 cells and HMEC-LX vector controls treated with 1.0 μ M Tam. Expression is normalized to beta-actin. These data are the average of three separate determinations. (*: p-value < 0.01)

(C) ChIP was performed to test for STAT1, CBP, and IRF-1 recruitment to the *IFI 6-16* ISRE promoter element as a function of Tam treatment. Early passage acutely damaged HMEC-E6 cells (passage 11) were treated with 1.0 μ M Tam for 0, 30 min, 2, and 6 hr as described in Materials and Methods. Input controls tested the integrity of the DNA samples. These data represent three separate experiments.

(D) Baseline phosphorylation of STAT1 in early passage HMEC-E6 cells (passage 11). Membrane was incubated with antibodies specific for STAT1-phosphoserine-727 (STAT1-pSer727), and STAT1 (total STAT1). Equal amounts of protein lysate were loaded in each lane. Beta-actin serves as a loading control.

Figure 5: Tam promotes caspase-1 activation in acutely damaged HMEC-E6 cells.

(A) HMEC-LX vector controls (passage 10) and HMEC-E6 cells (passage 10) were treated with either 1.0 μ M Tam or an equivalent volume of solvent for 0 to 6 hr, to test for caspase-1 activity. Cells were harvested by trypsinization, washed, and pelleted. The pellets were lysed and assayed according to the manufacturer's instructions. Assays were performed in duplicate. A positive control was provided by THP-1 cells (+cont). These data are the mean of three separate experiments with standard deviation (**: p-value < 0.025).

(B) Caspase-1 activation by Tam in acutely damaged HMEC-E6 cells (passage 11) is blocked by pretreatment with 15 nM Caspase-1 inhibitor IV for 4 hr. HMEC-E6 cells were treated with either 1.0 μ M Tam (**TAM**) or an equivalent volume of solvent for 4 hr. Caspase-1 activity was assayed as above. A positive control was provided by THP-1 cells. These data are the mean of three separate experiments performed in duplicate.

(C) Caspase-3 activation by Tam in acutely damaged HMEC-E6 cells (passage 11) is blocked by pretreatment with 15 nM Caspase-1 inhibitor IV for 3 hr. HMEC-E6 cells were treated with either 1.0 μ M Tam (**TAM**) or an equivalent volume of solvent. Caspase-3 activity was assayed as above. These data are the mean of three separate experiments performed in duplicate.

(D) Pretreatment with 15 mM Caspase-1 inhibitor IV for 3 hr blocks Tam-induced apoptosis in acutely damaged HMEC-E6 cells (passage 11). Cells were treated with

or without 1.0 μ M Tam and harvested after an 18 hr treatment. Control cells received an equivalent volume of solvent. Detection of apoptotic cells was performed with FITC-conjugated Annexin V as described in Materials and Methods. These data are representative of three experiments.

Figure 6: Inhibition of IRF-1 expression blocks Tam-induced caspase-1/3 activation and apoptosis in acutely damaged HMEC-E6 cells.

(A) Suppression levels of IRF-1 protein expression in early passage HMEC-E6 cells (passage 11) treated with siRNA #1, siRNA #4, and Cellfectin™ for 12hr. Equal amounts of protein lysate were loaded in each lane. Beta-actin serves as a loading control.

(B) siRNA directed against IRF-1 blocks Tam-mediated caspase-1 activation in acutely damaged HMEC-E6 cells (passage 11). Cells were treated with 1.0 μ M Tam (**Tam**) or an equivalent volume of solvent (**No TX**) for 4 hr. Caspase-1 activity was assayed as described in Materials and Methods. A positive control was provided by THP-1 cells (**pos. control**). These data are the mean of three experiments performed in duplicate.

(C) siRNA directed against IRF-1 blocks Tam-mediated caspase-3 activation in acutely damaged HMEC-E6 cells (passage 11). Cells were treated with 1.0 μ M Tam (**Tam**) or an equivalent volume of solvent (**No TX**) for 12 hr. Caspase-3 activity was assayed as per manufacturer's instructions using the caspase-3 assay kit (Clontech, Palo Alto, CA, USA). A positive control was provided by THP-1 cells (**pos. control**). These data are the mean of three experiments performed in duplicate.

(D) siRNA directed against IRF-1 blocks Tam-induced apoptosis in acutely damaged HMEC-E6 cells (passage 11). Cells were treated with 1.0 μ M Tam (**Tam**) or an equivalent volume of solvent (**No TX**) for 18 hr. Detection of apoptotic cells was

performed with FITC-conjugated Annexin V as described in Materials and Methods.

These data are representative of three experiments.

In each experiment HMEC-E6 cells were pretreated with Cellfectin™, control siRNA, siRNA #1 or siRNA #4 for 12 hr, and then treated with either 1.0 μM Tam (**Tam**) or an equivalent volume of solvent (**No TX**) for the time indicated. Control cells (**Control**) were not exposed to either siRNA or Cellfectin™. Cellfectin™ controls (**Cellfectin**) were exposed to Cellfectin™ alone.

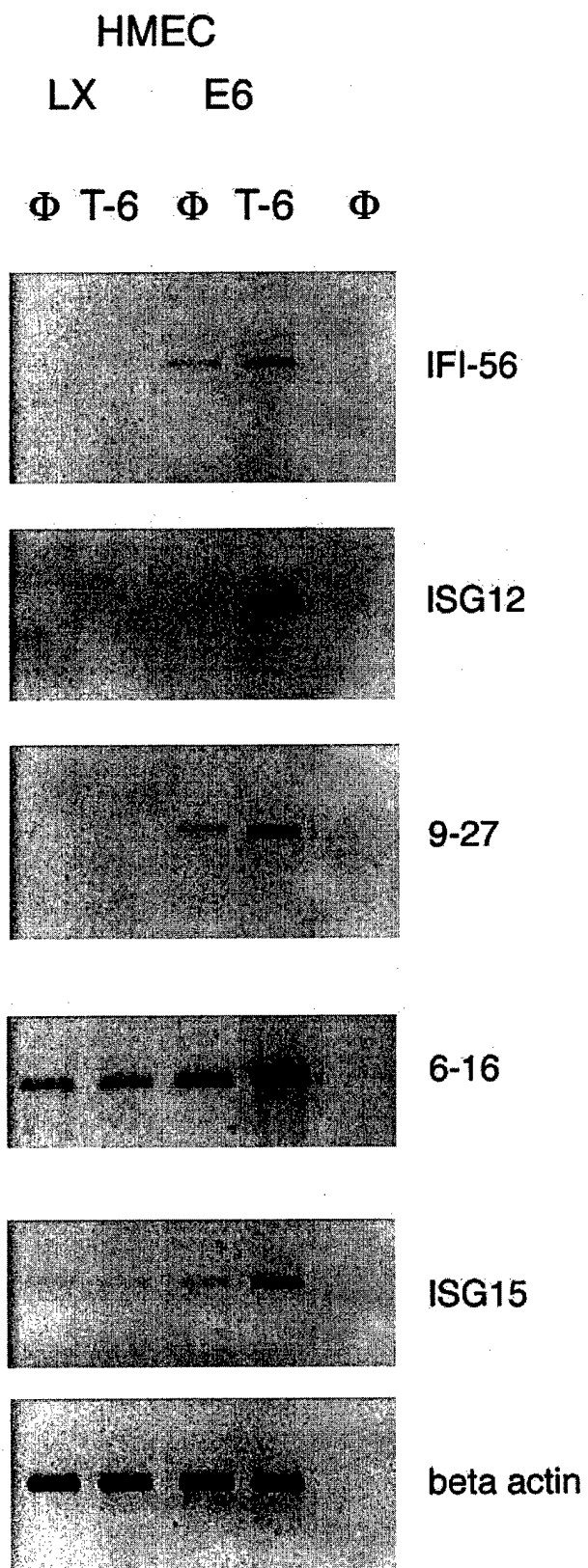
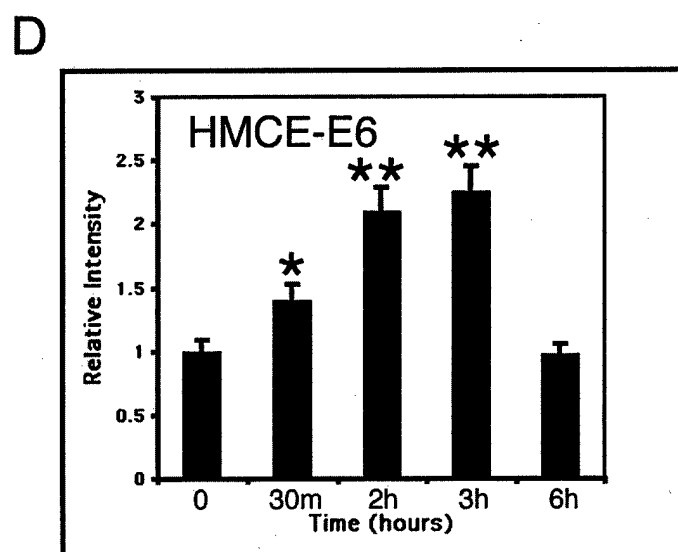
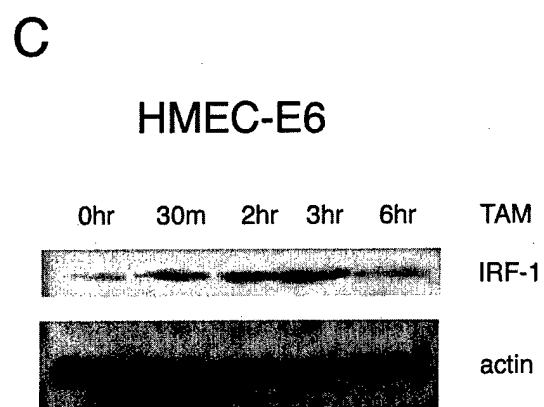
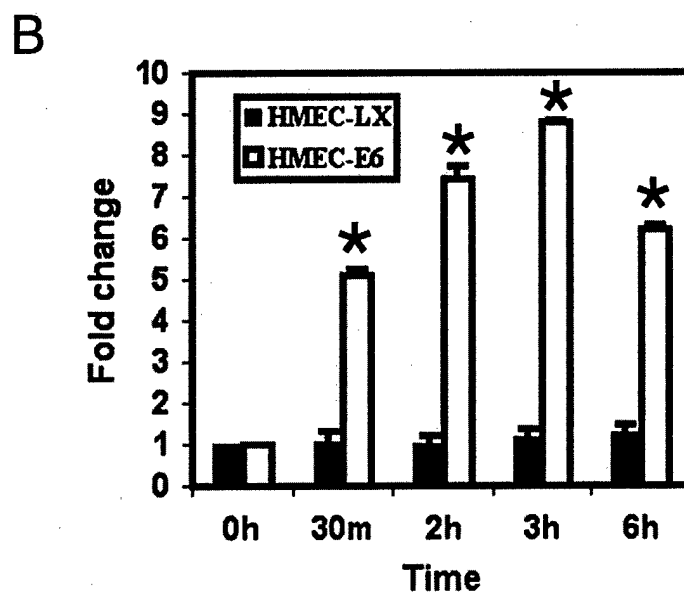
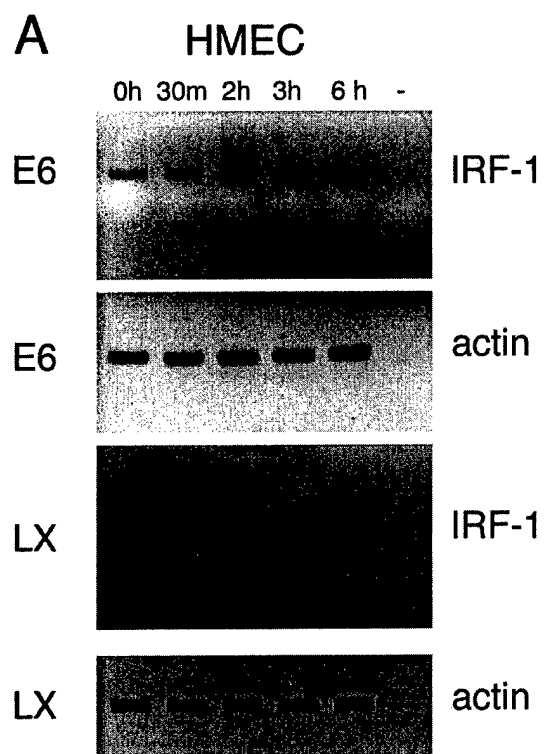


Fig. 1

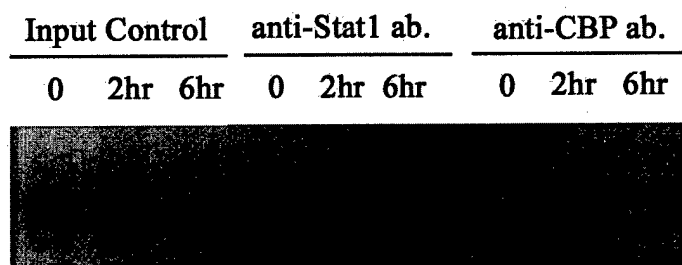
Figure 2.



A

HMEC-E6

IRF-1 promoter GAS element



B

HMEC-E6

IRF-1 promoter GAS element

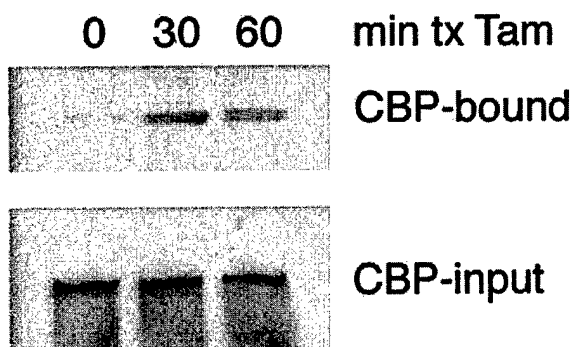


Fig. 3

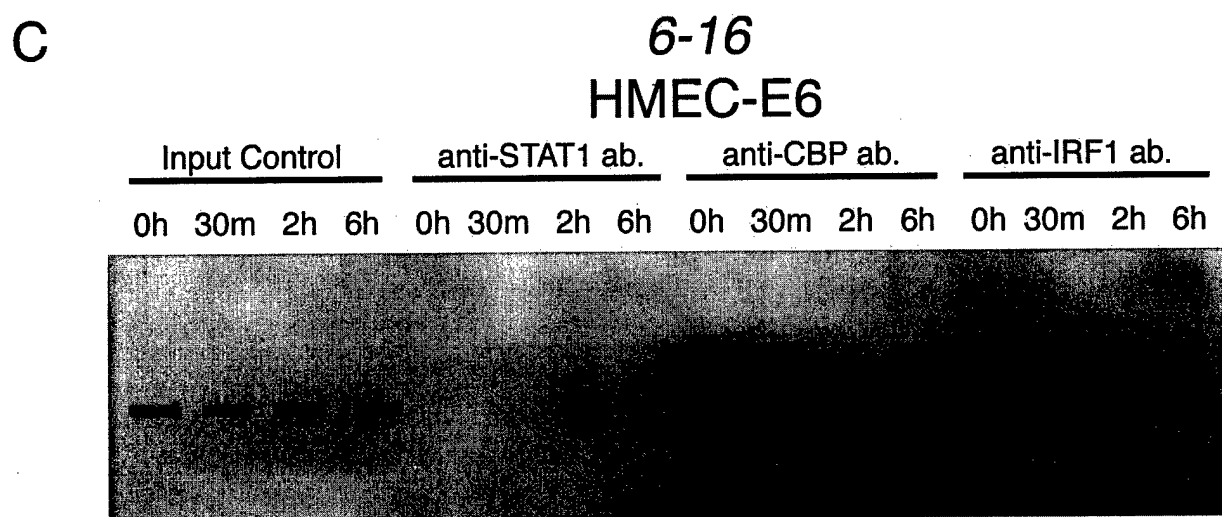
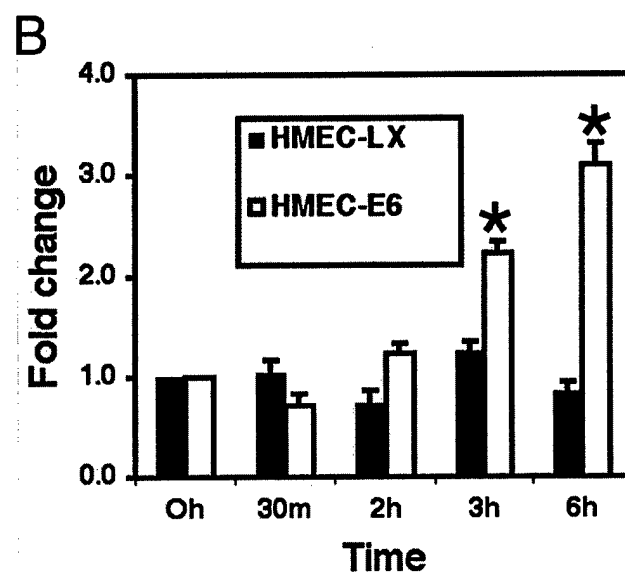
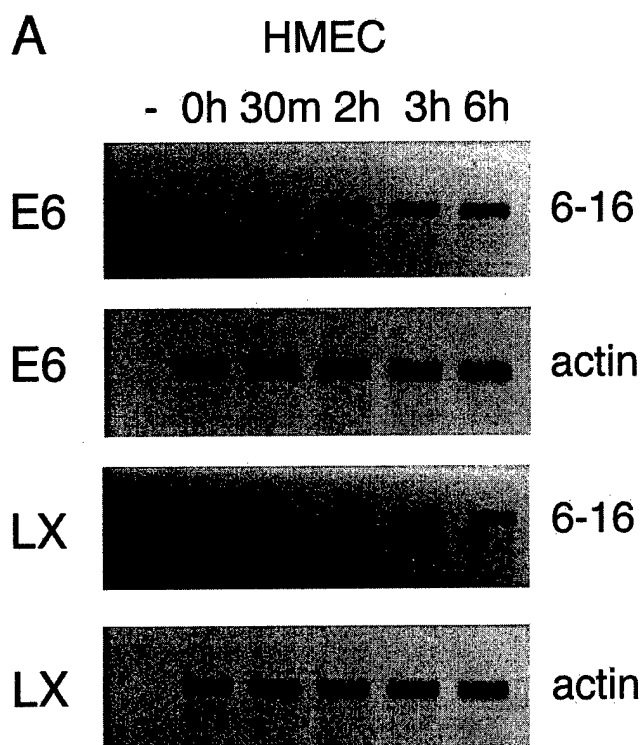
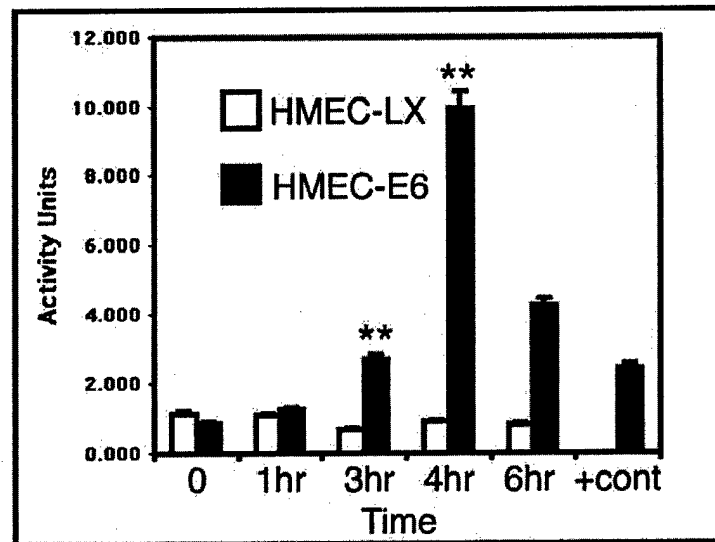
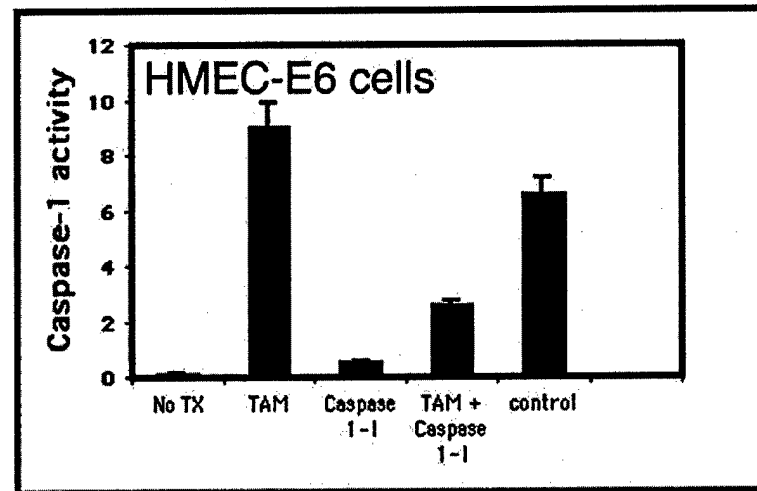


Fig. 4

A



B



C

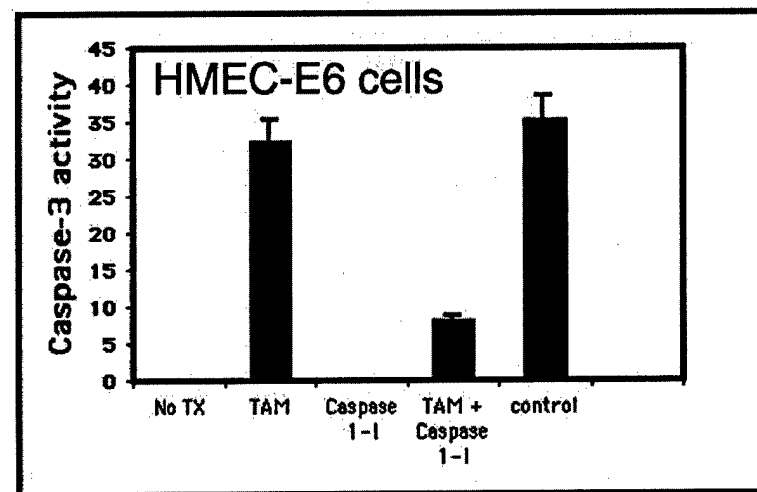


Figure 5 A-C

D

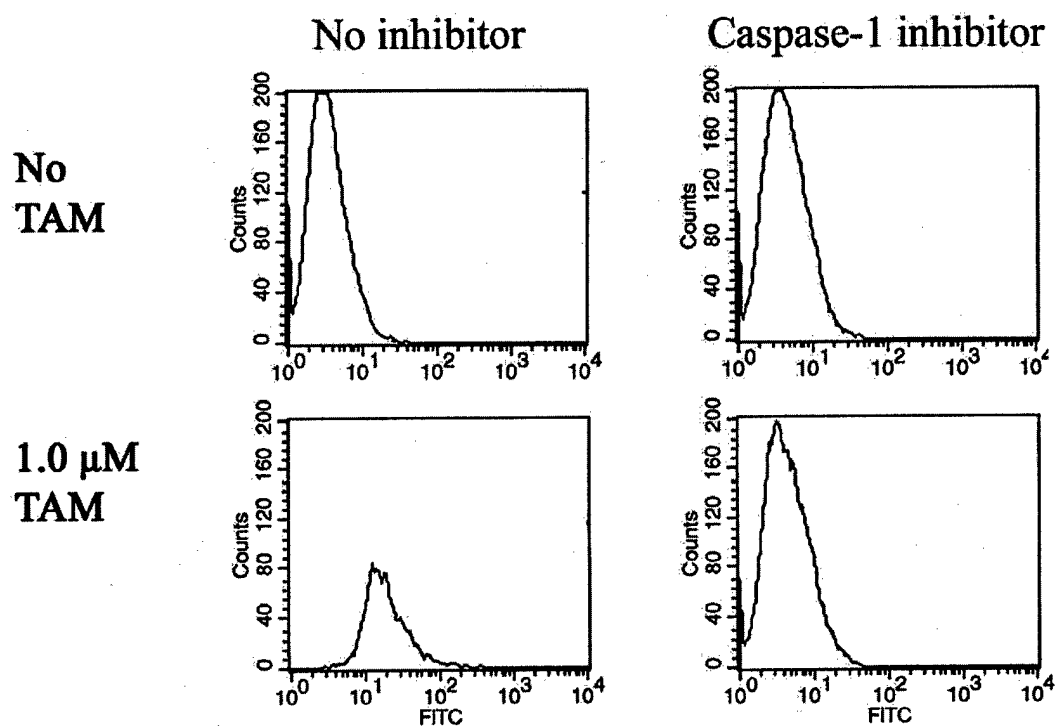
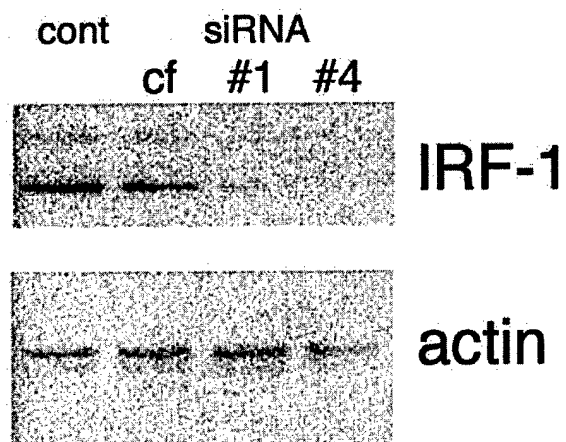
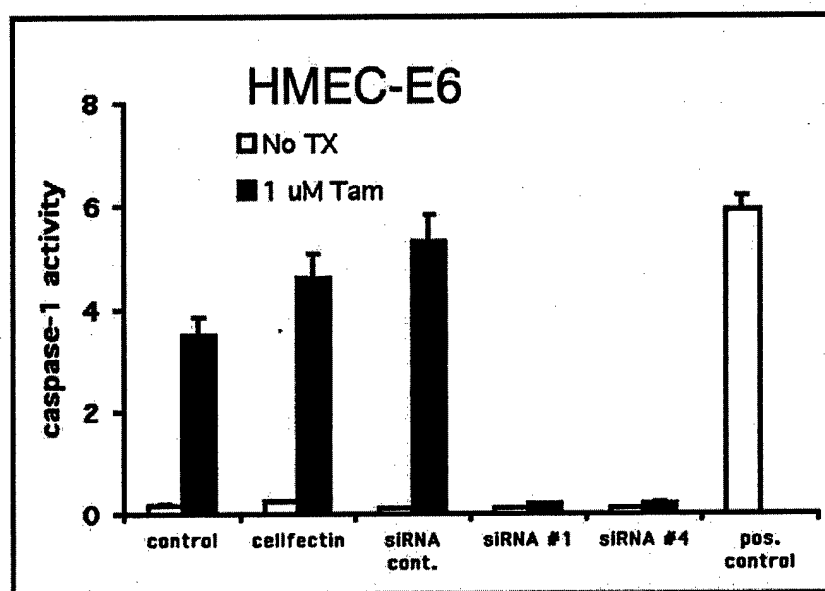


Figure 5 D

A



B



C

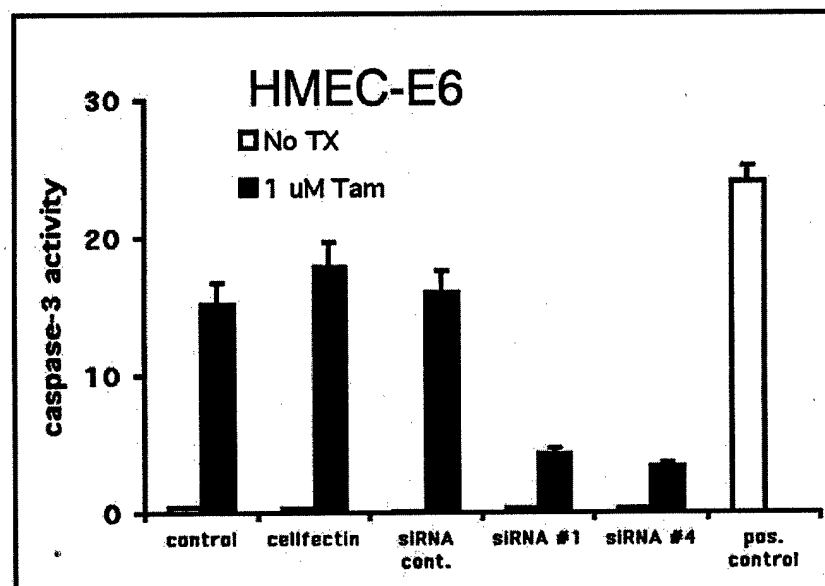


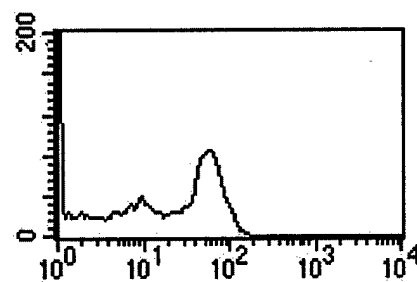
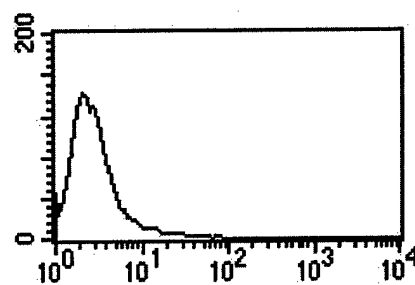
Figure 6 A-C

D

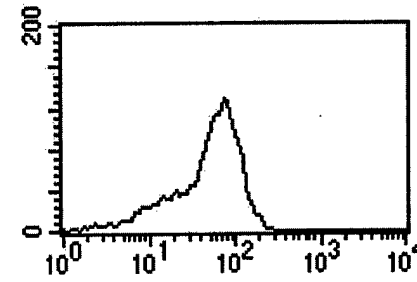
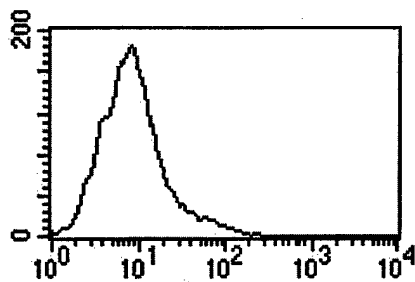
No TX

1 μ M Tam

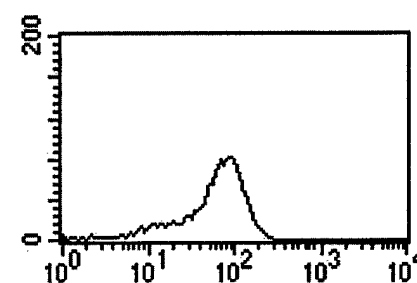
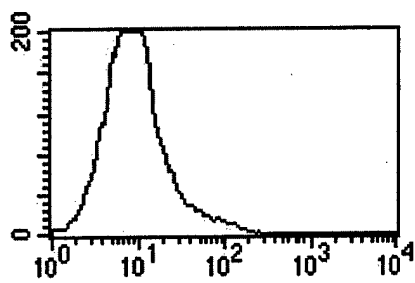
Control



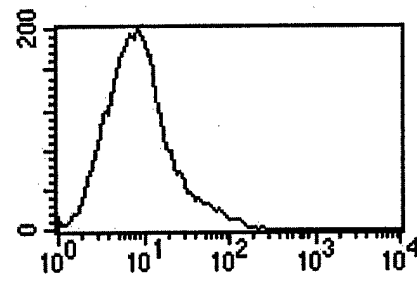
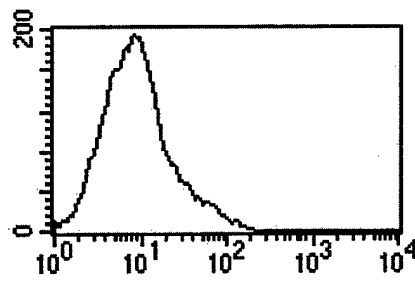
Cellfectin



Control
siRNA



IRF-1 #1
siRNA



IRF-1 #4
siRNA

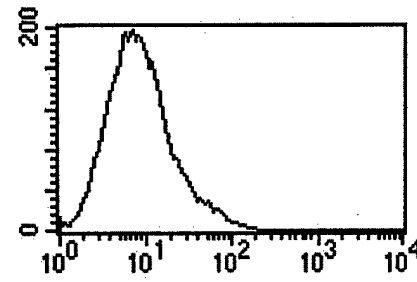
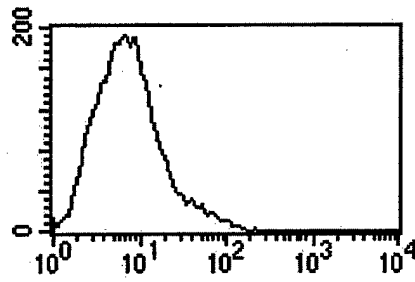


Figure 6D.

Retinoic Acid Receptor-beta2 Promoter Methylation in Random
Periareolar Fine Needle Aspiration

GREGORY R. BEAN, VICTORIA SCOTT, LISA YEE³, BROOKE RATLIFF-DANIEL³,
MICHELLE M. TROCH, MICHELLE L. BOWIE, PAUL K. MARCOM, JAIMIE SLADE, BRUCE
F. KIMLER, CAROL J. FABIAN, CAROLA M. ZALLES, GLORIA BROADWATER, JOSEPH C.
BAKER, JR., CASSANDRA MOORE, AND VICTORIA L. SEEWALDT²

Division of Medical Oncology, Duke University Medical Center, Durham, NC 27710
[G.R.B., V.S., B.R.D., M.M.T., M.L.B., P.K.M., J.S., G.B., J.C.B., C.M., V.L.S.],
Department of Surgery and the Comprehensive Cancer Center, The Ohio State
University, Columbus, OH 43210 [L.Y.], University of Kansas Medical Center, Kansas
City, Kansas [B.F.K., C.J.F., C.M.Z.].

Abstract

Methylation of the RAR β 2 P2 promoter is hypothesized to be an important mechanism for loss of RAR β 2 function during early mammary carcinogenesis. The frequency of RAR β 2 P2 methylation was tested in 1) sixteen early stage breast cancers and 2) sixty-seven Random Periareolar Fine Needle Aspiration (RPFNA) samples obtained from 38 asymptomatic women who were at increased risk for breast cancer. Risk was defined as either 1) 5 year Gail risk calculation $\geq 1.7\%$, 2) prior biopsy exhibiting atypical hyperplasia, LCIS/DCIS, or 3) known BRCA1/2 mutation carrier. RAR β 2 P2 promoter methylation was assessed at two regions, M3 (-51 to +162 bp) and M4 (+104 to +251 bp). In early stage cancers, M4 methylation was observed in 11/16 (69%) cases; in RPFNA aspirates, methylation was present at M3 and M4 in 28/56 (50%) and 19/56 (38%) cases, respectively. RPFNAs were stratified for cytologic atypia using the Masood cytology index. The distribution of RAR β 2 P2 promoter methylation was reported as a function of increased cytologic abnormality. Methylation at both M3 and M4 was observed in 1) 0/10 (0%) of RPFNAs with Masood scores of 10 or less (non-proliferative), 2) 3/20 (15%) with Masood scores of 11-12 (low-grade proliferative), 2) 3/10 (30%) with Masood scores of 13 (high-grade proliferative), and 3) 7/14 (50%) with Masood scores of 14-15 (atypia). Results from this study indicate that the RAR β 2 P2 promoter is frequently methylated (69%) in primary breast cancers and demonstrates a positive association with increasing cytologic abnormality in RPFNA.

Introduction

Recent studies suggest that breast cancer incidence may be substantially reduced in high-risk women by tamoxifen treatment and/or prophylactic mastectomy (1-3). Although these reports are encouraging, current prevention strategies are expensive and can be associated with significant side effects. Biomarkers are needed to accurately predict short-term breast cancer risk so that 1) women who are most likely to benefit from preventive therapy can be identified and 2) response to chemoprevention can be accurately assessed.

Retinoids are important mediators of growth and differentiation in normal human mammary epithelial cells (HMECs) and regulate the expression of many pharmacologic targets for prevention such as cyclooxygenase-2 (COX-2) (4-6). The majority of retinoid actions are mediated through specific nuclear retinoid receptors (RAR- α , - β , and - γ) and rexinoid receptors (RXR- α , - β , and - γ). These nuclear receptors act as transcription regulators and establish genetic communication networks that are essential in regulating cell growth, differentiation, and apoptosis (4). The transcriptional activity of RARs and RXRs is primarily modulated through the formation of RAR-RXR heterodimers (4). These heterodimers have two distinct functions: 1) they modulate transcription initiation after binding to retinoic acid response elements (RAREs) in the promoter of target genes and 2) they promote "cross-talk" with other steroid signaling pathways, perhaps through promoting co-activator shifts.

RAR β 2 is unique because it is 1) primarily expressed in epithelial cells and 2) positively regulated by retinoids and the RAR β 2 P2 promoter retinoic acid response element (4).

We have shown that RAR β 2 is a tumor suppressor in breast cancer (7) and progressive loss of RAR β 2 expression is observed during breast carcinogenesis (8, 9). Importantly, while retinoids and RAR β 2 mediate growth arrest and differentiation in HMECs, restoration of RAR β 2 function in breast cancer cells promotes apoptotic cell death (5, 10-12). Noncancerous epithelial cells adjacent to invasive breast cancer also exhibit markedly decreased RAR β 2 mRNA expression (8, 9). This has led to the hypothesis that loss of RAR β 2 expression may provide a local cellular environment (field effect) that promotes mammary carcinogenesis.

Tumorigenesis is thought to be a multistep process resulting from the accumulation of genetic losses and epigenetic changes. Epigenetic changes, mainly DNA methylation and modification of histones, are now recognized as playing a critical role in carcinogenesis (13). A multitude of studies using the candidate gene approach have established the importance of DNA hypermethylation in tumor suppressor gene silencing (13-24). Several important observations have been made. First, many tumor suppressor genes have been found to be hypermethylated in multiple tumor types. For example, BRCA1 promoter hypermethylation has been observed in breast and ovarian cancer (16, 21). Second, DNA hypermethylation events occur early in carcinogenesis, which makes hypermethylation a potentially important marker of risk and a target for prevention. Third, evidence also suggests that hypermethylation of DNA repair genes may profoundly affect overall and disease-free survival in patients with malignancy (13).

Loss of RAR β 2 function in mammary epithelial cells is hypothesized to be the result of both genetic and epigenetic events. Two mechanisms have been proposed: 1) loss of

heterozygosity (LOH) and 2) promoter hypermethylation (6, 8, 9, 14, 15). LOH at the RAR β 2 locus (3p24) is frequently observed in invasive breast cancers and is thought to be a late mechanism for loss of RAR β 2 expression (6, 8). In contrast, RAR β 2 P2 promoter methylation has been observed in dysplastic mammary epithelial cells and is thought to be an important early mechanism for loss of RAR β 2 expression (9, 14, 15).

Random Periareolar Fine Needle Aspiration (RPFNA) is a research technique developed to repeatedly sample mammary cells from the whole breast of asymptomatic high-risk women to assess both 1) breast cancer risk and 2) response to chemoprevention (25, 26). RPFNA is distinct from diagnostic FNA: diagnostic FNA is a standard clinical technique used to evaluate a clinically identifiable breast mass, while breast RPFNA is analogous to a cervical pap-smear in its ability to obtain a representative sampling of cells from the entire breast of asymptomatic women. RPFNA has the advantage of being able to provide a "snap-shot" of the whole breast, and, unlike ductal lavage, 1) can be performed successfully in a majority of high-risk women (72-85% cell yield for RPFNA vs. 20-40% for ductal lavage) and 2) has been validated in long-term chemoprevention cohorts (25-27). A great strength of RPFNA is the willingness of high-risk women to undergo subsequent RPFNA; approximately 80% of women who undergo initial RPFNA undergo subsequent RPFNA (25, 26). Breast RPFNA has been successfully used to predict breast cancer risk in women at increased risk for breast cancer. The presence of cellular atypia in a breast RPFNA specimen is associated with a 5-fold increase in breast cancer risk in high-risk women (25). These observations validate the use of cellular atypia obtained by RPFNA as a surrogate marker of short-term breast cancer risk in high-risk populations.

The frequency of RAR β 2 P2 promoter methylation and resulting loss of RAR β 2 expression in breast RPFNA is currently unknown. RAR β 2 P2 methylation is 1) frequently (74%) detected in fluid from mammary ducts containing ductal carcinoma *in situ* and invasive carcinomas and 2) observed in 2/5 (40%) atypical ductal lavage specimens (28, 29). While these data are extremely limited (n=5), they provide evidence for the feasibility of testing for RAR β 2 P2 methylation in cytological specimens. As described in this study, we demonstrate that RAR β 2 P2 methylation 1) is observed in 68.8% of primary breast cancers and 2) correlates with the presence of increasing cytologic abnormality in RPFNA samples obtained in high risk women.

Methods

Informed Consent: The study was approved by the Human Subjects Committee and Institutional Review Board at the Ohio State University (for biopsy assessment) and Duke University Medical Center (for RPFNA studies), in accordance with assurances filed with and approved by the Department of Health and Human Services.

Biopsy Tissue: Paraffin-embedded fixed breast biopsy tissue was tested from subjects with Stage I or II invasive breast cancer.

Eligibility: To be eligible for screening by RPFNA, women were required to have at least one of the following major risk factors for breast cancer: 1) 5 year Gail risk calculation $\geq 1.7\%$, 2) prior biopsy exhibiting atypical hyperplasia, lobular carcinoma *in situ* (LCIS), ductal carcinoma *in situ* (DCIS), or 3) known BRCA1/2 mutation carrier. In subjects with prior DCIS/LCIS or radiation, only the contralateral breast was aspirated. In general, women were required to be between 30 and 60 years of age, as women younger than 30 years have a low short-term risk of breast cancer and women older than 60 years often have involutional breasts that are unlikely to yield sufficient cells for analysis (25). Women younger than 30 years could only be aspirated if they were within 10 years of the age of onset in a first degree relative. Women older than 55 could only participate if they had prior evidence of generalized proliferative breast disease. All women were required to have a mammogram interpreted as "not suspicious for breast cancer" within 2 months of entry, plus a breast examination on the day of aspiration that was interpreted as normal or not sufficiently abnormal to warrant a diagnostic biopsy. Clinical parameters evaluated included age, menopausal status, hormone and oral

contraceptive use, parity, age of menarche and menopause, lactation history, family cancer history (including family history of breast, ovarian, colon, and prostate cancer), radiation exposure, and other environmental exposures.

RPFNA: RPFNA was performed as previously published (25, 26). All investigators were trained to perform RPFNA by Carol Fabian. To control for hormonal effects on mammary cell proliferation, menstruating women were aspirated between Days 1-12 of their cycle. The breast was anesthetized with 5 cc of 1% lidocaine, immediately adjacent to the areola, at approximately 3 and 9 o'clock. Eight to ten aspirations were performed per breast for random sampling of epithelial cells. After the aspiration, cold packs were applied to the breasts for 10 min, and then both breasts were bound in kerlex gauze for 12-24 hr. Epithelial cells were pooled and placed in modified CytoLyt™ (Cytoc Corporation) with 1% formalin for 24 hr. Cells from the right and left breast were pooled separately, so as to obtain one sample per aspirated breast. Epithelial cells were split into two pools, with half designated for cytology and half designated for DNA extraction.

Cytologic Assessment: Slides for cytology were prepared by filtration and Papinicolus Stained as described previously (25, 26). Cells were classified as nonproliferative, hyperplasia, or hyperplasia with atypia (30). Cytology preparations were also given a semiquantitative index score through evaluation by the Masood Cytology Index (25, 26). As previously described, cells were given a score of 1-4 points for each of six morphological characteristics that include cell arrangement, pleomorphism, number of myoepithelial cells, anisonucleosis, nucleoli, and chromatin clumping (25, 26). Morphological assessment, Masood Cytology Index scores, and cell count were assigned

by a single dedicated pathologist from University of Kansas Medical Center (C.M.Z.) without knowledge of the subjects' clinical history.

Materials and Cell Culture Lines: Sodium bisulfite (Sigma, A.C.S.) and hydroquinone (Sigma, 99+%) were used under reduced lighting and stored in a dessicator. 2-pyrrolidinone (99+%) was purchased from Fluka. HS578T and ZR751 cell lines were obtained from American Type Culture Collection (Manassas, VA) and grown in supplemented α MEM (GibcoBRL) as previously described (5). HMEC-SR is a cell line derived from Human Papillomavirus E6-immortalized, normal human mammary epithelial cell (HMEC) strain AG11132 (M. Stampfer #172R/AA7) (31). This cell strain was purchased from the National Institute of Aging, Cell Culture Repository (Coriell Institute, Camden, NJ) and grown in supplemented MEM (Cambrex) as previously described (11, 32). E6-transduction is as previously described (33, 34).

DNA Extraction from Fixed Tissue: DNA was extracted from paraffin-embedded tissue using the Pico Pure DNA Extraction Kit (Arcturus) according to manufacturer's instructions. The DNA was then purified with a phenol-chloroform extraction, ethanol precipitated, and resuspended in 10 mM Tris (pH 7.5). Samples were stored at -80°C.

DNA Extraction from RPFNA: The RPFNA samples were washed with unmodified CytoLytTM to eliminate red blood cells. The cells were treated with proteinase K digestion buffer [50 mM Tris (pH 8.1), 1 mM EDTA, 0.5% Tween 20, 0.1 mg/ml proteinase K] and incubated overnight at 40°C (35). The proteinase K was inactivated by

incubation at 95°C for 10 min, the samples were spun, and the supernatant was collected and stored at -80°C.

Confirmation of Genomic Integrity: To confirm the integrity of the extracted genomic DNA from fixed tissue, PCR analysis was used to detect β -actin. PCR reactions consisted of 50 ng DNA, 1x PCR buffer (Roche), 250 μ M of each dNTP, 200 nM of each primer, and 2.5 U of Taq polymerase (Roche) in 30 μ l total volume. Amplification was carried out in a GeneAmp PCR System 9700 (Applied Biosystems) as follows: initial 95°C for 5 min followed by 40 amplification cycles (94°C for 30 sec, 59°C for 30 sec, 72°C for 1 min) and a final extension of 72°C for 4 min. Primer sequences were as follows: 5'-CCC GCT ACC TCT TCT GGT G-3' (sense) and 5'-GGG GTG TTG AAG GTC TCA AA-3' (antisense).

Bisulfite Treatment: Extracted DNA from both RPFNA and fixed tissue was sodium bisulfite treated following the protocol of Grunau, et al (2001), with some modifications (36). Treatments on positive and negative controls were performed simultaneously. Briefly, 1 μ g of genomic DNA was denatured with 3 M NaOH for 20 min at 42°C, followed by deanimation in saturated sodium bisulfite and 10 mM hydroquinone solution (pH 5.0) for 4 hr at 55°C in the dark. The samples were desalted using the Wizard DNA Clean-Up System (Promega) according to the manufacturer's protocol. The DNA was then desulfonated in 3 M NaOH for 20 min at 37°C, ethanol precipitated, and resuspended in 1 mM Tris (pH 8.0) for storage in aliquots at -20°C.

MS-PCR: This assay takes advantage of discriminatory primers for methylated and unmethylated DNA, as the primers bind or do not bind depending on methylation status. Previous work has elucidated four CpG regions where methylation is known to occur upstream from the RAR β 2 gene; region 3 (M3) includes the RARE and TATAA box and region 4 (M4) includes the 5' end of the transcribed message (14). Region 4 was first studied in the fixed tumor samples, while both regions 3 and 4 were investigated in the RPFNA samples. All PCR reactions consisted of 50 ng DNA, 1x PCR buffer (see Table 2), 250 μ M of each dNTP, 200 nM of each primer, and 2.5 U of HotStar Taq polymerase (Qiagen) in 30 μ l total volume. Each PCR thermal cycle consisted of 95°C for 5 min followed by 40 amplification cycles (94°C for 1 min, annealing temp for 1 min, 72°C for 1 min) and a final extension of 72°C for 4 min. See Table 1 for primer sequences and annealing temperatures (14). A GeneAmp PCR System 9700 (Applied Biosystems) was used for all amplifications. PCR products were visualized on 1.5% ethidium bromide agarose gels using an Image Station 440 (Kodak).

MS-PCR Sensitivity Experiment: Previous studies have investigated the methylation status of breast cancer cell lines at both regions 3 and 4 (14, 15). It was confirmed that cells of the HMEC-SR line were unmethylated at region 3, HS578T cells were unmethylated at region 4, and ZR751 cells were methylated at both regions. As an estimate of PCR sensitivity, two experiments were set up where known amounts of methylated cells were titrated in unmethylated cells of each negative type. For the purposes of testing, the RPFNA procedure was estimated to yield an average of two million epithelial cells. Thus, titrated amounts of ZR751 cells (from 0 to 100,000 cells) were used to spike two million cells of each negative type. Each sample was DNA

extracted, bisulfite treated, and subjected to PCR as outlined above to determine the sensitivity of our method at each region.

Statistical Methods: The Wilcoxon Rank-Sums test was used to compare the median Masood score based on M3 methylation, M4 methylation, and a combination of both M3 and M4 methylation. Median cell counts for the two groups defined by M3 or M4 methylation were also compared using the Wilcoxon Rank-Sums test. The Spearman Correlation Coefficient was used to determine the association between cell count and Masood score.

Results

Study Demographics: Sixteen women with early stage breast cancer (Stages 0-2) were enrolled at Ohio State University from April 1999 to December 1999. Six percent had Stage 0 breast cancer (DCIS), 50% had Stage 1 breast cancer, and 44% had Stage 2 breast cancer. The average tumor size was 3.2 cm (range 0.5 cm to 5 cm). Thirty-one percent of the women had lymph node positive disease. Sixty-nine percent of the tumors were estrogen receptor positive and 50% were progesterone receptor positive. The mean age of the women was 57 years old (range 34-82 years old). Eighty-eight percent of the women were Caucasian and 12% were African American. Sixty-nine percent of the women were postmenopausal. A summary of clinical characteristics of subjects with early stage breast cancers whose primary breast biopsy specimens were tested for RAR β 2 P2 promoter methylation are listed in Table 2.

Thirty-eight women underwent RPFNA at Duke University Medical Center from March 2003 to March 2004. Clinical characteristics of subjects undergoing RPFNA are listed in Table 3. The mean age was 46 (range 29-64). Forty-seven percent of the women were either peri- or postmenopausal; 53% were premenopausal. Sixty-seven percent of the women had bilateral RPFNA. The mean Masood Cytology Index was 12. Eighty-seven percent (33/38) of the women were Caucasian and 13% (5/38) were African American. Five percent (2/38) of the women were currently on hormone replacement at the time of RPFNA. Twenty-four percent (9/38) of the women had been on estrogen replacement in the past and had a mean of 9 years of exposure (range 1-25 years). Thirteen percent (5/38) received tamoxifen, raloxifene, or an aromatase inhibitor at time of RPFNA. Of the 67 RPFNA samples that were collected, 11 were unsuccessful in obtaining sufficient epithelial cells for cytologic testing so 56 samples were submitted for full pathology analysis. Of the samples that contained insufficient cell counts for cytologic analysis, 6 samples both yielded methylation information and were positive for beta-actin by PCR

amplification (data not shown). Of the RPFNA samples, 33% (18/56) were from participants with a prior abnormal biopsy (20% ADH, 11% DCIS, 2% LCIS), 8/56 had history of contralateral breast cancer, 20/56 had strong family history, and 2/56 were BRCA2 mutation carriers.

Methylation Analysis: In this study, two known potential hypermethylation regions of the RAR β 2 P2 promoter were examined in mammary epithelial cells. These regions are detailed in Figure 1. Region 3 (M3) contains the RARE (nt -52 to nt -36), TATAA box (nt -28 to -24), and the transcription start region; methylation region 4 (M4) contains an Sp1 element (nt 230 to nt 235) (14). In the RPFNA samples, either only an unmethylated band or both methylated and unmethylated bands were observed. The presence of unmethylated RAR β 2 promoter sequences confirmed the integrity of the DNA in all samples and was expected given the global nature of the sampling. In this heterogeneous environment, the MS-PCR assay was sensitive enough to detect 0.005% methylation at region 3 and 0.05% methylation at region 4 (data not shown).

Incidence of RAR β 2 P2 promoter methylation in primary breast cancers: The frequency of RAR β 2 P2 promoter methylation was tested in primary breast cancer samples at methylation region 4 (M4). PCR amplification of β -actin was used to confirm DNA integrity (data not shown). Sixty-nine percent (11 of 16) of primary tumors demonstrated M4 methylation (data not shown). These results are similar to previously published reports (14).

Incidence of RAR β 2 P2 promoter methylation in RPFNA: Methylation specific PCR at the M3 and M4 regions was tested in 67 RPFNA specimens (Figure 2). Fifty-six out

of 67 samples (84%) had sufficient cellular material for cytologic analysis. MS-PCR analysis of these 56 samples demonstrated methylation in 50.0% (28/56) of RPFNA samples at region M3 and 37.5% (21/56) of RPFNA samples at region M4. All included samples exhibited strong unmethylated bands at both regions, confirming both the presence of DNA and the promoter sequence itself (Figure 2b). Sixty-four percent (36/56) of RPFNA samples demonstrated methylation at either M3 or M4; 23.2% (13/56) demonstrated methylation at both M3 and M4. Seventeen of the subjects had bilateral RPFNAs; one paired sample did not have sufficient cellular material so only sixteen paired samples were analyzed. Of these samples, 5/16 (31.2%) demonstrated methylation in RPFNA bilaterally, 7/16 (43.8%) demonstrated methylation in RPFNA unilaterally and 4/16 (25.0%) demonstrated the absence of methylation in either breast.

Correlation of RAR β 2 P2 Promoter Methylation in RPFNA with Masood Cytology

Index Scores: RPFNA aspirates were stratified for cytologic atypia using the Masood cytology index. The distribution of RAR β 2 P2 promoter methylation was reported as a function of increased cytologic abnormality. Figure 3a shows the number of samples with M3 region methylation for each Masood score. As the Masood score increased, the percentage of samples with M3 region methylation increased. Importantly, no sample with a Masood score of 10 or less exhibited RAR β 2 P2 promoter methylation at either the M3 or M4 region. The 28 samples without M3 region methylation had a median Masood score of 11, while the 29 samples with M3 region methylation had a median Masood score of 13. There was a significant difference between the two groups ($p=0.0018$). Figure 3b shows the number of samples with M4 region methylation for each Masood score. The 35 samples without M4 region methylation had a median score of 12, while the 20 samples with M4 region methylation had a median Masood score of 13.5 ($p=0.0002$). Figure 3c shows the presence of both M3 and M4 region methylation for each Masood score. The 42 samples without methylation at both regions had a median

Masood score of 12. The 13 samples with both M3 and M4 region methylation had a median Masood score of 14 ($p=0.0051$).

Correlation of RAR β 2 P2 Promoter Methylation in RPFNA with Cell Count: The presence of RAR β 2 P2 promoter methylation was compared to total cell count of each corresponding RPFNA slide. The 22 samples without M3 or M4 region methylation has a median cell count of 10, while the 34 samples with either M3 or M4 region methylation had a median cell count of 300 ($p=0.003$) (Figure 4a,b).

Correlation of Masood Score with Cell Count: RPFNA Masood scores were compared to the total cell count of each sample (Figure 4c). The Spearman Correlation Coefficient is 0.67 and indicates a significant correlation between the cell count and the Masood score ($p<0.0001$).

Discussion

Tumorigenesis is hypothesized to be a multistep process resulting from the accumulation of genetic losses and epigenetic changes. Epigenetic changes, mainly DNA methylation and modification of histones are now recognized as playing a critical role in mammary carcinogenesis (13, 37). To better define the role of promoter hypermethylation in early mammary carcinogenesis, we prospectively tested 1) the frequency of RAR β 2 P2 promoter hypermethylation in RFPNA specimens obtained from women at high-risk for breast cancer and 2) whether the presence of RAR β 2 P2 promoter hypermethylation correlates with the presence of early cytologic changes.

In 1996, the late Helene Smith proposed a model of mammary carcinogenesis where breast cancer developed in a "high-risk epithelial field" in which some of the genetic and epigenetic aberrations found in cancer may also be present in the morphologically normal surrounding epithelium (8). Loss of heterozygosity of RAR β 2 has been detected in normal epithelium adjacent to breast cancer but not in distal epithelium, supporting a "field effect" of increased risk (8). Yet it has been found that LOH cannot fully account for the frequent loss of RAR β 2 expression in breast cancer (38). Further, the presence of methylation has been shown to correlate between tumor and the apparently normal adjacent tissue. For example, RAR β 2 P2 promoter methylation has been detected in normal adjacent tissue of head and neck squamous cell carcinoma (HNSCC) tumors where RAR β 2 P2 promoter methylation was also present; RAR β 2 P2 methylation was not detected in normal epithelium near unmethylated HNSCC (39). Taken together, an early epigenetic change such as methylation may contribute to this "field effect" seen in breast cancer, and RAR β 2 P2 promoter methylation occurs early enough along this progression to potentially serve as an effective biomarker.

In this study we observe that RPFNA specimens obtained in women at high-risk for

breast cancer exhibit 1) a high frequency of methylation at the M3 and M4 regions of the RAR β 2 P2 promoter and 2) a positive correlation between the presence of RAR β 2 P2 promoter methylation and increasing Masood cytologic abnormalities (Figure 3). RAR β 2 P2 promoter methylation was also observed in 69% of primary low risk breast cancers and, importantly, was not observed in ten non-proliferative, cytologically normal RPFNA specimens (Masood index ≤ 10). The frequency of RAR β 2 P2 promoter methylation at the M3 region was unexpectedly high in RPFNA exhibiting low-grade proliferative changes (Masood index 11-12) which may reflect the overall breast cancer risk of this cohort. However, the presence of both M3 and M4 RAR β 2 P2 promoter methylation in RPFNA was 15% for specimens with low-grade proliferative changes and 30% for RPFNA specimens exhibiting high-grade proliferative changes (Masood index 13). Studies are in progress to test whether the presence of RAR β 2 P2 methylation can be used to further risk stratify high-risk patients with proliferative changes.

These studies used MS-PCR to detect the presence of RAR β 2 P2 promoter methylation at two target regions. MS-PCR is an established method for detecting methylation in DNA sequences. The method has been successfully used to examine methylation in relatively homogenous samples such as cancer cell lines and tumor specimens. In such samples, primers anneal to plentiful "target" sequences readily. However, RPFNA samples consist of cells from the whole breast—a heterogeneous collection that may or may not include "fields" of increased risk. Assuming RAR β 2 P2 promoter methylation is present in an RPFNA sample, MS-PCR primers would have far less "target" DNA to possibly bind, compared to in homogeneous samples with potentially greater amounts of "target". MS-PCR in RPFNA samples is then complicated by two factors: 1) less "target" DNA and 2) a sea of presumably unmethylated DNA from the whole breast that partially impairs proper annealing of methylated primers. These factors are more easily overcome in cell lines and tumor specimens, but require additional PCR optimization in RPFNA samples.

It is for these reasons that the PCR was optimized with such specific buffers and additives. Additionally, the cellular sensitivity experiment was set up for each region to gauge the effect of unmethylated DNA during amplification of the methylated "target" DNA. The optimization also included refining the program to ensure small amounts of "target" positive control (as low as ~5 pg DNA) could be amplified, to mirror the small amounts of potentially methylated sequences in the RPFNA samples. When optimized, the MS-PCR assay was able to detect 0.005% methylation at the M3 region and 0.05% methylation at the M4 region. Thus, the final optimized programs are quite sensitive, so each program was run in triplicate and only repeatable bands were counted as methylated.

Breast RPFNA has been used to predict both short-term breast cancer risk and monitor response to chemoprevention agents (25, 26). There are, however, some current limitations of breast RPFNA. First, much of the assessment of RPFNA samples has been focused on morphologic analysis. Molecular analysis of RPFNA samples may have the potential to enhance both the reproducibility and prognostic value of RPFNA. Second, many breast cancer prevention agents inhibit mammary cell proliferation and therefore have the potential to reduce the cell yield from RPFNA. As seen in our study as well as others' (29), MS-PCR studies on methylated genes such as RAR β 2 can still be performed even when epithelial samples are inadequate for cytology. The statistically significant correlation between increasingly atypical morphologic appearance and the increase in rates of detectable methylation at the RAR β promoter site supports the concept that the methylation assay is accurately detecting an early step in carcinogenesis. The addition of MS-PCR-based marker analysis of RPFNA provides additional sensitivity to assist in determining whether a prevention agent 1) solely acted to decrease proliferation or 2) was also successful in eliminating abnormal cells. Thus, RPFNA coupled with methylation studies shows promise for the early detection of breast cancer risk and

provides an extremely sensitive marker to track response to breast cancer prevention agents.

References

1. Fisher, B., Costantino, J. P., Wickerham, D. L., Redmond, C. K., Kavanah, M., Cronin, W. M., Vogel, V., Robidoux, A., Dimitrov, N., Atkins, J., Daly, M., Wieand, S., Tan-Chiu, E., Ford, L., and Wolmark, N. Tamoxifen for prevention of breast cancer: report of the National Surgical Adjuvant Breast and Bowel Project P-1 Study.[comment]. *Journal of the National Cancer Institute*, 90: 1371-88, 1998.
2. Rebbeck, T. R. Prophylactic oophorectomy in BRCA1 and BRCA2 mutation carriers. *European Journal of Cancer*, 38 Suppl 6: S15-7, 2002.
3. Hartmann, L. C., Schaid, D. J., Woods, J. E., Crotty, T. P., Myers, J. L., Arnold, P. G., Petty, P. M., Sellers, T. A., Johnson, J. L., McDonnell, S. K., Frost, M. H., and Jenkins, R. B. Efficacy of bilateral prophylactic mastectomy in women with a family history of breast cancer.[see comment]. *New England Journal of Medicine*, 340: 77-84, 1999.
4. Altucci, L., and Gronemeyer, H. The promise of retinoids to fight against cancer. *Nature Reviews. Cancer*, 1: 181-93, 2001.
5. Seewaldt, V. L., Johnson, B. S., Parker, M. B., Collins, S. J., and Swisshelm, K. Expression of retinoic acid receptor beta mediates retinoic acid-induced growth arrest and apoptosis in breast cancer cells. *Cell Growth Differ*, 6: 1077-88., 1995.
6. Subbaramaiah, K., Cole, P. A., and Dannenberg, A. J. Retinoids and carnosol suppress cyclooxygenase-2 transcription by CREB-binding protein/p300-dependent and -independent mechanisms. *Cancer Research*, 62: 2522-30, 2002.
7. Treuting, P. M., Chen, L. I., Buetow, B. S., Zeng, W., Birkebak, T. A., Seewaldt, V. L., Sommer, K. M., Emond, M., Maggio-Price, L., and Swisshelm, K. Retinoic Acid Receptor β 2 Inhibition of Metastasis in Mouse Mammary Gland Xenografts. *Breast Cancer Research and Treatment*, 72: 79-88, 2002.
8. Deng, G., Lu, Y., Zlotnikov, G., Thor, A. D., and Smith, H. S. Loss of heterozygosity in normal tissue adjacent to breast carcinomas. *Science*, 274: 2057-9, 1996.
9. Widschwendter, M., Berger, J., Daxenbichler, G., Muller-Holzner, E., Widschwendter, A., Mayr, A., Marth, C., and Zeimet, A. G. Loss of retinoic acid receptor beta expression in breast cancer and morphologically normal adjacent tissue but not in the normal breast tissue distant from the cancer. *Cancer Res*, 57: 4158-61., 1997.
10. Seewaldt, V. L., Kim, J. H., Caldwell, L. E., Johnson, B. S., Swisshelm, K., and Collins, S. J. All-trans-retinoic acid mediates G1 arrest but not apoptosis of normal human mammary epithelial cells. *Cell Growth & Differentiation*, 8: 631-41, 1997.

11. Seewaldt, V. L., Caldwell, L. E., Johnson, B. S., Swisshelm, K., Collins, S. J., and Tsai, S. Inhibition of retinoic acid receptor function in normal human mammary epithelial cells results in increased cellular proliferation and inhibits the formation of a polarized epithelium in vitro. *Experimental Cell Research*, 236: 16-28, 1997.
12. Dietze, E. C., Caldwell, L. E., Marcom, K., Collins, S. J., Yee, L., Swisshelm, K., Hobbs, K. B., Bean, G. R., and Seewaldt, V. L. Retinoids and retinoic acid receptors regulate growth arrest and apoptosis in human mammary epithelial cells and modulate expression of CBP/p300. *Microsc Res Tech*, 59: 23-40, 2002.
13. Kopelovich, L., Crowell, J. A., and Fay, J. R. The epigenome as a target for cancer chemoprevention. *J Natl Cancer Inst*, 95: 1747-57, 2003.
14. Sirchia, S. M., Ferguson, A. T., Sironi, E., Subramanyan, S., Orlandi, R., Sukumar, S., and Sacchi, N. Evidence of epigenetic changes affecting the chromatin state of the retinoic acid receptor beta2 promoter in breast cancer cells. *Oncogene*, 19: 1556-63, 2000.
15. Widschwendter, M., Berger, J., Hermann, M., Muller, H. M., Amberger, A., Zeschnigk, M., Widschwendter, A., Abendstein, B., Zeimet, A. G., Daxenbichler, G., and Marth, C. Methylation and silencing of the retinoic acid receptor-beta2 gene in breast cancer. *J Natl Cancer Inst*, 92: 826-32., 2000.
16. Esteller, M., Silva, J. M., Dominguez, G., Bonilla, F., Matias-Guiu, X., Lerma, E., Bussaglia, E., Prat, J., Harkes, I. C., Repasky, E. A., Gabrielson, E., Schutte, M., Baylin, S. B., and Herman, J. G. Promoter hypermethylation and BRCA1 inactivation in sporadic breast and ovarian tumors. *J Natl Cancer Inst*, 92: 564-9, 2000.
17. Fackler, M. J., McVeigh, M., Evron, E., Garrett, E., Mehrotra, J., Polyak, K., Sukumar, S., and Argani, P. DNA methylation of RASSF1A, HIN-1, RAR-beta, Cyclin D2 and Twist in in situ and invasive lobular breast carcinoma. *Int J Cancer*, 107: 970-5, 2003.
18. Lapidus, R. G., Nass, S. J., Butash, K. A., Parl, F. F., Weitzman, S. A., Graff, J. G., Herman, J. G., and Davidson, N. E. Mapping of ER gene CpG island methylation-specific polymerase chain reaction. *Cancer Res*, 58: 2515-9, 1998.
19. Lehmann, U., Langer, F., Feist, H., Glockner, S., Hasemeier, B., and Kreipe, H. Quantitative assessment of promoter hypermethylation during breast cancer development. *Am J Pathol*, 160: 605-12, 2002.
20. Liu, Z. J., Maekawa, M., Horii, T., and Morita, M. The multiple promoter methylation profile of PR gene and ERalpha gene in tumor cell lines. *Life Sci*, 73: 1963-72, 2003.
21. Mancini, D. N., Rodenhiser, D. I., Ainsworth, P. J., O'Malley, F. P., Singh, S. M., Xing, W., and Archer, T. K. CpG methylation within the 5' regulatory region of the

BRCA1 gene is tumor specific and includes a putative CREB binding site. *Oncogene*, 16: 1161-9, 1998.

22. Nass, S. J., Herman, J. G., Gabrielson, E., Iversen, P. W., Parl, F. F., Davidson, N. E., and Graff, J. R. Aberrant methylation of the estrogen receptor and E-cadherin 5' CpG islands increases with malignant progression in human breast cancer. *Cancer Res*, 60: 4346-8, 2000.

23. Sathyanarayana, U. G., Padar, A., Suzuki, M., Maruyama, R., Shigematsu, H., Hsieh, J. T., Frenkel, E. P., and Gazdar, A. F. Aberrant promoter methylation of laminin-5-encoding genes in prostate cancers and its relationship to clinicopathological features. *Clin Cancer Res*, 9: 6395-400, 2003.

24. Umbricht, C. B., Evron, E., Gabrielson, E., Ferguson, A., Marks, J., and Sukumar, S. Hypermethylation of 14-3-3 sigma (stratifin) is an early event in breast cancer. *Oncogene*, 20: 3348-53, 2001.

25. Fabian, C. J., Kimler, B. F., Zalles, C. M., Klemp, J. R., Kamel, S., Zeiger, S., and Mayo, M. S. Short-term breast cancer prediction by random periareolar fine-needle aspiration cytology and the Gail risk model. *J Natl Cancer Inst*, 92: 1217-27, 2000.

26. Fabian, C. J., and Kimler, B. F. Beyond tamoxifen new endpoints for breast cancer chemoprevention, new drugs for breast cancer prevention. *Ann N Y Acad Sci*, 952: 44-59, 2001.

27. Dooley, W. C., Ljung, B. M., Veronesi, U., Cazzaniga, M., Elledge, R. M., O'Shaughnessy, J. A., Kuerer, H. M., Hung, D. T., Khan, S. A., Phillips, R. F., Ganz, P. A., Euhus, D. M., Esserman, L. J., Haffty, B. G., King, B. L., Kelley, M. C., Anderson, M. M., Schmit, P. J., Clark, R. R., Kass, F. C., Anderson, B. O., Troyan, S. L., Arias, R. D., Quiring, J. N., Love, S. M., Page, D. L., and King, E. B. Ductal lavage for detection of cellular atypia in women at high risk for breast cancer. *J Natl Cancer Inst*, 93: 1624-32, 2001.

28. Sirchia, S. M., Ren, M., Pili, R., Sironi, E., Somenzi, G., Ghidoni, R., Toma, S., Nicolo, G., and Sacchi, N. Endogenous reactivation of the RARbeta2 tumor suppressor gene epigenetically silenced in breast cancer. *Cancer Res*, 62: 2455-61, 2002.

29. Evron, E., Dooley, W. C., Umbricht, C. B., Rosenthal, D., Sacchi, N., Gabrielson, E., Soito, A. B., Hung, D. T., Ljung, B., Davidson, N. E., and Sukumar, S. Detection of breast cancer cells in ductal lavage fluid by methylation-specific PCR. *Lancet*, 357: 1335-6, 2001.

30. Zalles, C. M., Kimler, B. F., Kamel, S., McKittrick, R., and Fabian, C. J. Cytology patterns in random aspirates from women at high and low risk for breast cancer. *Breast Journal*, 1: 343-9, 1995.

31. Stampfer, M. R. Isolation and growth of human mammary epithelial cells. *J Tissue Cult Meth*, 9: 107-15, 1985.

32. Seewaldt, V. L., Caldwell, L. E., Johnson, B. S., Swisshelm, K., Collins, S. J., and Tsai, S. Inhibition of retinoic acid receptor function in normal human mammary epithelial cells results in increased cellular proliferation and inhibits the formation of a polarized epithelium in vitro. *Exp Cell Res*, 236: 16-28, 1997.
33. Seewaldt, V. L., Mrozek, K., Dietze, E. C., Parker, M., and Caldwell, L. E. Human papillomavirus type 16 E6 inactivation of p53 in normal human mammary epithelial cells promotes tamoxifen-mediated apoptosis. *Cancer Research*, 61: 616-24, 2001.
34. Seewaldt, V. L., Mrozek, K., Sigle, R., Dietze, E. C., Heine, K., Hockenbery, D. M., Hobbs, K. B., and Caldwell, L. E. Suppression of p53 function in normal human mammary epithelial cells increases sensitivity to extracellular matrix-induced apoptosis. *Journal of Cell Biology*, 155: 471-86, 2001.
35. Lehmann, U., and Kreipe, H. Real-time PCR analysis of DNA and RNA extracted from formalin-fixed and paraffin-embedded biopsies. *Methods*, 25: 409-18, 2001.
36. Grunau, C., Clark, S. J., and Rosenthal, A. Bisulfite genomic sequencing: systematic investigation of critical experimental parameters. *Nucleic Acids Res*, 29: E65-5, 2001.
37. Widschwendter, M., and Jones, P. A. DNA methylation and breast carcinogenesis. *Oncogene*, 21: 5462-82, 2002.
38. Yang, Q., Yoshimura, G., Nakamura, M., Nakamura, Y., Shan, L., Suzuma, T., Tamaki, T., Umemura, T., Mori, I., and Kakudo, K. Allelic loss of chromosome 3p24 correlates with tumor progression rather than with retinoic acid receptor beta2 expression in breast carcinoma. *Breast Cancer Res Treat*, 70: 39-45, 2001.
39. Youssef, E. M., Lotan, D., Issa, J. P., Wakasa, K., Fan, Y. H., Mao, L., Hassan, K., Feng, L., Lee, J. J., Lippman, S. M., Hong, W. K., and Lotan, R. Hypermethylation of the retinoic acid receptor-beta(2) gene in head and neck carcinogenesis. *Clin Cancer Res*, 10: 1733-42, 2004.

Footnotes:

¹ This work is supported by NIH/NCI grants CA68438-AV13 [AVON/NCI Partners in Progress], 2P30CA14236-26 [to V.L.S.], R01CA88799 [to V.L.S.], R01CA98441 [to V.L.S.], Susan G. Komen Breast Cancer Award BCTR0402720 [to V.L.S.], DAMD-98-1-851 and DAMD-010919 [to V.L.S.], American Cancer Society Award CCE-99898 [to V.L.S.], a V-Foundation Award [to V.L.S.], and a Charlotte Geyer Award [to V.L.S.].

² To whom correspondence should be addressed: Box 2628, Duke University Medical Center, Durham, NC, 27710. Phone: (919) 668-2455. Fax: (919) 668-2458. email: seewa001@mc.duke.edu

³ These authors made equal contributions as third authors.

⁴ Abbreviations: **RAR**, retinoic acid receptor; **RPFNA**, Random Periareolar Fine Needle Aspiration; **LCIS**, lobular carcinoma *in situ*; **DCIS**, ductal carcinoma *in situ*; **BRCA1/2**, breast cancer 1/2 gene; **HMEC**, human mammary epithelial cell; **RXR**, retinoid X receptor; **RARE**, retinoic acid receptor element; **LOH**, loss of heterozygosity; **HNSCC**, head and neck squamous cell carcinoma

Table 1: MS-PCR Primer Sequences and Reaction Conditions

	sequences	1x buffer (& additives)	annealing temp
M3	S 5'-GGT TAG TAG TTC GGG TAG GGT TTA TC-3' AS 5'-CCG AAT CCT ACC CCG ACG-3'	16.6 mM (NH ₄) ₂ SO ₄ 67 Tris (pH 9.1) 3.0 mM MgCl ₂	57°C
U3	S 5'-TTA GTA GTT TGG GTA GGG TTT ATT-3' AS 5'-CCA AAT CCT ACC CCA ACA-3'	15 mM (NH ₄) ₂ SO ₄ 60 Tris (pH 8.5) 4.5 mM MgCl ₂	57°C
M4	S 5'-GTC GAG AAC GCG AGC GAT TC-3' AS 5'-CGA CCA ATC CAA CCG AAA CG-3'	15 mM (NH ₄) ₂ SO ₄ 60 Tris (pH 9.0) 3.5 mM MgCl ₂ 0.15 M 2-pyrrolidinone	55°C
U4	S 5'-GAT GTT GAG AAT GTG AGT GAT TT-3' AS 5'-AAC CAA TCC AAC CAA AAC A-3'	15 mM (NH ₄) ₂ SO ₄ 60 Tris (pH 8.5) 4.5 mM MgCl ₂	57°C

Table 2: Patient Characteristics of Early Stage Breast Cancer

Women Enrolled in Study		16
Number of Biopsy Samples Taken		17
		N= 16
Age (years)		57 (34-82)
Race	Caucasian	14 (87.5%)
	African-American	2 (12.5%)
Menopausal Status	Postmenopausal	11 (68.8%)
	Premenopausal	5 (31.2%)
Stage of Breast Cancer	Stage 0/DCIS	1 (6.3%)
	Stage 1	8 (50.0%)
	Stage 2	7 (43.7%)
Tumor Size (cm)		3.2 (0.5-5.0)
Type of Tumor	Invasive Ductal	12 (75.0%)
	Invasive Lobular	1 (6.3%)
	Mixed Ductal/Lobular	2 (12.4%)
	DCIS	1 (6.3%)
Tumor Receptor Status	ER+	11 (68.9%)
	PR+	8 (50.0%)
Lymph Node Positive Disease		5 (31.2%)

Table 3: Patient Characteristics for RPFNA

Women Enrolled in Study	38
FNA Samples Collected	67
Number of RPFNAs with Insufficient Epithelial Cell Count	11
Number of RPFNAs Submitted for Analysis	56
	N = 38
Average Age and Range (years)	46 (29- 64)
Race	Caucasian 33 (86.8%) African-American 5 (13.2%)
Menopausal Status	Postmenopausal 18 (47.4%) Pre/Perimenopausal 20 (52.6%)
Hormone Replacement Use	Current 2 (5.3%) Ever-use 9 (23.7%) Never use 27 (71.0%)
Anti-Estrogen Therapy (at the time of RFPNA)	Tamoxifen 2 (5.3%) Raloxifene 1 (2.6%) Aromatase Inhibitor 2 (5.3%)
Family History of Breast Cancer	17 (44.7%)
Prior Abnormal Biopsies	LCIS 1 (2.6%) DCIS 5 (13.2%) ADH 10 (26.3%) Hx. Contralateral Br.CA 5 (13.2%)
Number of Bilateral RPFNA	17 (44.7%)

Figure 1: MS-PCR Targets. MS-PCR primers were designed to amplify regions of known methylation regions in the RAR β 2 P2 promoter (14). M3 region (methylated nt -51 to nt 162; unmethylated nt -49 to nt 162) includes the RARE, TATAA box, and transcription start region; M4 region (methylated nt 104 to nt 251; unmethylated nt 101 to nt 250) contains an Sp1 element. Methylated CpGs were previously identified by sequencing of cell lines and primary tumor samples and are depicted as filled circles (14, 15).

Figure 2: RPFNA Cytology and Methylation of RAR β 2 P2 Promoter. (a)

Representative RPFNA specimens in high-risk women. The numeric value denotes the Masood Cytology Index Score for this specimen. The presence of RAR β 2 P2 promoter methylation at either the M3 or M4 region is denoted as **Methylated**. If neither region is methylated, the specimen is labeled **Unmethylated**. (b) Hypermethylation of RAR β 2 P2 promoter M3 and M4 regions in RPFNA obtained from 5 high-risk women. (M3) and (M4) denote the use of primers to identify methylated RAR β 2 P2 regions 3 and 4, respectively. (U3) and (U4) denote the use of primers to identify unmethylated RAR β 2 P2 regions 3 and 4, respectively. (+) denotes a methylated positive control in the M3 and M4 gels, HMEC-SR in the U3 gel, and HS578T in the U4 gel. (-) denotes the negative control.

Figure 3: Correlation between RAR β 2 P2 Promoter Methylation in RPFNA with Masood Cytology Index Scores. RPFNA aspirates were assessed for cytologic atypia using the Masood cytology index. The distribution of RAR β 2 P2 promoter methylation is depicted as a function of increased cytologic abnormality. *(a)* The distribution of RPFNA samples with M3 region methylation relative to Masood cytology score. *(b)* The distribution of RPFNA samples with M4 region methylation relative to Masood cytology score. *(c)* RPFNA samples containing methylation at both the M3 and M4 regions relative to Masood cytology score.

Figure 4: Correlation between RPFNA Cell Count and RAR β 2 P2 Promoter Methylation and Masood Score. *(a, b)* The presence of RAR β 2 P2 promoter methylation at the M3 *(a)* and M4 *(b)* region is depicted relative to total cell count of each RPFNA sample. *(c)* RPFNA Masood cytology index scores are reported relative to the total cell count of each sample.

Figure 1

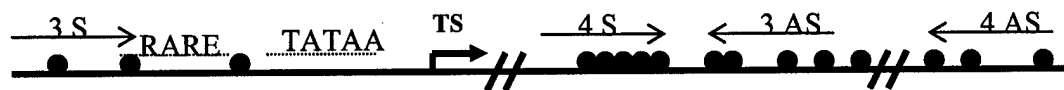
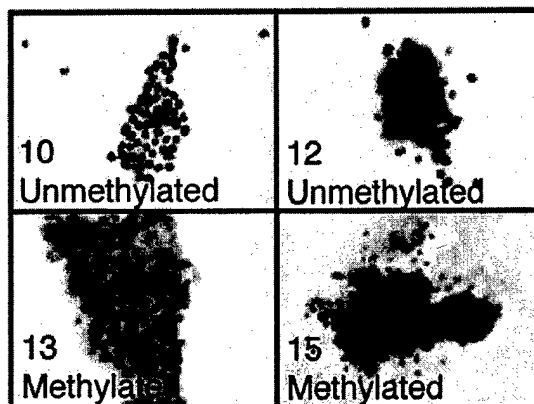


Figure 2

a



b

RPFNA

27 28 28 29 29 30 30 31 31 (+) (-)
L L R L R L R L R



M3



M4



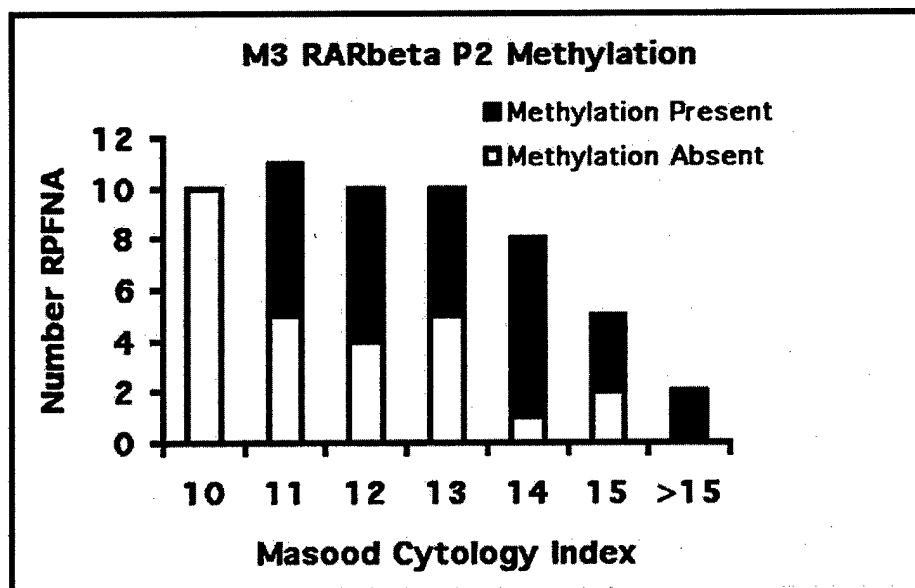
U3



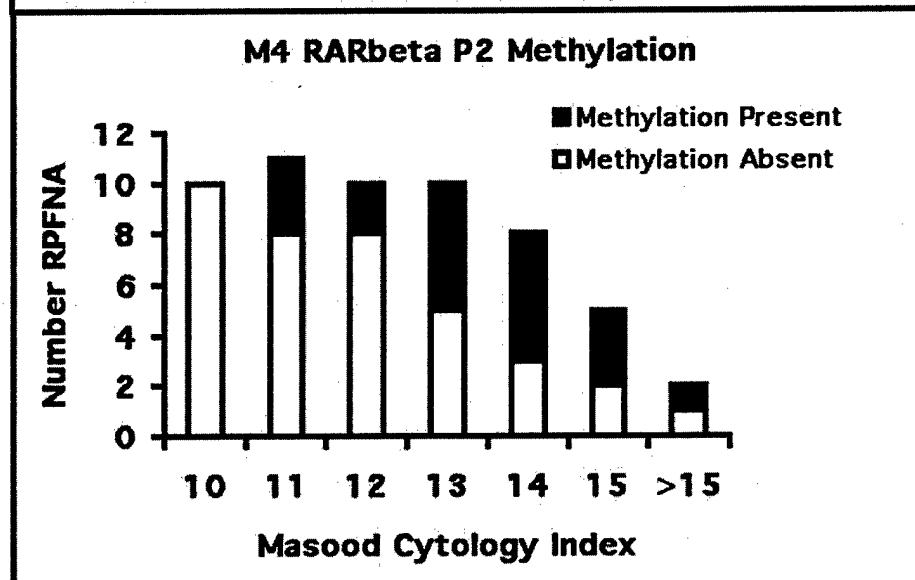
U4

Figure 3

a



b



c

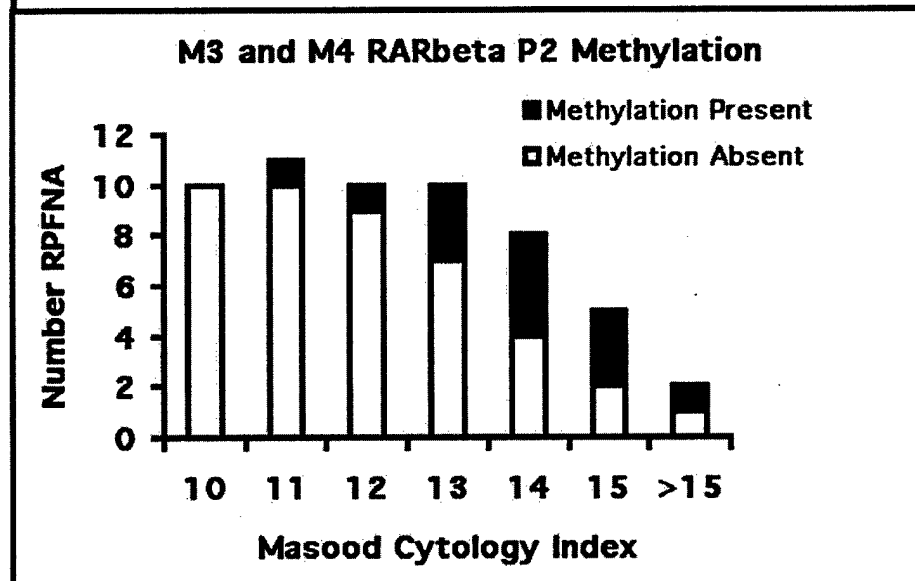
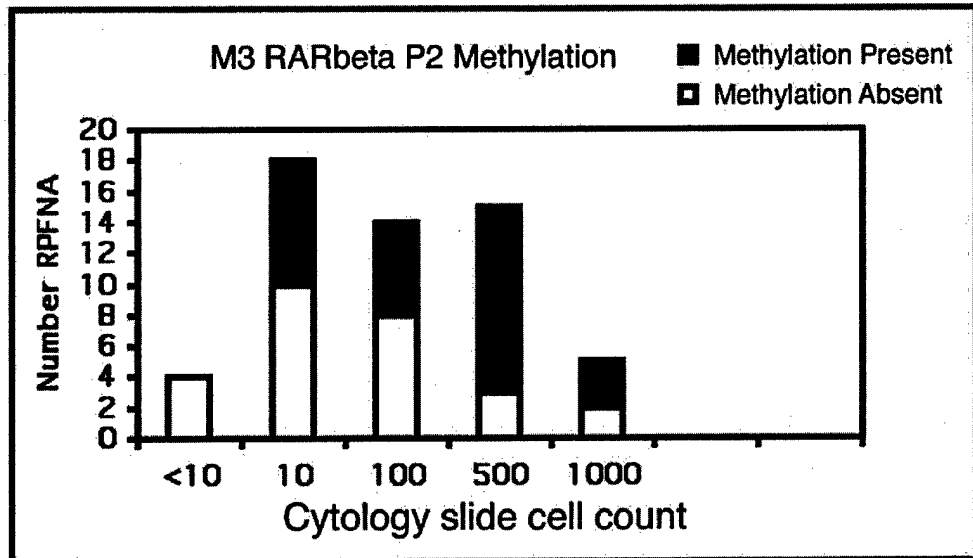
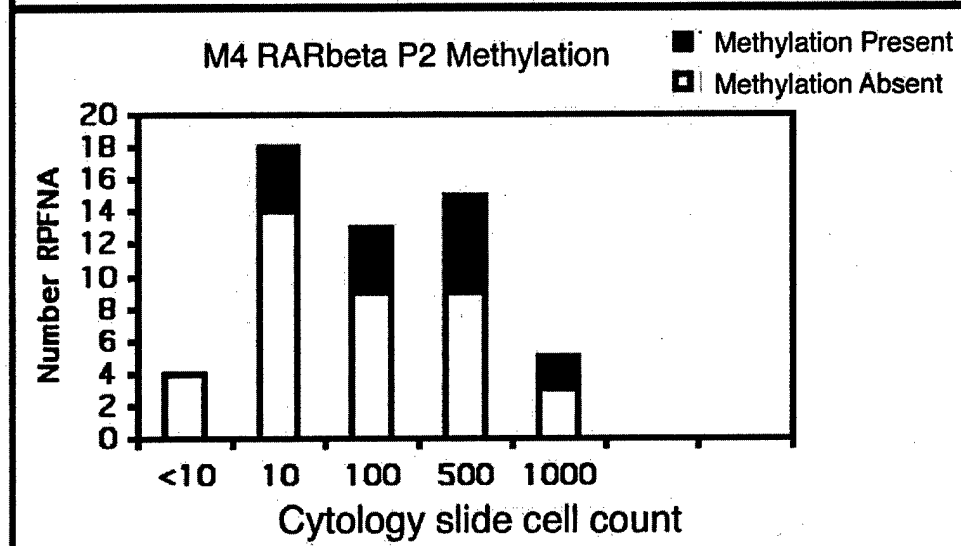


Figure 4

a



b



c

